UPPSALA UNIVERSITET

UNIVERSITAT DE BARCELONA

Synthesis, characterization and study of Stiff-Stilbene based Photo-switchable Cyclic Ethers

Óscar Benito Pérez

Project in Chemistry, 30 credits
Treball Final de Grau – BSc Final Project

22nd June 2016

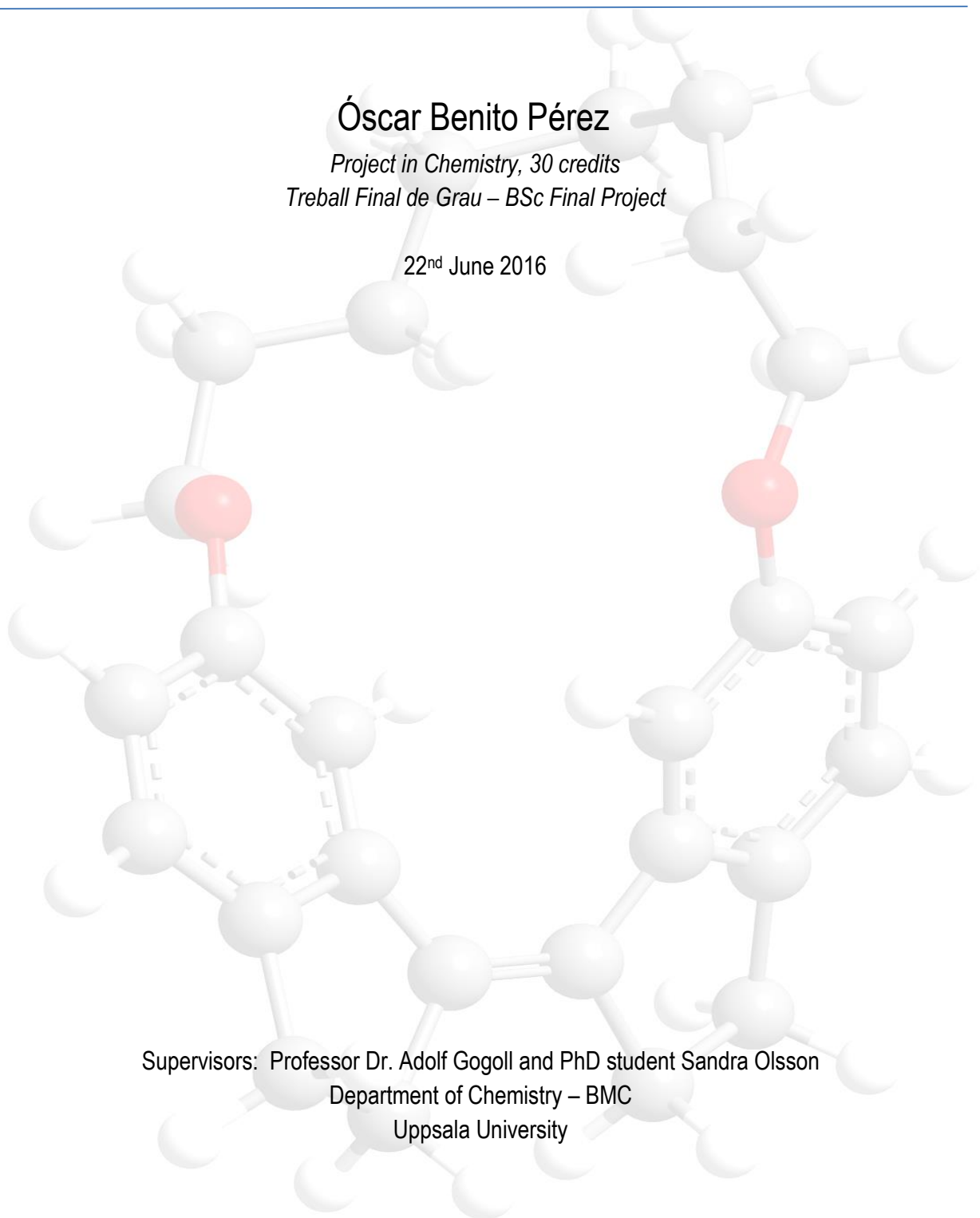

Supervisors: Professor Dr. Adolf Gogoll and PhD student Sandra Olsson
Department of Chemistry – BMC
Uppsala University

”That all our knowledge begins with experience there can be no doubt. […] In respect of time, therefore, no knowledge of ours is antecedent to experience, but begins with it”

Immanuel Kant, from *Critique of Pure Reason* (1781)

ABSTRACT

Photo-switchable molecules undergo configurational changes between two or more isomeric states upon irradiation by light. One of those photo-switchable molecules is stiff-stilbene. It is used in many applications in a wide range of fields from material science to biologic systems. In some of these applications stiff-stilbene is the backbone of cyclic molecules. In this project, a model system was designed introducing different length linkers between stiff-stilbene aromatic rings. The main aim is to study the dependence of photo-isomerization properties on the linker length. A good synthetic route to target molecules was planned and followed giving moderate to good yields. The photo-switching study of the target molecules revealed that the linker length has a large impact on the photo-isomerization process. NMR spectroscopy was used to follow the progress of the isomerization.

TABLE OF CONTENTS

ABBREVIATIONS

A	Absorption
A.U.	Absorbance units
abs	Absorbance
AFM	Atomic force microscope
APCI	Atmospheric-pressure chemical ionization
bp	Broad peak
calcd.	Calculated
CC	Column chromatography
conc.	Concentrated
COSY	Correlation spectroscopy
d	Doublet
DCM	Dichloromethane
dd	Doublet of doublets
DMF	N,N-dimethylformamide
DOSY	Diffusion-ordered spectroscopy
dt	Doublet of triplets
eq.	Equivalent
EtOAc	Ethyl acetate
F	Fluorescence
HMBC	Heteronuclear multiple bond correlation
HSQC	Heteronuclear single quantum correlation
i.e.	*id est* (that is)
IC	Internal conversion
ISC	Intersystem crossing
J	Coupling constant
LG	Leaving group
m	multiplet
MS	Mass spectroscopy
MW	Microwave
NMR	Nuclear magnetic resonance
NOESY	Nuclear overhauser effect spectroscopy
Nu	Nucleophile
P	Phosphorescence
RT	Room temperature
s	Singlet
S_EAr	Electrophilic aromatic substitution
S_N1	Nucleophilic substitution (first order kinetics)
S_N2	Nucleophilic substitution (second order kinetics)
t	triplet
TBAB	Tetra-n butylammonium bromide
TfOH	Trifluoromethanesulfonic acid
THF	Tetrahydrofuran
TOCSY	Total Correlation Spectroscopy
UV	Ultraviolet light
VC	Vibrational cascade
vis	Visible light

1. INTRODUCTION

1.1 Background

1.1.1 Photochemistry

Photochemistry is the study of chemical reactions initiated by light.[1] This field of chemistry studies interactions between molecules and light, which is energy as electromagnetic radiation. Some authors, as J. Knowles[2] or A. Natarajan,[3] dated the origin of photochemistry to the 19th century when H. Trommsdorff[4] discovered and described a kind of reaction of crystals of the sesquiterpene santonin upon interaction with sunlight. The establishment of quantum mechanical foundations during the first half of the 20th century helped especially in this field since they explain the interaction between light and molecules.[5] A more extensive development of photochemistry started at the turn of 20th century when G. Ciamician[6] described some of the nowadays well-known photochemical reactions, pericyclic reactions, and introduced some fundamental concepts of this field. After the 1950s many examples of photochemistry applications have been described such as photo-reductions and photo-cyclizations of tryptophan,[7] Paterno-Büchi reactions,[8] Corey's synthesis of carophyllene alcohol[9] or synthesis of the anti-malaria drug Artemisinin.[10] However, the most famous photochemical example is the natural biologic process called photosynthesis.[11,12]

Quantum mechanics[5] describes the dual nature of electromagnetic radiation. It behaves as a wave, which explains how it propagates through the space, and it behaves as discrete particles (photons), which allows us to understand how molecules and light interact. When a molecule absorbs a photon it is electronically excited from its ground state, the minimum energy level, to an excited state of higher energy. This happens when the molecule is irradiated with light that corresponds to the energy difference between the ground state and an excited state. Jablonski diagrams[13] schematize the transitions between the electronic states of a molecule as it is shown in Figure 1.

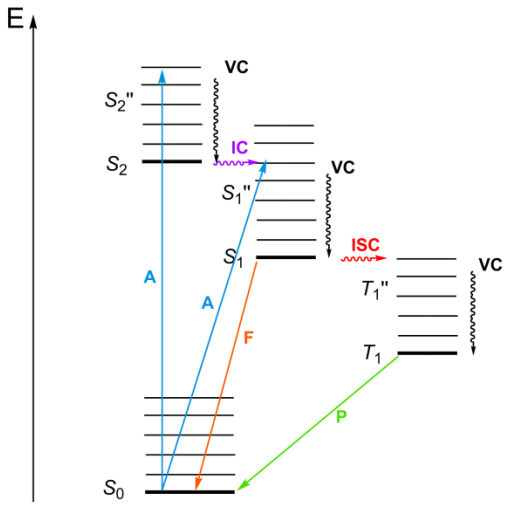

Figure 1. *Jablonski diagram showing excitation and relaxation routes. Radiative transitions are indicated as A (Absorption), F (fluorescence) and P (Phosphorescence) whereas non-radiative transitions are represented with IC (Internal conversion), ISC (Intersystem crossing) and VC (Vibrational cascade). S_0 indicates the ground state while S_1, S_2 and T_1, singlet and triplet excited states.*

Direct transitions between S_0 and T_1 are forbidden by Franck-Condon principle which states that molecular structure and spin state must remain unaltered during electronic transitions between ground and excited states.[14,15]

Two additional laws have to be considered regarding photochemistry reactions: Grotthus-Draper and Stark-Einstein laws. The first states that radiation has to be absorbed by a molecule in order to promote a chemical change. Nevertheless, photon absorption does not necessarily mean that a chemical reaction will occur, since it can also be followed by deactivation processes. Fluorescence and phosphorescence are radiative deactivation processes whereas internal conversion, intersystem crossing and vibrational cascade are non-radiative ones. Thus, it is important to measure the efficiency of a photochemical process which is defined by the quantum yield, Φ, (1). The Stark-Einstein law states that only one molecule can be activated with each photon absorbed by a chemical system.[1]

$$\phi = \frac{number\ of\ molecules\ reacting\ per\ unit\ volume\ per\ unit\ time}{number\ of\ photons\ absorbed\ per\ unit\ volume\ per\ unit\ time} \quad (1)$$

1.1.2 Photo-switchable molecules

Photo-switchable molecules are those which undergo configurational changes between two or more isomeric states upon irradiation by light.[16] The photo-switchable molecules studied in this project are formed by two subunits linked by a double bound. The double bond provides the molecule with two configurations: isomer *trans*, or *E*; and isomer *cis*, or *Z*. The studied photo-switchable molecules have extended conjugated systems and high degrees of aromaticity which make them able to absorb electromagnetic radiation at a wavelength corresponding to visible/UV light. Because of the absorbed energy, they undergo isomerization from *E* to *Z* and from *Z* to *E*.

Discovered at the end of the 19th century, these compounds have been extensively investigated and many applications have been suggested in such diverse areas as material science and biological systems.[17,18,19,20] Some photo-switchable molecules are shown in Figure 2.

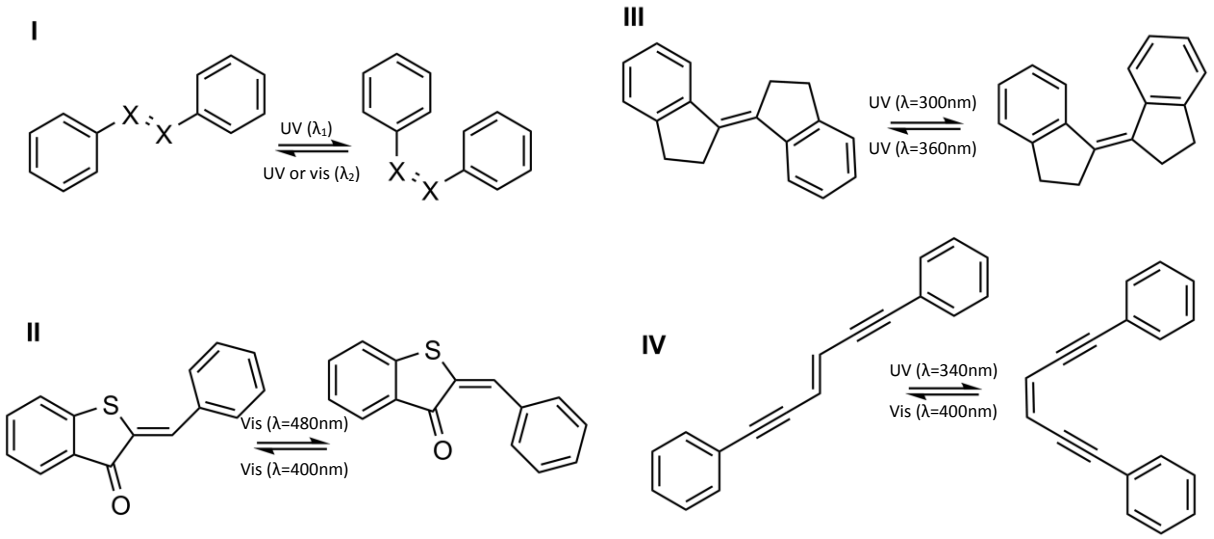

Figure 2. *Some examples of photo-switchable units: (I) X=CH, stilbene (λ_1 = 300nm, λ_2 = 280nm); (I) X=N, azobenzene (λ_1 = 350nm, λ_2 = 450nm); (II) thioaurone; (III) stiff-stilbene; (IV) enediyne.*

1.1.3 Stiff-stilbene

Stiff-stilbene is one of the photo-switchable molecules shown in Figure 2. It shows interesting properties such as thermal, chemical and photochemical stability. Regarding its structure, it is a rigid chromophore since the aromatic ring rotation is restricted by the cyclopentane ring. This results in a larger difference between *E* and Z isomers absorption wavelengths which, in addition, are red-shifted with respect to the stilbene molecule described above.[21] Moreover, J.F. Xu compared the stiff-stilbene with the azobenzene as a backbone. Photo-isomerization of stiff-stilbene derivatives proceeded with a 50 % quantum yield whereas azobenzene derivatives proceeded with a 20% (λ < 320nm) or 35% (λ >400nm) quantum yield.[22]

Stiff-stilbene has been studied on many occasions as a photo-switchable molecule.[23,24,25,26] Recently, M. Quick has done a comprehensive study of the photo-isomerization dynamics of stiff-stilbene in solution.[27] Furthermore, there are quite many applications of stiff-stilbene related with its photo-isomerization ability in such diverse fields, as material science[28] to biological systems.[29] Stiff-stilbene has been used as photo-switchable monomer in polymer synthesis,[30] it has been tested as a backbone of Host-Guest systems[31] and recent projects in our research group have demonstrated its potential ability to be used as backbone of peptidomimetics for the inhibition of *Mycobacterium tuberculosis* ribonucleotide reductase. Stiff-stilbene has been also used as backbone in cyclic molecules, i.e. adding a linker between the two aromatic rings of the stiff-stilbene unit. These cyclic molecules have been used as molecular force probes[32,33,34] and in asymmetric catalysis.[35]

Force probes aim to measure reaction rates relating them with the restoring force in a molecule that has been stretched or compressed.[36] This stretch can be caused by microscopic force probes (AFM) which are useful to study reactions involving structural changes at nanometer scale such as protein unfolding. However, because of their surface roughness and thermal fluctuations, it is not suitable to

study more localized chemical reactions. These issues can be overcome using molecular force probes. They are molecular systems that have the same effect as microscopic force probes but at molecular level, therefore they can be used to study localized chemical reactions (reacting group, blue spheres in Figure 3). One example of molecular force probe are cyclic molecular systems with a stiff-stilbene backbone. The reaction which is investigated or the corresponding functional groups are placed in the linker between the two aromatic rings of stiff-stilbene. A photo-isomerization of stiff-stilbene backbone from the *Z* to the *E* isomer causes a strain on the linker that gives rise to the restoring force. Restoring forces can be calculated as the release of energy while the perturbed system returns back to equilibrium. Then, reaction rates can be calculated by means of chemomechanical kinetics.[32] Our target molecules are model systems similar to that used as a molecular force probes. In Figure 3, both systems, microscopic force probes and molecular force probes, are compared.

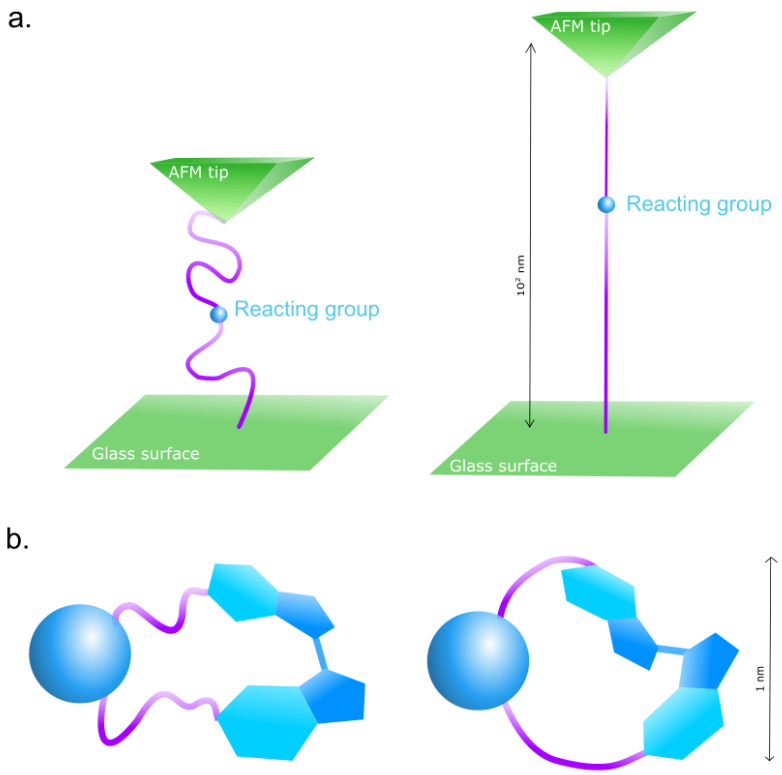

Figure 3. *Representation of (a) microscopic force probe and (b) molecular force probe with stiff-stilbene as backbone. In both systems it is shown the relaxed (left) and stretched (right) forms. Microscopic force probe system (a) is about 100 nm long whereas molecular force probe (b) is 1 nm. Blue spheres represent reacting groups.*

1.2 The project

Molecular tools is one of the research topics in our group. It consists of design, synthesis and characterization of molecules that have some utility at molecular level, for example, as host-guest systems.[31] In this context, one of the most important challenges is to find out how to control those

systems. Photo-switchable molecules are important tools that allow us to achieve this control. Irradiating the molecule with light we can manipulate its cis/trans configuration, thereby changing its properties. As we have presented in previous sections, we will focus on one of those photo-switchable units: stiff-stilbene. A small library of molecules was designed as a model system introducing different length linkers between stiff-stilbene aromatic rings. The main aim is to determine if the linker length has an important effect on the photo-isomerization process.

1.2.1 Target molecules

Stiff-stilbene is the photo-switchable unit chosen for this project. As can be seen in figure 3 a linker can be introduced between the two aromatic rings. This kind of molecules are used in many applications as described in the previous section, therefore, a fundamental study of this system will be useful for those who are working with it. Thus, we have designed a small library of model molecules similar to the previously described force probes systems[33,35] with the main purpose of studying its photo-switching properties. We want to determine if photo-switchable properties depend on the linker length and how.

These designed molecules, as it is shown in Figure 4, are cyclic diethers containing a stiff-stilbene backbone and different linkers between the two aromatic rings. These linkers are aliphatic unbranched chains from six to twelve carbons.

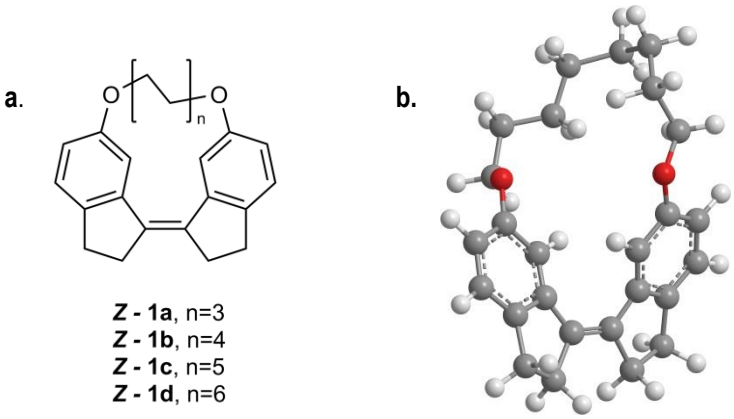

Figure 4. *(a) Designed target molecules in this project. (b) Example of target molecule, Z-1b (n=4).*

These molecules have not been previously reported in the literature. A Retrosynthetic analysis of these target molecules is shown in Scheme 1.

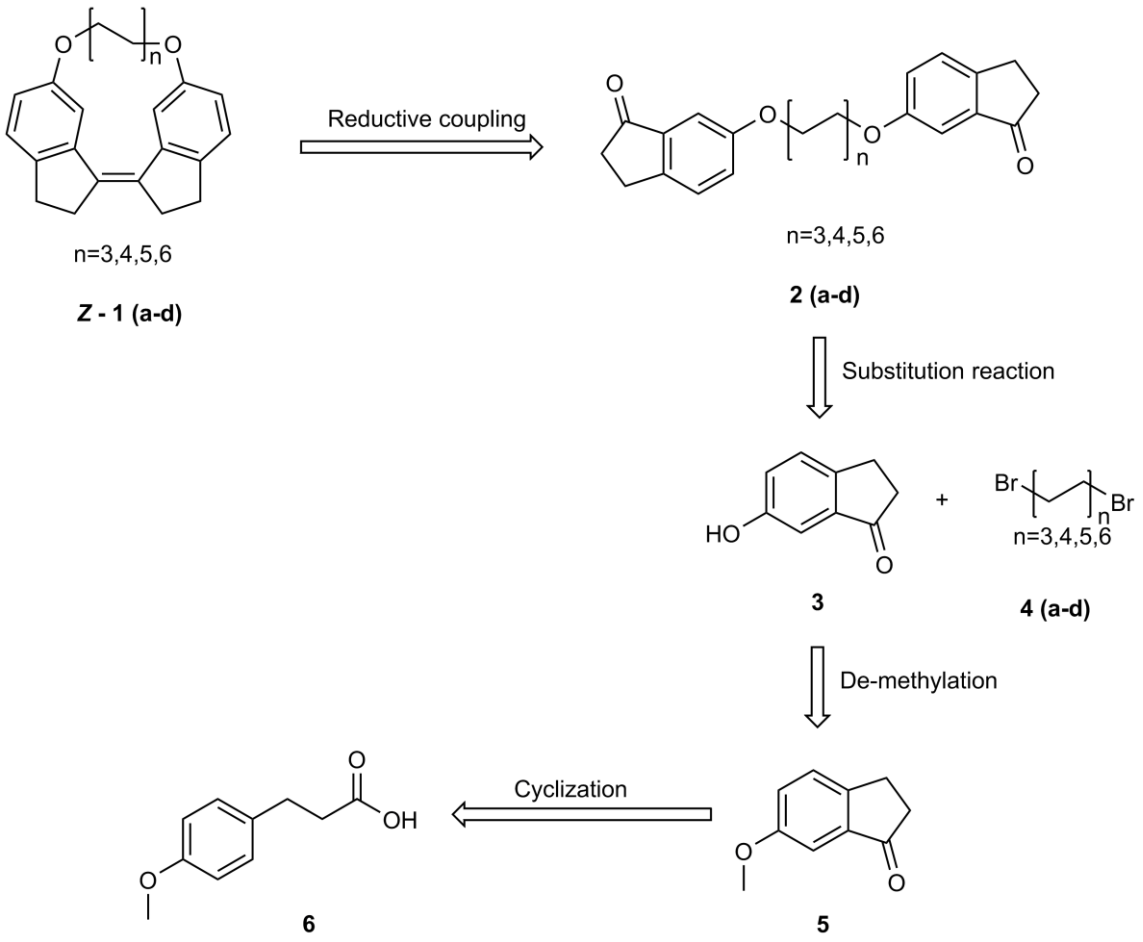

Scheme 1. *Retrosynthetic analysis of the target molecules.*

As the retrosynthetic analysis shows, starting from our target molecules, the double bond between the cyclopentane rings can be broken leading to an open di-ketone compound. Then, the two ether bonds can be broken and di-ketone compounds split into three parts, two units of 6-hydroxy-1-indanone with a hydroxyl group where the ether oxygen were before; and an aliphatic unbranched chain as the di-bromo analogue compound. From 6-hydroxy-1-indanone, a methyl group can be bonded to the hydroxyl oxygen to get 6-methoxy-1-indanone. Finally, the bond between the carbonyl carbon and the aromatic one can be broken to open the ring and get compound 6.

Therefore, the target molecules, *Z*-1, can be synthesized from di-ketone compounds via McMurry coupling. Di-ketone compounds, 2, can be obtained from 6-hydroxy-1-indanone introducing the linkers with different lengths via Williamson ether synthesis. 6-hydroxy-1-indanone can be prepared in two steps from 3-(4-methoxyphenyl)propionic acid via an intramolecular Friedel-Crafts acylation followed by a de-methylation reaction. The proposed synthetic route is presented in Scheme 2.

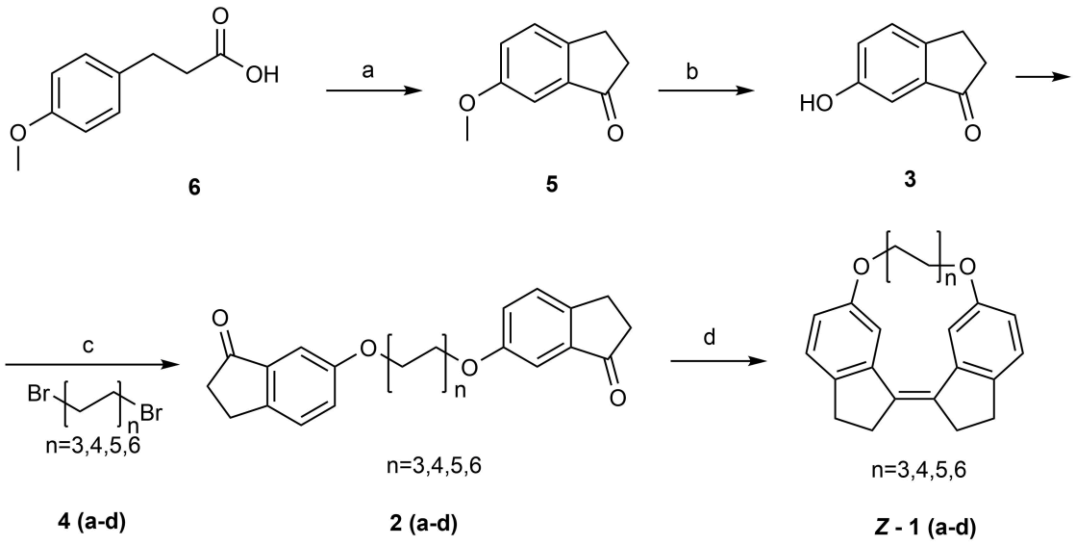

Scheme 2. *Designed synthetic route towards target molecules. (a) Intramolecular Friedel-Crafts acylation, (b) de-methylation, (c) Williamson ether synthesis, (d) McMurry coupling.*

1.2.2 Nuclear Magnetic Resonance spectroscopy

Developed in the late 1940s to study the properties of atomic nuclei,[37] nuclear magnetic resonance spectroscopy started to be used in 1951 to determine structures of organic compounds. Nowadays, NMR spectroscopy is the most useful tool to determine structures of chemical compounds, pure or as mixtures, solids or liquids.[38]

Basically, we can obtain information from NMR spectra about chemical shifts (δ) and coupling constants (*J*). By means of chemical shifts, one can determine the environment of the atom corresponding to that signal and by analyzing coupling constants and splitting patterns, connectivity between neighbouring atoms can be detected.

In this project, NMR spectroscopy will be used at two stages. First, we will work with NMR spectroscopy to characterize the products, i.e. determine the chemical structure of the synthesized compounds and check that we have obtained the correct ones. In the second part of the project, the photo-switching analysis, we will use NMR to follow the course of the photo-isomerization. As the isomerization from *Z* to *E* isomer causes a change on the environment of some atoms, especially those corresponding to the linker and those of the aromatic ring, chemical shift and coupling pattern changes can be used to monitor the reaction.

2D NMR techniques such as gCOSY,[39,40] TOCSY,[41] gHSQC[42] and gHMBC,[43] will be used to assign all the ^{1}H and ^{13}C NMR signals.[38]

1.2.3 Summary

Photo-switching, i.e. isomerization by means of light stimulus, is an appreciated property of molecules and many studies have been conducted around this topic. In this project, we study a small library of cyclic molecules with a stiff-stilbene backbone and an aliphatic linker of varying lengths between the aromatic rings. The main aim is to determine if different chain lengths affect photo-switching and how they affect it. We will try to establish the limit of the linker, in term of length, to make the molecule able to undergo photo-isomerization.

1.3 Reactions involved in this project

1.3.1 Friedel-Crafts acylation

Friedel-Crafts acylation was discovered by C. Friedel and J. M. Crafts in 1877.[37] This reaction is one of the most important electrophilic aromatic substitution (S_EAr) reactions because it forms a carbon-carbon bond. Through this reaction, an acyl group is linked to an aromatic carbon (Scheme 3).

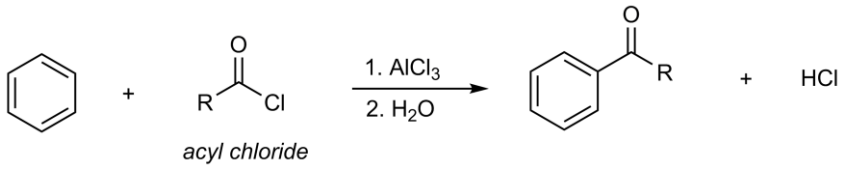

Scheme 3. *Friedel-Craft acylation model reaction*

The mechanism of Friedel-Crafts acylation (Scheme 4) can be divided into 3 steps:

- Formation of an acylium ion with $AlCl_3$, a Lewis acid.
- Electrophile attack on the ring
- Recovery of aromaticity by losing a proton caught by a base in the reaction mixture.

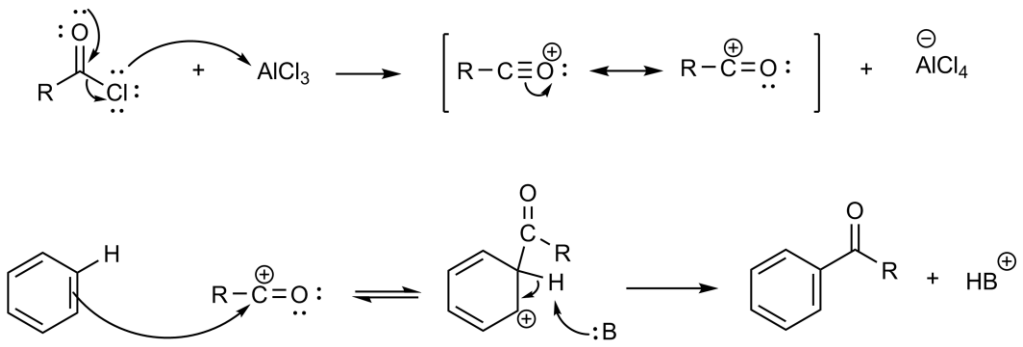

Scheme 4. *Friedel-Crafts acylation mechanism*

An important fact to consider is that the reaction product contains a carbonyl group which can form a complex with the $AlCl_3$, therefore more than 1 mol eq. must be used in this reaction and water is added as a last step to separate the Lewis acid from the product as it can be seen in Scheme 5.

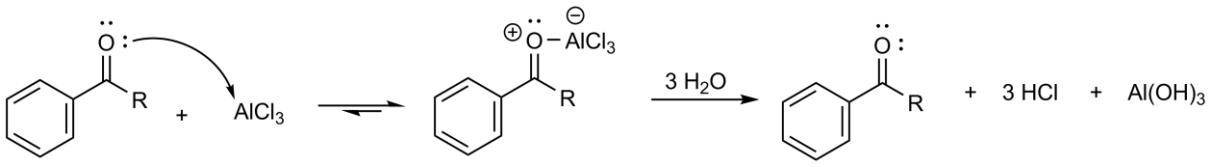

Scheme 5. *Carbonyl-$AlCl_3$ complex formation during Friedel-Crafts reaction and hydrolysis.*

In Friedel-Crafts acylations an acyl chloride or an acid anhydride can be used as starting materials.

Many applications of Friedel-Crafts acylation in organic synthesis have been described in the literature since it was first presented, some of them last year.[44,45,46]

1.3.2 De-methylation

A de-methylation reaction is a removal of a methyl group from a molecule. When an ether undergoes a process of de-methylation an alcohol is the result. This kind of reactions is extensively applied in aryl ethers using boron tribromide as a main reagent.[47] Nevertheless, in this project we use $AlCl_3$ which is an analogue reagent. A mechanism for this reactions was proposed by J.F.W. McOmie[48] and is shown in Scheme 6.

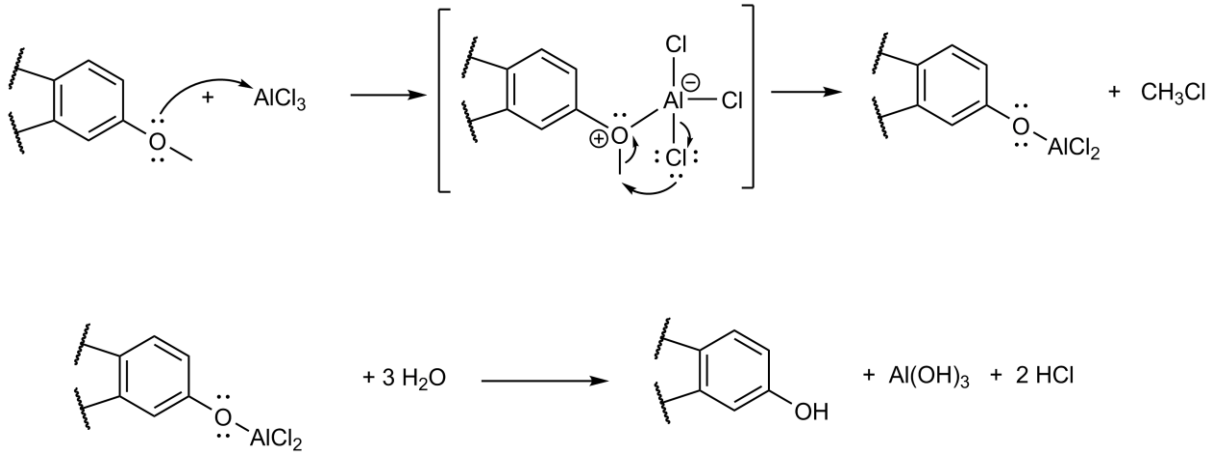

Scheme 6. *De-methylation reaction mechanism.*

1.3.3 Nucleophilic substitution

Nucleophilic substitution reactions (Scheme 7), as the name suggests, consist in replacing a part of a molecule, which we call leaving group (LG), for another atom or group which we name nucleophile (Nu).

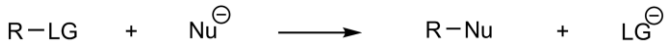

Scheme 7. *General nucleophilic substitution reaction.*

E. Hughes and C. Ingold proposed two mechanisms for this reaction[49] in 1937: S_N1 and S_N2, where "S" means substitution, "N" nucleophilic and the number unimolecular (1) or bimolecular (2) and also the kinetic order of the reaction.[37] S_N2 is a concerted mechanism, i.e. the R-LG bond is broken at the same time that R-Nu bond is formed, thus the reaction is bimolecular and the kinetics is affected by concentration of both reactants. Hughes and Ingold described a backside attack of the nucleophile as it is shown in Scheme 8a. On the other hand, S_N1 mechanism proceeds through the formation of an intermediate carbocation. This is a unimolecular mechanism since reaction kinetic is only affected by the substrate concentration. S_N1 mechanism is shown in Scheme 8b. If the substrate presents an asymmetric center and it undergoes a nucleophilic substitution, which mechanism the reaction goes will affect the product. In the S_N2 mechanism, a transition state where both LG and Nu are "semi-bonded" to the center promotes an inversion of configuration and a single product with inverted stereochemistry will be obtained. Alternatively, in the S_N1 mechanism, a planar carbocation is formed as intermediate so all previous stereochemical information will be lost and the final product will be a racemic mixture of both possible stereoisomers.

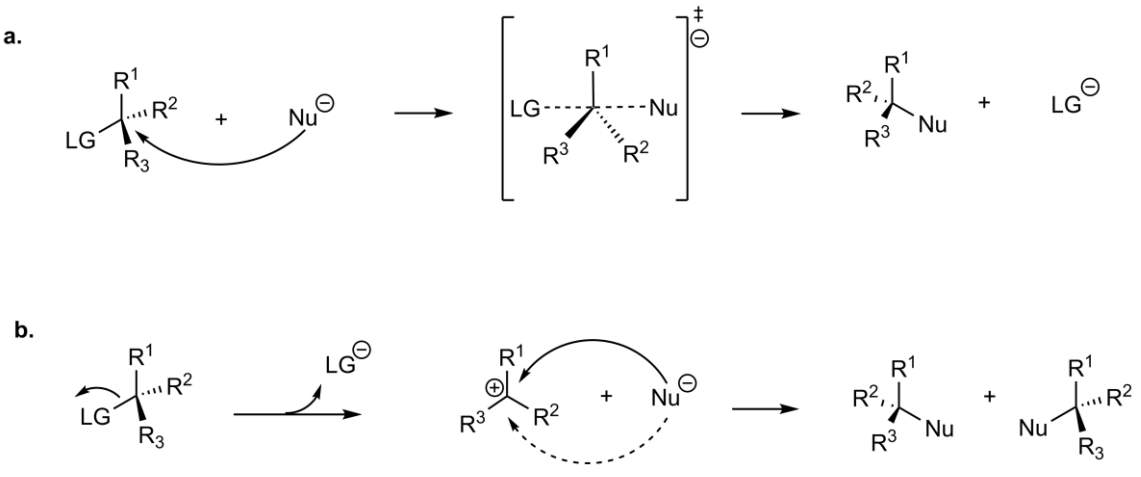

Scheme 8. *Nucleophilic substitution reaction mechanism. (a) S_N2 mechanism through a transition state involving both LG and Nu and leading to a racemic-pure product. (b) S_N1 mechanism through a plane carbocation what give to the nucleophile the chance to attack from the top (solid line) or from the bottom (dashed line) giving a racemic mixture as products.*

Both mechanisms are always in competition and the observed product will be that which was most favored by reaction conditions and reactant type. For example, a primary carbon substrate will react via S_N2 because a primary carbocation is not much stable. On the other hand, in tertiary carbon substrates we observe an S_N1 mechanism reaction since a tertiary carbocation is the most stable carbocation and the substrate center is too sterically hidden to undergo an S_N2 reaction. However, this is not so simple in all cases and more complicated scenarios have been described in the literature.[50,51]

1.3.4 Williamson ether synthesis

This reaction was discovered by Alexander Williamson in 1850.[52] To synthesize an ether, an alkyl halide reacts with an alkoxide ion as shown in Scheme 9.

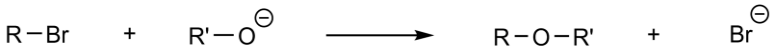

Scheme 9. *Model reaction in Williamson ether synthesis.*

The conventional method to prepare an alkoxide ion for this reaction is using sodium metal or sodium hydride (Scheme 10).

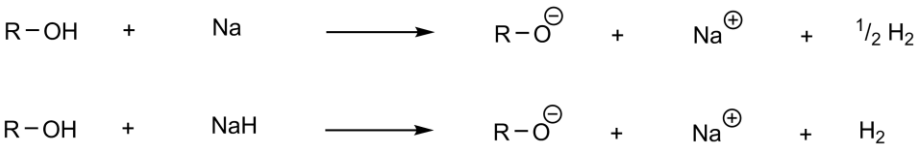

Scheme 10. *Conventional method to prepare an alkoxide ion.*

Williamson ether synthesis follows the S_N2 mechanism[37] explained in the previous section.

1.3.5 McMurry coupling

The McMurry coupling reaction is named after one of its discoverers, John McMurry.[53] However, this reaction was discovered simultaneously by three independent research groups. J. McMurry's, T. Mukaiyama's[54] and S. Tyrlik's[55] groups. This reaction is basically a reductive coupling of ketones and aldehydes to get olefins using low-valent titanium as a reagent (Scheme 11). The authors described different reagent systems: $TiCl_3/LiAlH_4$ (McMurry), $TiCl_4/Zn$ (Mukaiyama) and $TiCl_3/Mg$ (Tyrlik).

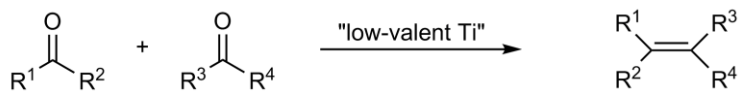

R^1, R^2, R^3, R^4 = H, alkyl or aryl

Scheme 11. *McMurry coupling reaction.*

Mukaiyama and Tyrlik systems are limited to aromatic cases whereas McMurry reagent can be also used with aliphatic substrates.[56] Some years later, a reagent system based on $TiCl_3$/Zn-Cu showed better results and with this reagent most couplings are now done. Afterwards, other different reagent systems were also described.[57]

We can consider McMurry coupling an important reaction in organic synthesis since many published synthetic procedures use it.[56,58,59]

The most accepted mechanism for the titanium catalyzed reaction is through pinacolate intermediates as it is shown in Scheme 12. However, other reaction mechanisms involving carbenoid intermediates when tungsten or molybdenum were used as reagents have been described in the literature.[56,60,61]

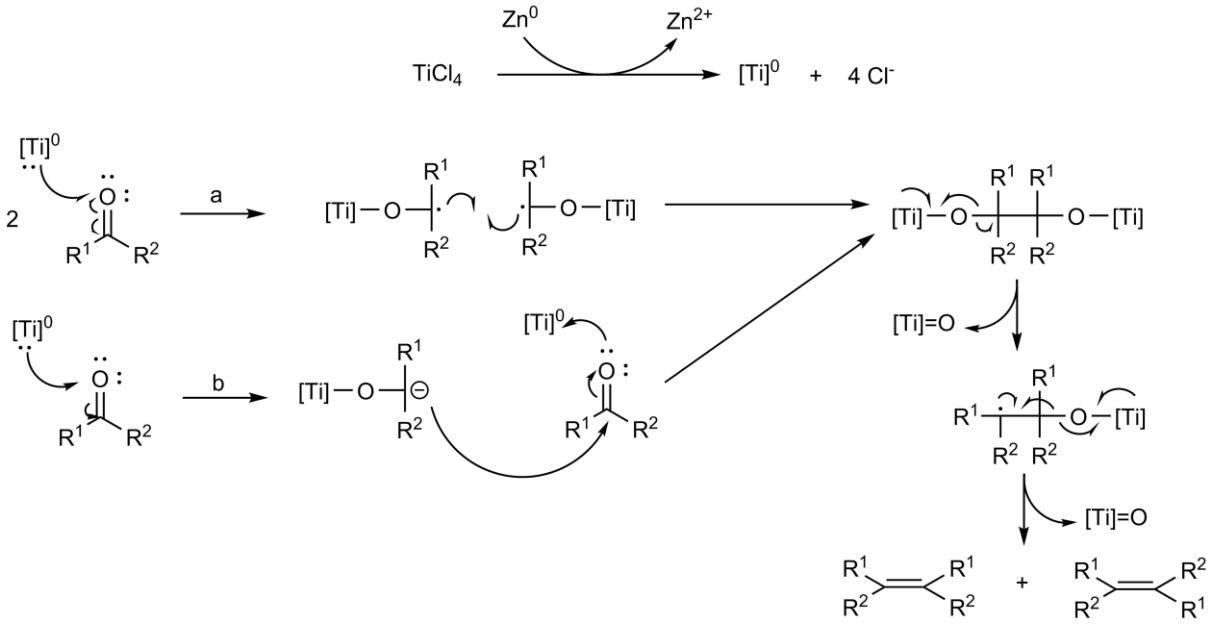

Scheme 12. *McMurry coupling reaction suggested mechanism mediated by titanium through Ti-pinacolate intermediate via 1 (a) or 2 (b) electron transfer.*

2. OBJECTIVES

The aim of this project, as its title suggests, is to synthesize, characterize and study a small library of stiff-stilbene based photo-switchable cyclic ethers with varying chain length, like those described in chapter 1.2 (Figure 4). Two parts form this project: synthesis of the target molecules and a photo-switching analysis of them in order to determine how much the differences of chain length affect photo-switching.

2.1 Synthesis of the target molecules

All targeted products are new compounds that have not been previously reported in the literature, neither have the products used as starting material in the last synthesis step. Thus, the synthesis route planned was based on previous projects of our research groups (Scheme 13) and some other routes described in the literature leading to similar compounds (Scheme 14).[31,62]

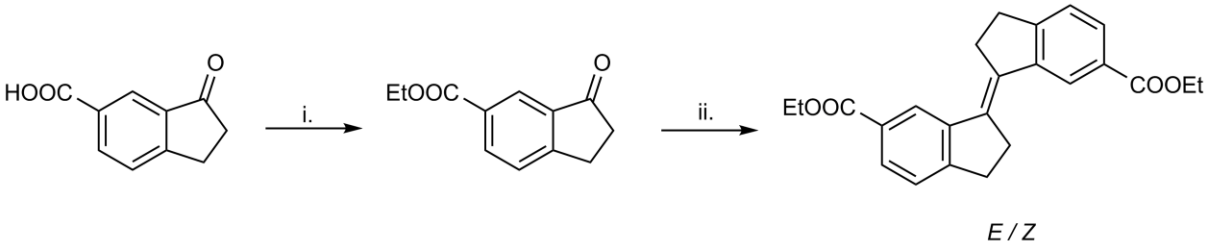

Scheme 13. *Synthetic route towards non-cyclic stiff-stilbene dimer reported by M. Blom;[31] (i) HCl conc. (1 mol eq.), ethanol, reflux 12 h; (ii) $TiCl_4$ (3 eq.), Zn powder (6 eq.), THF, reflux 12 h.*

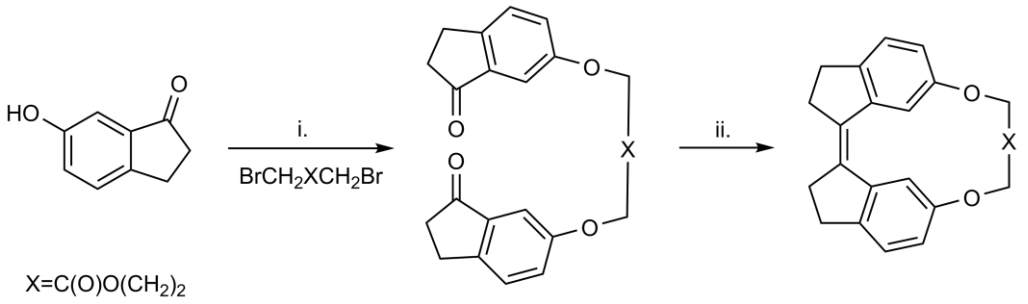

Scheme 14*. Synthetic route towards a similar compound reported by T. Kucharski ;[62] (i) TBAB (0.1 mol eq.), K_2CO_3 (2 eq.), DMF, 65-70 ˚C 12 h.; (ii) $TICl_4$ (6 eq.), Zn (12 eq.), THF, reflux 9 h.*

Di-ketone compounds are synthesized from 6-hydroxy-1-indanone via Williamson ether synthesis introducing the linker between the two indanone units using dibromoalkane analogues. After that, McMurry coupling is performed to reach the cyclic diethers. Kutcharski described the synthesis of compounds similar to our target molecules. They contained a disulfide moiety in the linker between the two aromatic rings of stiff-stilbene and were molecular force probes. Kutcharski's group determined the reaction rates when their compounds underwent reduction reactions to form di-thiol products.[62]

In order to synthesize 6-hydroxy-1-indanone several procedures have been described in the literature[63,64,65,66] starting from 3-(4-methoxyphenyl)propionic acid which is the main starting material available for this project. The designed synthetic route is presented in Scheme 2, section 1.2.1.

2.2 Photo-switching analysis

Once we have successfully prepared all the target molecules we will perform a photo-switching study. The aim of this study is to compare the different photo-switching behavior of the target molecules and to determine if it is related with the linker length between the two aromatics rings, i.e. to study how switching is affected by conformational strain (Figure 5). We will try to establish the limit, in terms of length, of the linker chain for this kind of systems. To achieve that, we will need to consider the strain caused because of the stiff-stilbene backbone isomerization from *Z* to *E* isomer.

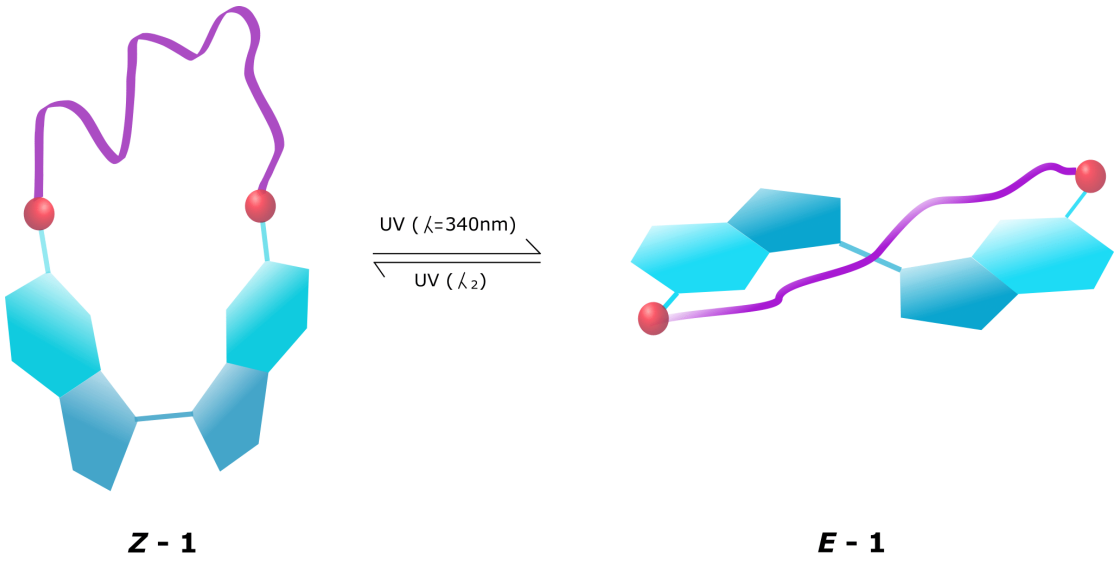

Figure 5. *Photo-isomerization of a model compound from isomer Z to E. It can be observed that in E isomers the linker chain is more stretched with respect to Z isomers which is the relaxed form.*

Firstly, we will analyze the UV-vis spectrum to determine which wavelength is the optimal to photo-isomerize the molecule. Then, we will irradiate each compound with UV light of that wavelength. The isomerization process will be followed by NMR and we also want to determine how the NMR-shifts for the protons in the chain are affected during the photo-switching process.

Some photo-switching studies of stiff-stilbene have been conducted previously and reported in literature[67,68] but not any study with the molecules involved in this project.

3. RESULTS AND DISCUSSION

In this chapter, the results of our project are presented. They are divided in two parts: Synthesis and Photo-switching study.

3.1 Synthesis

3.1.1 Synthesis of the target molecules

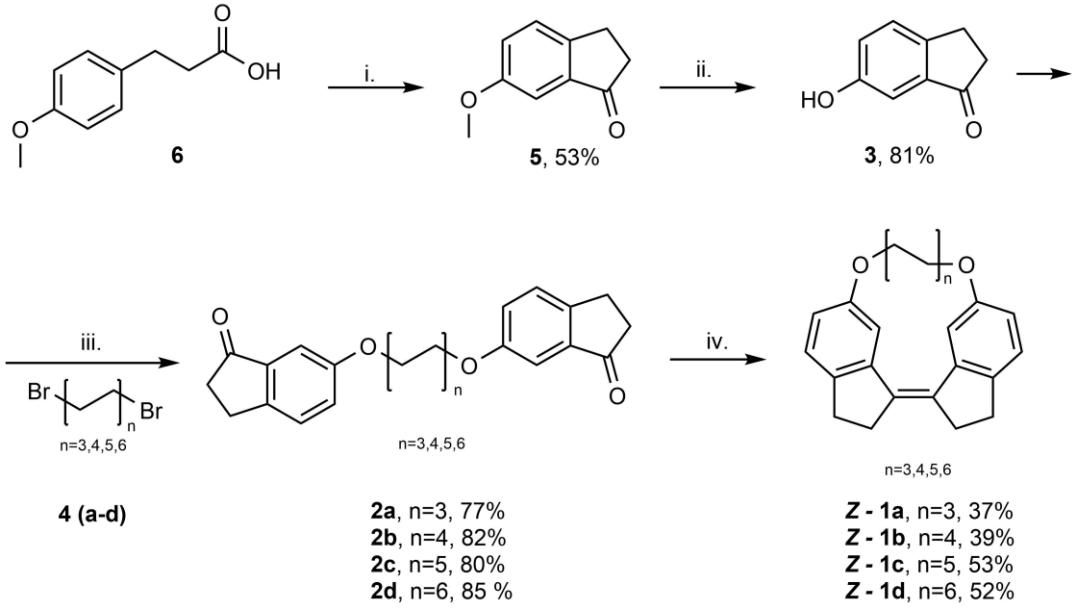

Scheme 15. *Synthetic route towards target molecules.* ***i.*** *(1) TfOH (3 eq.), DCM (dry), Ar-atm, MW (110 ˚C, 1h), (2) H_2O (0˚C).* ***ii.*** *(1) $AlCl_3$ (3 eq.), toluene (dry), Δ 1.5h, (2) H_2O.* ***iii.*** *(1) K_2CO_3 (4 eq.), TBAB (0.2 eq.), DMF (dry), Ar-atm, MW (150˚C, 20 min).* ***iv.*** *(1) $TiCl_4$ (3 eq.), Zn powder (6 eq.), THF, Δ 12h.*

Synthesis was performed as planned initially and divided into four steps (Scheme 15). The first step is a non-conventional intramolecular Friedel-Crafts acylation using methanesulfonic acid as a promoter instead of the typical $AlCl_3$. Brønsted acids have been used to promote Friedel-Crafts reactions as an alternative to $AlCl_3$ as described in literature.[69,70] The mechanism of this first reaction, scheme 16, differs slightly from that with $AlCl_3$ shown in scheme 3 in the first chapter. The procedure followed to carry out this reaction was described in literature[71] and also was the reaction mechanism of Friedel-Crafts acylation promoted by Brønsted acids (Scheme 16).[72]

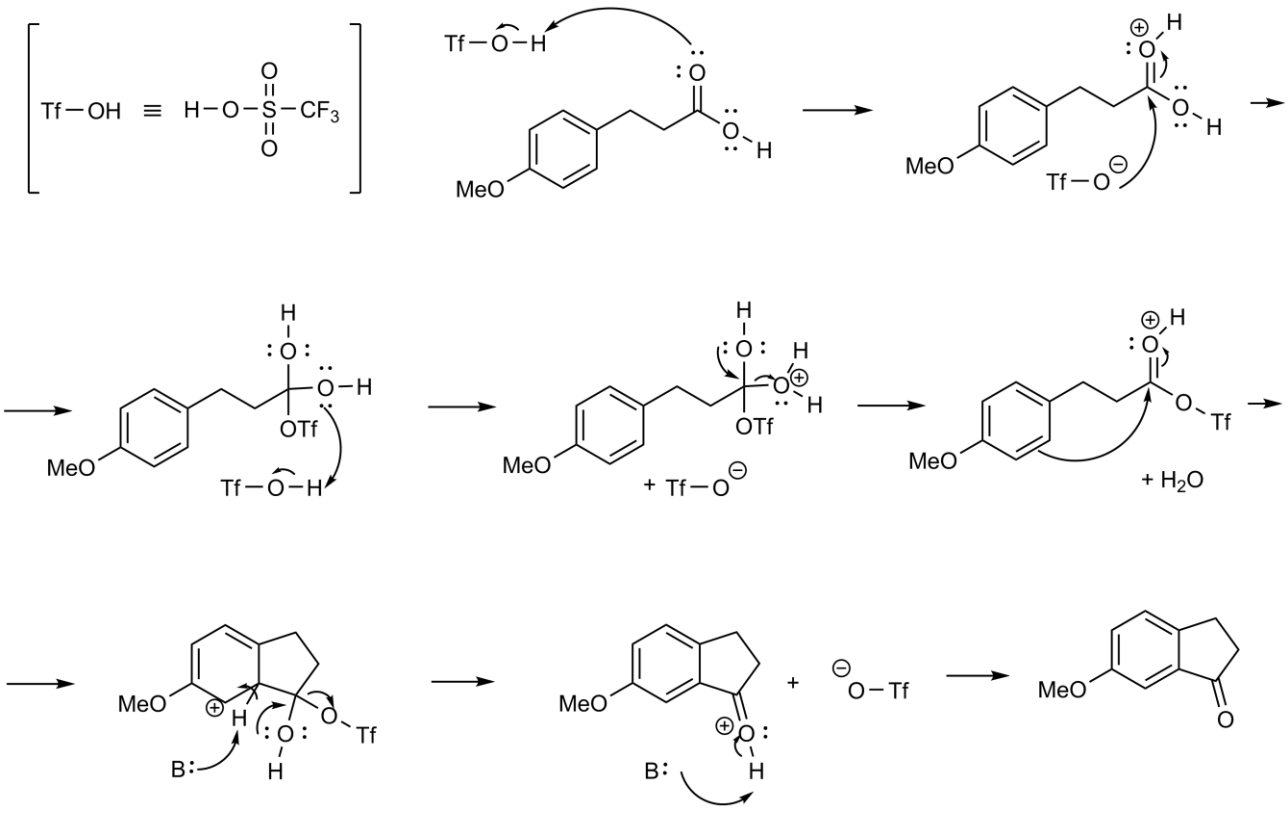

Scheme 16. *Friedel-Crafts acylation mechanism promoted by TfOH.*

The low yields obtained in this step can be explained by the intramolecular nature of the reaction. Since this reaction has been carried out in low solvent volume in MW vials, a high concentration of starting material favored intermolecular side reactions leading to some by-products. In a more diluted reaction mixture, intermolecular side reactions would have not been as numerous since reactant molecules would have been farther away from each other. This statement is supported by the first test reaction we performed where the initial reaction mixture was more diluted (six times) than later reactions and we obtained a yield of 90%. Thus, this reaction could be optimized further.

The second step, the de-methylation process, was performed following the procedure described by B. Wang[73] without significant problems.

Williamson ether synthesis was performed following a procedure described in literature[62] adapted to use the microwave reactor as a heating source. The reaction mechanism in our case is a bit different from that proposed in the first chapter. The reason is that a phenol is easier to deprotonate (pKa~10) than an aliphatic alcohol (pka~16),[37] thus a medium-strong base like potassium carbonate is enough to deprotonate it and sodium or sodium hydroxide are not necessary. Moreover, in this reaction the use of tetrabutylammonium bromide (TBAB) is necessary as a phase transfer catalyst to facilitate the solubility of salts (potassium carbonate) into the solution medium. We obtained yields about 80%.

Two different procedures in literature were tried for the last step reaction, McMurry coupling.[74,62] As we figured out that the second option was better, it was an easier procedure and better yields were obtained, we only followed the first procedure a couple of times. It is important to emphasize that this step is an intramolecular McMurry reaction, thus additional aspects had to be considered when this reaction was performed. To prevent the formation of intermolecular side products the starting material was added slowly by syringe pump to keep the concentration very low. These additions were performed overnight (12 h).

The McMurry reaction is a reductive coupling of ketones or aldehydes to get olefins and many reduction systems have been described in the literature over the years. We choose the $TiCl_4$/Zn which was reported to get compounds similar to our target molecules.[62] However, a reducing reagent system composed by $TiCl_3(DME)_{1.5}$ and Zn-Cu couple was reported by J. McMurry[75] as the best one giving yields from 80% to 97% even in intramolecular reactions. We have not used it because its preparation is complex taking several days and requiring argon atmosphere. But it can be investigated in future projects if the purposed goal is to improve this reactions yield.

3.1.2 Conversion study of McMurry coupling step

A conversion study of the McMurry coupling step was performed to determine the effect of the chain length on the yield of the reaction. To be sure that every compound reacts under the same conditions it was performed as an additional synthetic experiment where all the compounds react at the same time in the same flask. The relative composition of the crude reaction mixture was derived from a DOSY NMR spectrum. Results are shown in Table 1.

Table 1. *Results of the conversion study of McMurry coupling step.*

Entry	n[(a)]	Starting material mixture		Crude reaction mixture		Relative conversion[(b)]
		Reactant	mol%	Product	mol%	
1	3	**2a**	27.1	***Z* – 1a**	22.4	1
2	4	**2b**	24.0	***Z* – 1b**	21.1	1.1
3	5	**2c**	25.3	***Z* – 1c**	31.4	1.5
4	6	**2d**	23.6	***Z* – 1d**	25.1	1.3

(a) "n" is the number of (C_2H_4) units in the linker between stiff-stilbene backbone.
(b) This is not absolute conversion, but the relative conversion with respect to the lowest (n=3 linker length) one.

As initially expected, the compounds with the shortest linker have lower conversion. This could be explained by steric repulsion effects. In addition, the compound with the longest linker does not have the best conversion rate and could be because of entropic effects since a larger ring was formed.[76]

Nevertheless, these are preliminary results and more experiments have to be performed in order to confirm them.

3.1.3 Alternative synthetic procedures

The MW instrument was only accessible for part of the project. Since the procedures of the first and third step were based on this instrument we needed to find an alternative procedure and optimize it again. For the first step we tried different procedures from the literature.[77] These procedures are divided into two steps: Firstly, to synthesize an acyl chloride intermediate using $SOCl_2$ as reagent and then to obtain the compound 3 via a classical Friedel-Crafts acylation using $AlCl_3$ as it is shown in Scheme 17. However, several attempts have been made without success or with only poor yields (25%). Unsuccessful results can be explained by the high reactivity of acyl halides which could lead to a numerous by-products.

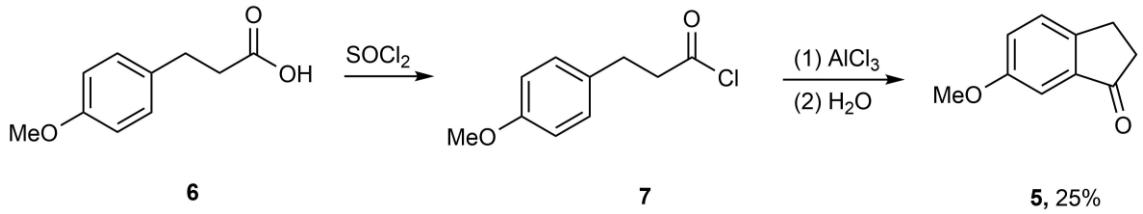

Scheme 17. *Alternative synthetic route towards compound 3.*

Afterwards, the initial procedure was used with an oil bath as heating source instead of the microwave instrument and similar results to the initial method, in terms of yield, were obtained.

In order to perform the third step reaction without microwave, a procedure similar to that followed initially was performed. Instead of using the microwave as a heating source, the reaction mixture was heated by means of regular reflux obtaining similar or better results in terms of yields. There is one disadvantage setting up a regular reflux system: a large volume of DMF is needed (30-50 ml) and a better and longer work-up is needed afterwards to get rid of all the DMF.

3.1.4 Synthesis of other compounds

1,8-Dibromooctane had to be prepared because only 1,8-octanediol was available as starting material in our lab. Synthesis followed a procedure described in the literature[78] without any problem (Scheme 18). This reaction follows the conventional S_N2 mechanism explained in chapter 1. The mono-brominated product could have been the main by-product obtained in this reaction if we had not left refluxing long enough, but in our case it was not detected.

Scheme 18*. Synthetic route to 1,8-octanediol*

3.2 Photo-switching analysis

A preliminary photo-switching study was conducted. The isomer synthesized was the *Z* one. It was determined by NMR spectroscopy since some signals are different in *Z* and *E* isomers. M. Bloom described these signal changes when a similar compound underwent photo-isomerization and assigned them to the different isomers by NOESY.[31] A NOESY study can be performed in the future to verify this.

Firstly, a UV-vis spectrum of each compound was obtained in order to determine the irradiation wavelength. Then, photo-isomerization from the *Z* isomers to the *E* ones was performed. Times stated in this report might be longer than real ones as the lamp used is suspected to be at the end of its lifetime. The photo-isomerization was followed by NMR spectroscopy. Decomposition was observed when our compounds were irradiated with non-selective wavelength.

3.2.1 Stiff-stilbene

Firstly, a photo-switching study of stiff-stilbene was performed. Photo-isomerization course from *E* to *Z* isomers was followed by UV-vis spectroscopy (Figure 6) and by NMR spectroscopy (Figure 7). The sample was irradiated with UV light of 340 nm wavelength

UV-vis spectrum shows two clear isobestic points which means that a clean photo-isomerization reaction happened without any simultaneous side reactions. Moreover, times are shorter than those stated when photo-isomerization was followed by NMR since much lower concentration is needed for UV-vis spectroscopy and the photo-isomerization process depends on the sample concentration.

NMR spectrum shows proton signal shifts when stiff-stilbene was photo-isomerized from *E* to *Z* isomer.

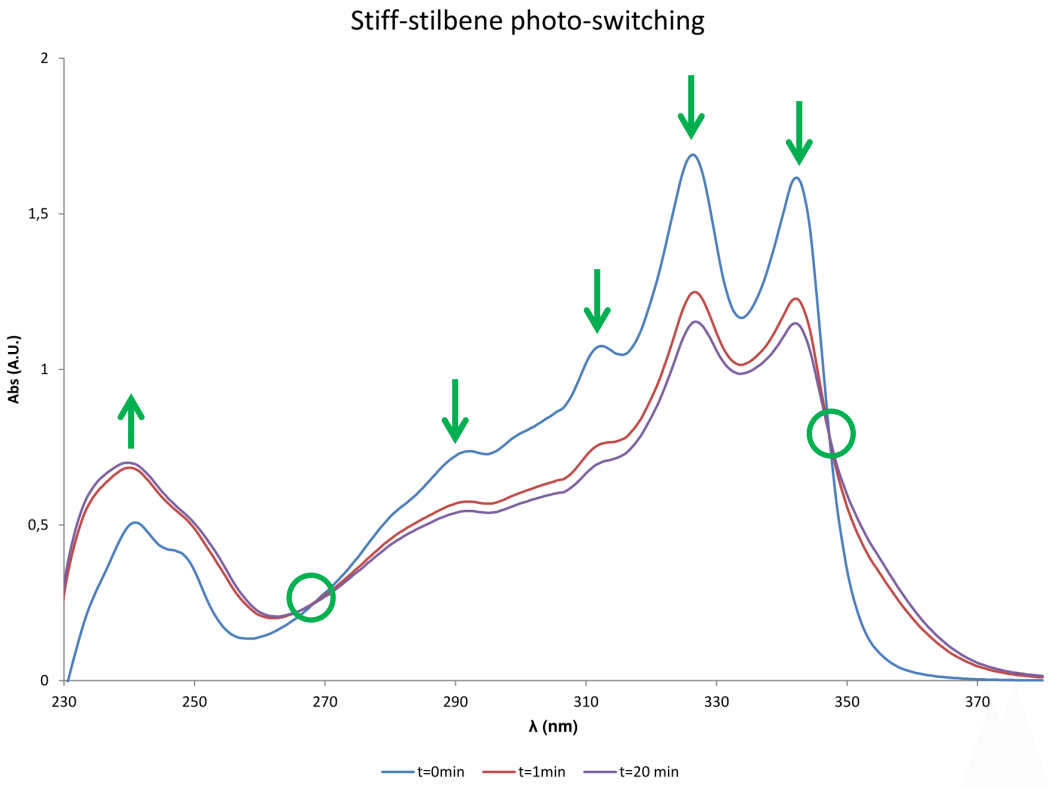

Figure 6. *Photo-isomerization process of stiff-stilbene followed by UV-vis spectroscopy.*

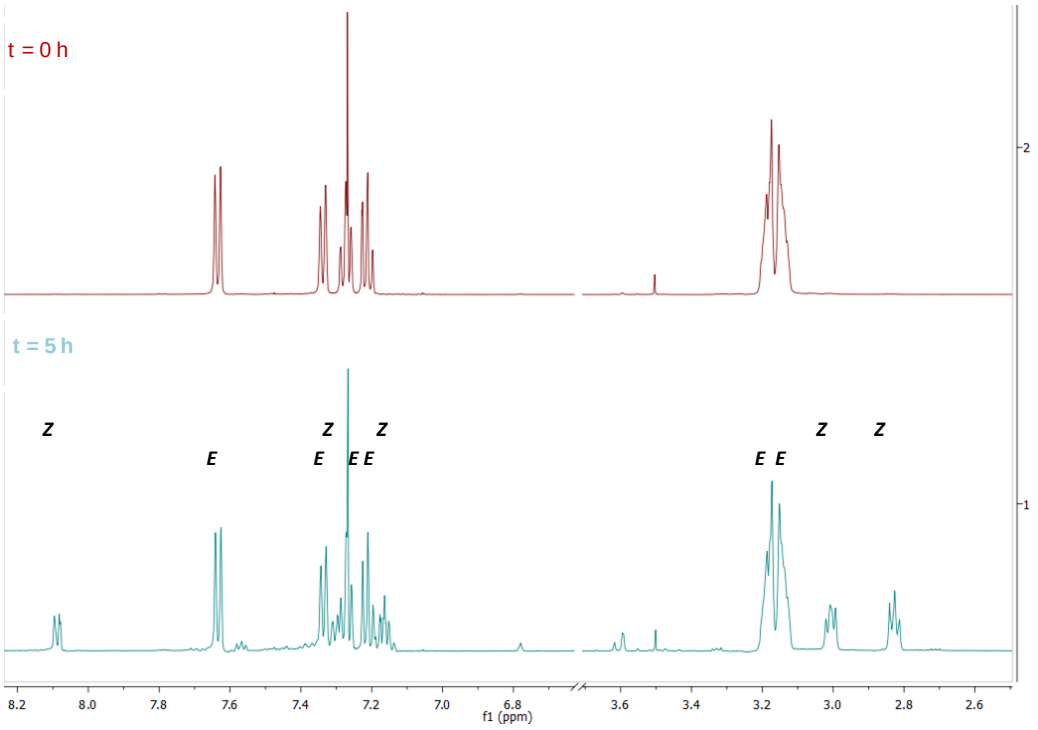

Figure 7. *Photo-isomerization process of stiff-stilbene followed by NMR spectroscopy.*

3.2.2 Compound Z-1a

Compound *Z*-1a almost did not show any photo-isomerization. The NMR spectrum showed little change after 7 hours of UV light radiation (360 nm). We have calculated a 2% conversion to isomer *E* from the NMR spectrum. This is the expected result as it is the molecule with the shortest linker and the *E* isomer is the most stretched. The irradiation course followed by NMR is shown in figure 8 and figure 9.

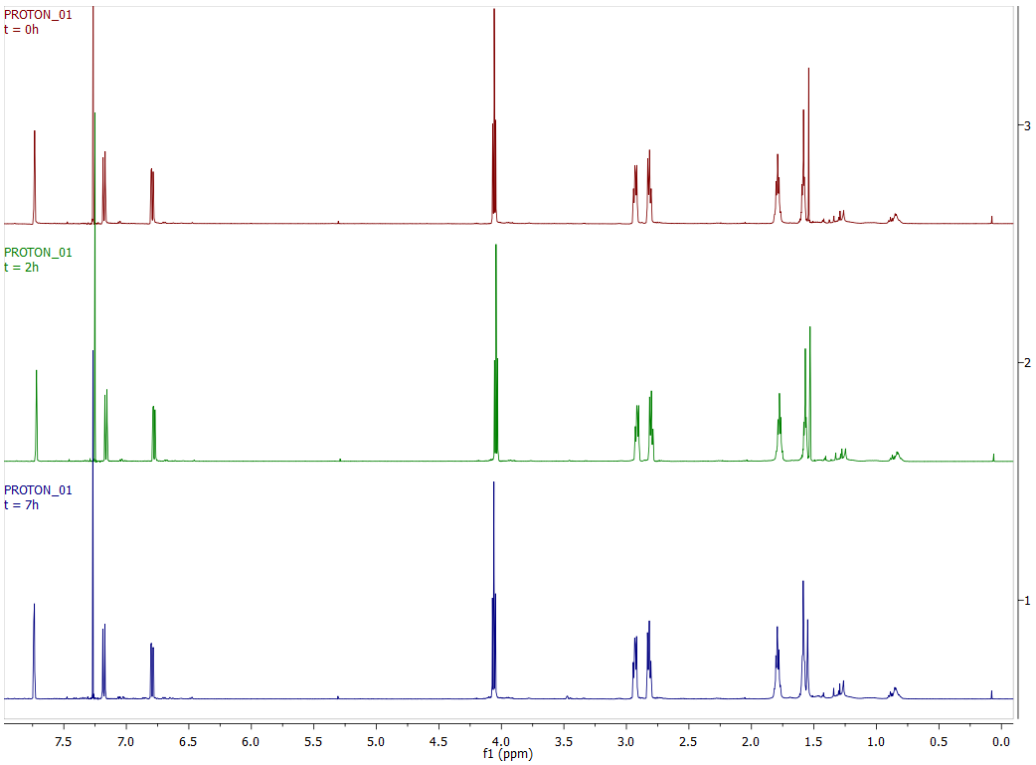

Figure 8. *Photo-isomerization process of compound Z-1a followed by NMR. Initial sample (top), after 2h (middle) and after 7h (bottom).*

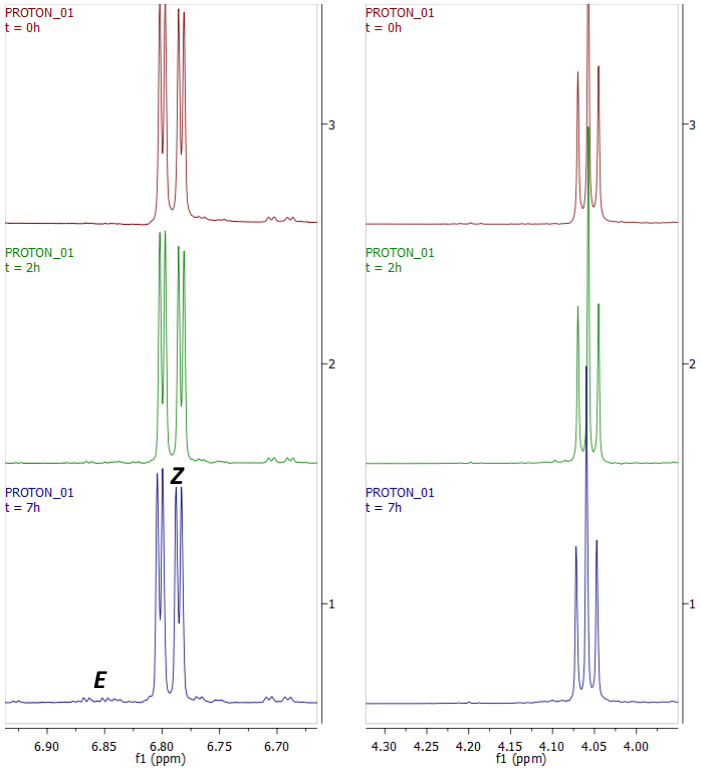

Figure 9. *Expansions of NMR spectra of figure 8 showing an aromatic proton shift (left) and the signals corresponding to the hydrogens bonded to the first carbon of the linker between the two aromatic rings of stiff-stilbene (right).*

3.2.3 Compound Z-1b

Although compound *Z*-1b was irradiated almost nine hours with UV light (λ=340nm), few changes were observed in the NMR spectra. After 5 hours, it had reached the stationary isomerization mixture corresponding to 8% conversion from isomer *Z* to *E*. Moreover, the sample was left overnight without light and no changes were observed in the NMR spectrum which suggests that these compounds are thermally stable. The isomerization course followed by NMR can be seen in figure 10 and figure 11.

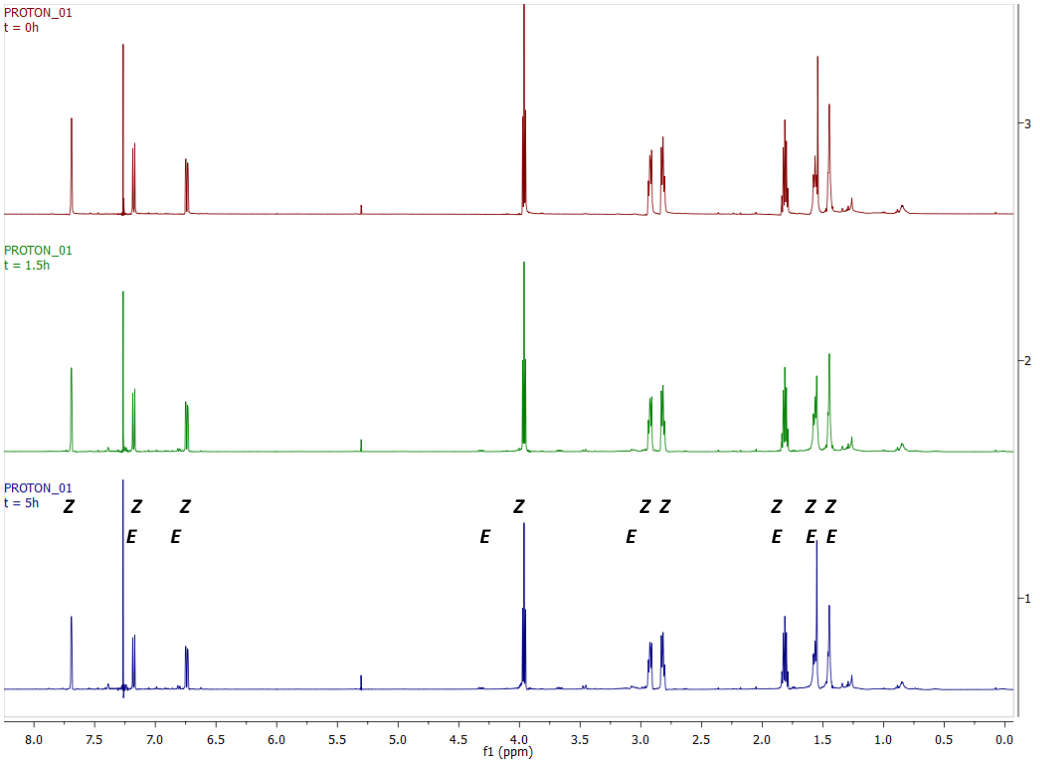

Figure 10. *Photo-isomerization process of compound Z-1b followed by NMR. Initial sample (top), after 1.5h (middle) and after 5h (bottom).*

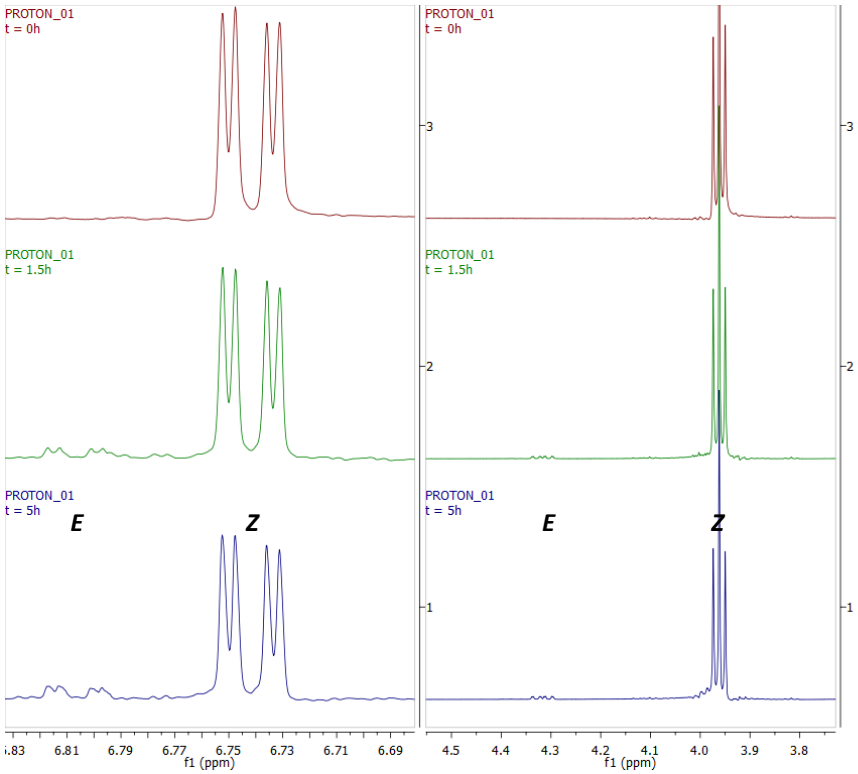

Figure 11. *Expansions of NMR spectra of figure 10 showing an aromatic proton shift (left) and the signals corresponding to the hydrogens bonded to the first carbon of the linker between the two aromatic rings of stiff-stilbene (right).*

3.2.4 Compound Z-1c

Compound Z-1c was irradiated with UV light of 340nm. After 10.5h irradiation of the sample, the stationary isomerization mixture was reached. A conversion of 19% from *Z* to *E* isomers was obtained. This compound shows a better conversion rate than the ones with shorter linkers (1a, 1b). In figure 12 and figure 13 the isomerization process followed by NMR spectroscopy is shown.

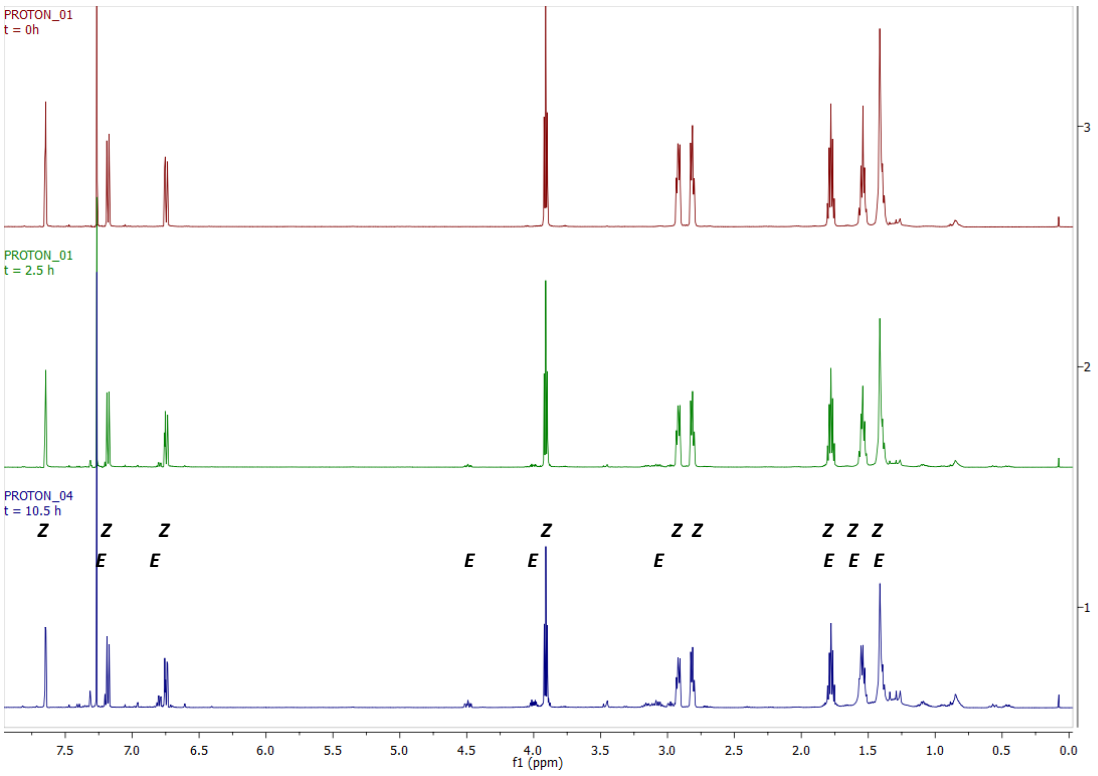

Figure 12. *Photo-isomerization process of compound Z-1c followed by NMR. Initial sample (top), mixture composition after 2.5h (middle) and after 10.5h (bottom).*

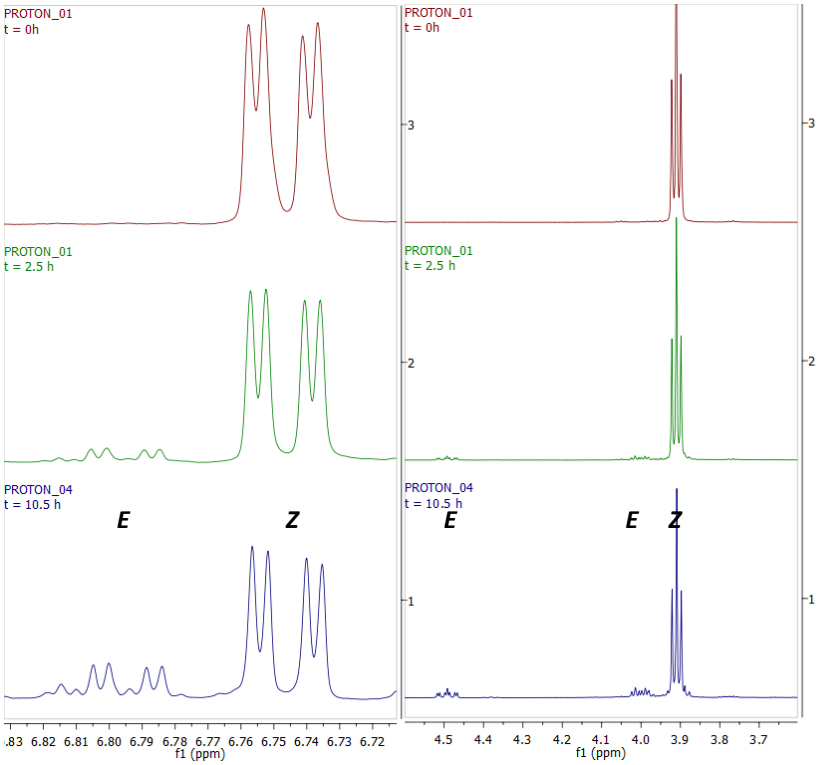

***Figure 13**. Expansions of NMR spectra of figure 12 showing an aromatic proton shift (left) and the signals corresponding to the hydrogens bonded to the first carbon of the linker between the two aromatic rings of stiff-stilbene (right).*

3.2.5 Compound Z-1d

Compound Z-1d was irradiated with UV light, first with 340nm and, after 5h, with 360nm. It showed the same behavior when it was irradiated by 340nm and 360nm as we expected studying the UV-vis spectrum (Appendices, Figure 89). The stationary isomerization mixture was reached after 10 hours irradiating the sample. A conversion of 38% from *Z* to *E* isomers was obtained. It was the best conversion rate obtained with our target molecules. In previous projects of our group it was described a 55% conversion rate in isomerization processes of similar acyclic compounds, i.e. less restricted. Thus, the conversion rate we obtained has to be considered good. In figure 14 and figure 15 the isomerization process followed by NMR spectroscopy is shown.

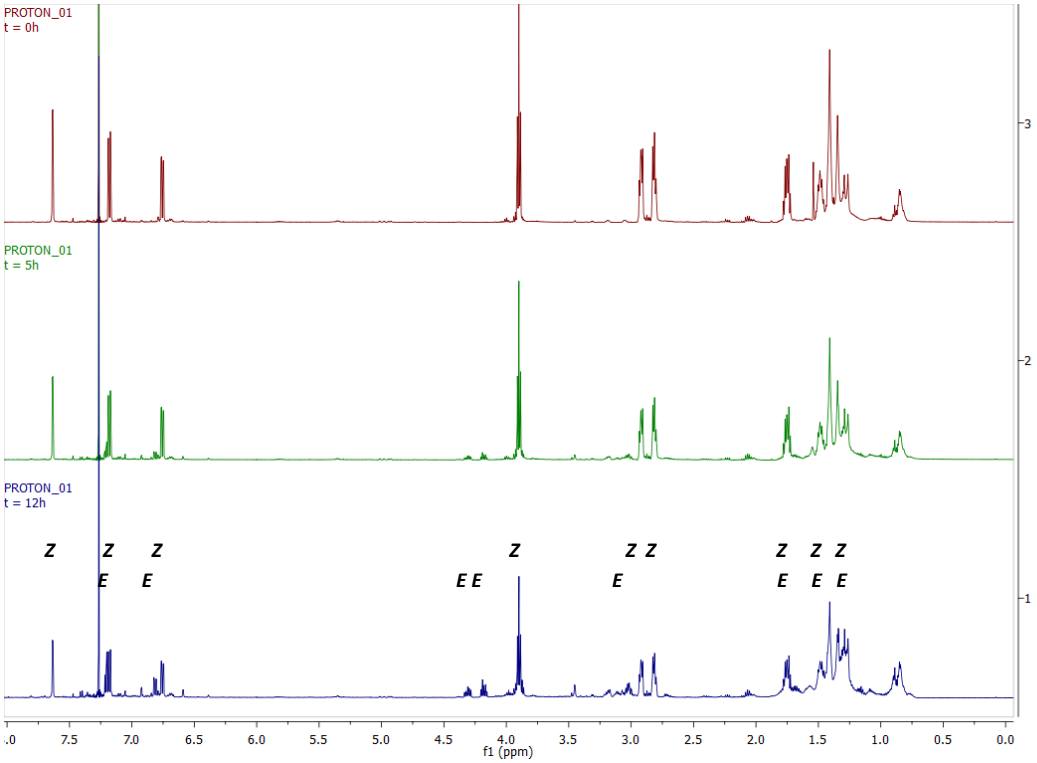

Figure 14. *Photo-isomerization process of compound Z-1d followed by NMR. Initial sample (top), mixture composition after 5h (middle) and after 12h (bottom).*

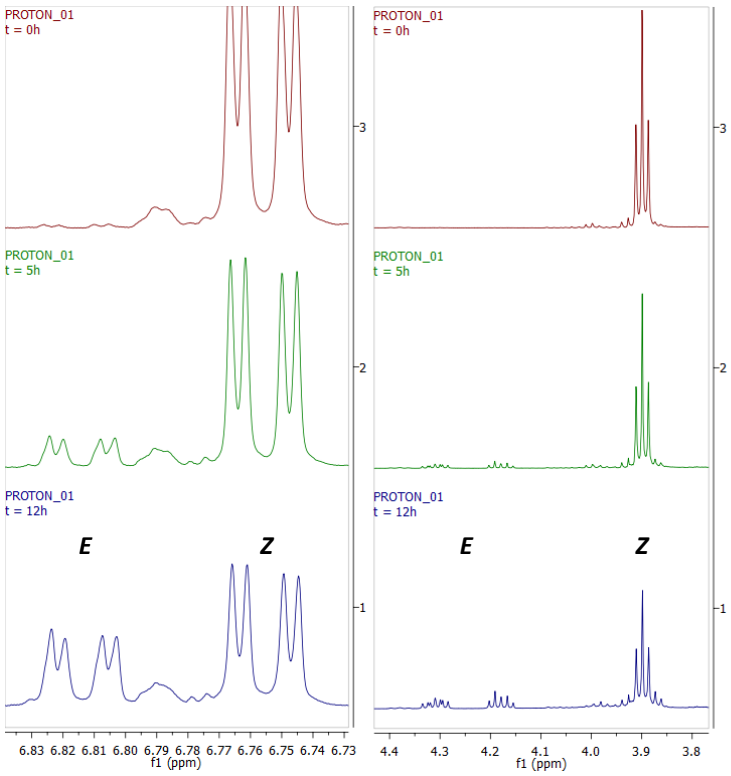

Figure 15. *Expansions of NMR spectra of figure 14 showing an aromatic proton shift (left) and the signals corresponding to the hydrogens bonded to the first carbon of the linker between the two aromatic rings of stiff-stilbene.(right).*

3.2.6 Study summary

A summary of the photo-switching results is presented in Table 2.

Table 2. *Results of photo-switching analysis.*

Entry	Compound	n[(a)]	Photo-stationary mixture (*Z*:*E*)	Photo-isomerization conversion [%] [(b)]	Photo-switchable
1	**1a**	3	50 : 1	2%	-
2	**1b**	4	11 : 1	8 %	+/-
3	**1c**	5	4.2 : 1	19 %	+
4	**1d**	6	1.6 : 1	38 %	+

(a) "n" is the number of (C_2H_4) units in the linker between stiff-stilbene backbone.
(b) Conversion of the photo-isomerization process to the *E*-isomer.

The photo-stationary mixture compositions shown in Table 2 are represented in Figure 16. It can be clearly seen that the longer the linker, the higher the isomerization rate obtained. In addition, in Figure 16 is represented as a reference the photo-stationary mixture composition of a diether acyclic similar compound studied in a previous project of our research group (Figure 17).

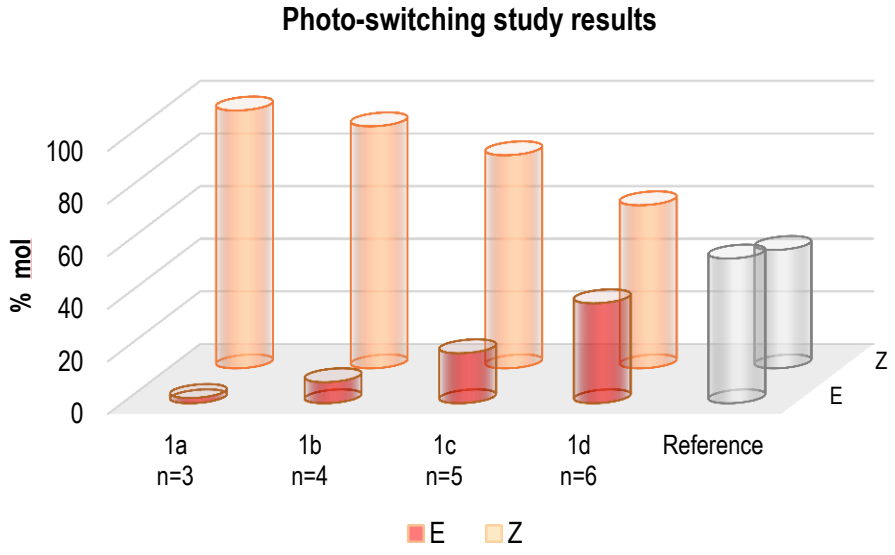

Figure 16. *Diagram representing the photo-switching study results.*

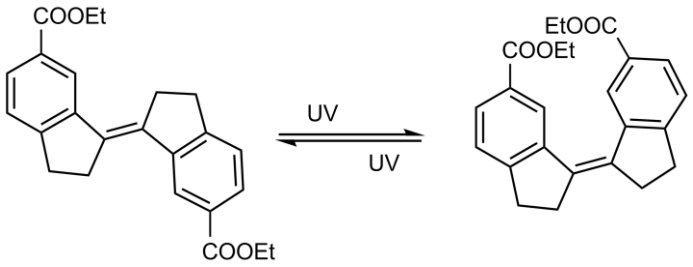

Figure 17. *Photo-isomerization of an acyclic diether compound similar to our target molecules. A photo-isomerization study of it was performed in previous projects of our group.*

3.2.7 Decomposition

Stiff-stilbene was irradiated with non-selective wavelength UV light, i.e. without filter. Photo-isomerization was speeded up since more energy was provided to the stiff-stilbene molecules. However, when our target molecules were irradiated with non-selective wavelength, they showed decomposition after 1 hour of irradiation (Figure 18).

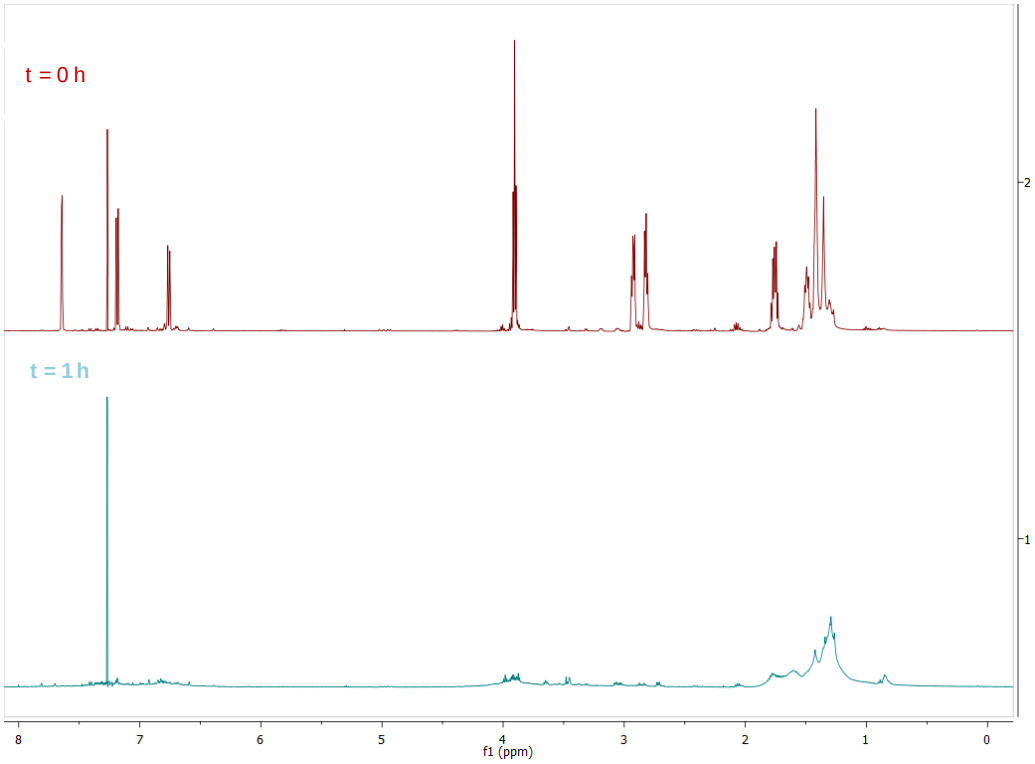

Figure 18. *NMR spectrum of compound Z-1a before (top) and after (bottom) 1 hour of irradiation with non-selective wavelength UV-light.*

4. CONCLUSIONS AND OUTLOOK

The aim of this project was to design and optimize a synthetic route towards the target molecules and, once synthesized, study its photo-switching behavior. The designed target molecules aim to simplify stiff-stilbene cyclic systems which have many applications related with their photo-switching ability. They were designed to study the limits to photo-switching related to the chain length. Thus, a study of this capacity would have a great significance for people who work with this system.

A good synthetic route to the target molecules was found in the first part of this project obtaining moderate to good yields. All the target molecules were synthesized. *However, a further optimization of this route, especially the first and last steps, could be possible and it will be discussed in future projects. A NOESY analysis will also be performed in order to verify that the synthesis lead to the Z-isomer only.*

Conversion study of McMurry coupling step shows that the best compound for this step is the one with ten-carbon length linker. Compounds with shorter linkers (six and eight carbons) showed lower conversion rates probably because of steric repulsion effects. The compound with the longest linker length (twelve carbons) also showed a lower conversion rate. In this case, we form a larger ring and a lower conversion rate could be explained by entropy effects. *The same study can be performed in a future if another catalyst system is tested in the McMurry reaction step to compare the behavior of the different reagent systems. It will also be repeated using the same reagent system to statistically confirm the obtained results.*

A preliminary photo-switching study was performed on compounds *Z*-1a, *Z*-1b, *Z*-1c and *Z*-1d. Compound *Z*-1a showed almost no conversion. Compound *Z*-1b showed low photo-switching activity since the conversion rate to the *E* isomer was only 8%. Isomers *Z*-1c and *Z*-1d gave higher conversion rates (19% and 38% respectively). The photo-isomerization course was followed successfully by NMR spectroscopy, which shows that it is an important characterization tool. It was demonstrated that the linker length between the two aromatic rings of stiff-stilbene is directly related with photo-switching properties of these cyclic compounds. However, an exact limit of the minimum linker length to make the molecule able to undergo photo-switching can not be stated since above 6 carbon length all molecules showed gradually incremented photo-isomerization activity. *An in-depth photo-switching study should be conducted in future projects in order to obtain more accurate data of the photo-isomerization processes, calculating, for instance, quantum yields.*

*Furthermore, in future projects, DFT calculations of the compounds **1** can be done in order to determine structural energies of both isomers and whether the photo-isomerization from Z to E is favorable or not. We expect that we will be able to correlate the energies to the linker length.*

The final stage will be to separate the isomer E from the mixture Z:E and perform a conformational analysis of both isomers by means of NAMFIS analysis.

5. EXPERIMENTAL

5.1 General

Starting materials, solvents and reagents were commercially available and used without further purification except dichloromethane, ethyl acetate, pentane, tetrahydrofuran and toluene that were distilled before use. N,N-dimethylformamide was used as supplied (biotech. grade, ≥ 99.9%). Unless stated differently, all reactions were carried out under atmospheric pressure and with argon atmosphere. Microwave heating was carried out in a Biotage+ Initiator microwave instrument using 10-20 ml Biotech MW vials, applying MW irradiation at 2.45 GHz, with a power setting up to 40 W and an average pressure of 4-5 bar when DCM was the solvent and 90 W / 1 bar when it was DMF. Analytical TLC was performed using Merck precoated silica gel 60 F_{254} plates and visualized with UV light and Hannessian´s stain (5% ammonium molybdate, 1% cerium sulfate and 10% sulfuric acid in water). Flash chromatography was done over Matrex silica gel (60 Á, 35-70 μm) on a regular column or on Revelis X2 Flash Chromatography System, GRACE.

^{1}H and ^{13}C NMR spectra were recorded on Varian Mercury Plus (^{1}H at 300.03 MHz), Agilent MR (^{1}H at 399.98 MHz, ^{13}C at 100.58 MHz) or Varian Unity Inova (^{1}H at 499.94 MHz) spectrometers at 25˚C. Chemical shifts (δ) are reported in ppm referenced indirectly to tetramethylsilane using the residual solvent signal ($CDCl_3$, ^{1}H at 7.26 and ^{13}C at 77.0 ppm) as internal standard. Signal assignments were derived from ^{1}H, ^{13}C, gCOSY,[39,40] gTOCSY,[41] gHSQC[42] and gHMBC[43] spectra.

Mass spectra were obtained on an Advion Expression-L CMS with APCI+ interface.

UV-vis spectra were recorded on a Shimadzu UV-1650PC spectrophotometer using 10mm quartz cuvettes. Photo-isomerizations were performed using an Oriel 1000 W Xe ARC light source equipped with a band pass filter 20BPF10-340 or 20BPF10-360.

5.2 Synthetic procedures

5.2.1 Synthesis of 6-methoxyindan-1-one, 5 (assisted by MW)

Compound **6** (2.523 g, 14.0 mmol) was dissolved in dry DCM (10 ml) in a flame-dried MW vial and cooled in ice-bath. TfOH (3.7 ml, 41.9 mmol) was added dropwise. The vial was sealed, put under argon and heated in the MW to 110˚C, 5 bar, for 1 h. The reaction mixture was poured on ice. The water phase was extracted three times with DCM (3x100 ml). The combined organic phases were dried over $MgSO_4$ and solvent was removed by rotary evaporation. The crude product was purified by CC (pentane/EtOAc 1:0 to 1:4). The solvent was evaporated, giving a light yellow solid, 1.204 g, 53% yield. **^{1}H NMR** ($CDCl_3$, 500 MHz): δ = 7.37 (m, 1H, Ar-*H*), 7.20 (m, 1H, Ar-*H*), 7.18 (m, 1H, Ar-*H*), 3.84 (s, 3H, O*CH*$_3$), 3.07 (m, 2H, C*H*$_2$CH$_2$CO), 2.72 (m, 2H, C*H*$_2$CO). **^{13}C NMR** ($CDCl_3$, 100.6 MHz): δ = 207.0 (*C*O), 159.4 (*C*-OCH$_3$), 148.0 (C, Ar), 138.2 (C, Ar), 127.3 (CH, Ar), 124.0 (CH, Ar), 104.9 (CH, Ar), 55.6 (O*C*H$_3$), 37.0 (*C*H$_2$CO), 25.1 (*C*H$_2$CH$_2$CO). **APCI-MS:** *m/z* calcd. for $C_{10}H_{10}O_2$, $[M+H]^+$: 163; found: 163. In agreement with literature.[77]

5.2.2 Synthesis of 6-methoxyindan-1-one, 5 (alternative procedure)

Compound **6** (2.551 g, 14.2 mmol) was dissolved in dry DCM (10 ml) in a flame-dried MW vial and cooled in ice-bath. TfOH (3.8 ml, 43.0 mmol) was added dropwise. The vial was sealed, put under argon and heated in oil bath to 110ºC, 5 bar, for 1.5 h. The reaction mixture was poured on ice. The water phase was extracted three times with DCM (3x100 ml). The combined organic phases were dried over $MgSO_4$ and solvent was removed by rotary evaporation. The black crude product was purified by CC (pentane/EtOAc 1:0 to 1:4). The solvent was evaporated, giving a light yellow solid, 1.192 g, 52% yield. Characterization data is described in the previous section in agreement with literature.[77]

5.2.3 Synthesis of 6-hydroxyindan-1-one, 3

Compound **5** (1.367 g, 8.4 mmol) and $AlCl_3$ (3.483 g, 26.1 mmol) were dissolved in dry toluene (50 ml) and refluxed for 1.5 h. The reaction was cooled to RT. H_2O (70 ml) was added and the organic phase collected. The water phase was extracted three times with EtOAc (3x50 ml). The combined organic phases were washed with brine two times (2x75 ml) and dried over $MgSO_4$. The solvent was removed by rotary evaporation. The orange crude product was purified by CC (pentane/EtOAc 1:0 to 1:4). The solvent was evaporated, giving a light orange solid, 1.103 g, 81% yield. **^{1}H NMR** ($CDCl_3$, 500 MHz): δ = 7.36 (d, *J* = 8.3 Hz, 1H, Ar-*H*), 7.22 (d, *J* = 2.4 Hz, 1H, Ar-*H*), 7.16 (dd, *J* = 2.4, 8.3 Hz, 1H, Ar-*H*), 5.67 (bp s, 1H, O*H*), 3.08 (m, 2H, C*H*$_2$CH$_2$CO), 2.73 (m, 2H, C*H*$_2$CO). **^{13}C NMR** ($CDCl_3$, 100.6 MHz): δ = 207.4 (*C*O), 155.4 (*C*-OH), 147.8 (C, Ar), 138.3 (C, Ar), 127.6 (CH, Ar), 123.4 (CH, Ar), 108.7 (CH, Ar), 37.0 (*C*H$_2$CO), 25.1 (*C*H$_2$CH$_2$CO). **APCI-MS**: *m/z* calcd. for $C_9H_8O_2$, $[M+H]^+$: 149; found: 149. In agreement with literature.[79]

5.2.4 General procedure A: Williamson ether synthesis (assisted by MW)

Compound **3** (2 eq.), dibromoalkane **4** (1 eq.), TBAB (0.2 eq.) and K_2CO_3 (4 eq.) were dissolved in dry DMF (15 ml) in a flame-dried MW vial. The vial was sealed, put under argon and heated in the MW to 150˚C for 15 min (the reaction was followed by NMR). The reaction mixture was cooled to RT and poured on DCM (40 ml), filtered and washed with water four times (4 x 50 ml) and brine three times (3x 50 ml). The organic phase was dried over $MgSO_4$ and solvent removed by rotary evaporation. The product was dried under high vacuum overnight.

5.2.5 General procedure B: Williamson ether synthesis (alternative procedure)

Compound **3** (2 eq.), dibromoalkane **4** (1 eq.), TBAB (0.4 eq.) and K_2CO_3 (6 eq.) were dissolved in dry DMF (35 ml) and refluxed for 1 h. The reaction mixture was cooled to RT and poured on DCM (100 ml), filtered and washed with water four times (4 x 100 ml) and brine three times (3x 100 ml). The organic phase was dried over $MgSO_4$ and solvent removed by rotary evaporation. The product was dried under high vacuum overnight.

5.2.6 Synthesis of 6-[2-(3-oxoindan-5-yl)oxyhexoxy]indan-1-one, 2a

The synthesis followed General procedure A with compound **3** (0.201 g, 1.4 mmol) and 1,6-dibromohexane **4a** (0.11 ml, 0.7 mmol) as starting materials, giving a brown solid which was sufficiently pure for subsequent steps, 0.176 g, 69% yield. **^{1}H NMR** ($CDCl_3$, 500 MHz): δ = 7.36 (m, 2H, H-7), 7.20-7.16 (m, 4H, H-4 H-6), 4.00 (t, *J* = 6.6 Hz, 4H, C*H*$_2$-1'), 3.07 (m, 4H, C*H*$_2$-1), 2.72 (m, 4H, C*H*$_2$-2), 1.84 (m, 4H, C*H*$_2$-2'), 1.54 (m, 4H, C*H*$_2$-3'). **^{13}C NMR** ($CDCl_3$, 100.6 MHz): δ = 207.1 (C, C-3), 158.8 (C, C-5), 147.8 (C, C-3a), 138.2 (C, C-7a), 127.3 (CH, C-7), 124.4 (CH, C-6), 105.6 (CH, C-4), 68.2 (CH_2, C-1'), 37.0 (CH_2, C-2), 29.0 (CH_2, C-2'), 25.8 (CH_2, C-3'), 25.1 (CH_2, C-1). **APCI-MS**: *m/z* calcd. for $C_{24}H_{26}O_4$, $[M+H]^+$: 379; found: 379. **UV-vis** (CH_2Cl_2) λ_{max}: 320, 249 nm. Not previously reported.

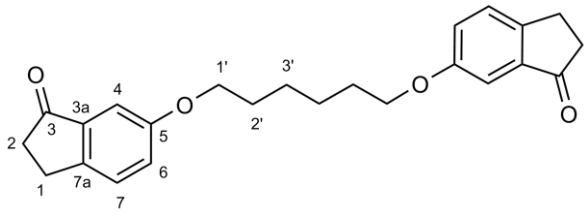

Figure 19**. Product **2a

Alternatively, the synthesis followed General procedure B with compound **3** (0.364 g, 2.5 mmol) and 1,6-dibromohexane **4a** (0.19 ml, 1.2 mmol) as starting materials, giving a red solid which was sufficiently pure for subsequent steps, 0.417 g, 77% yield (calculated from ^{1}H NMR spectrum).

5.2.7 Synthesis of 6-[2-(3-oxoindan-5-yl)oxyoctoxy]indan-1-one, 2b

The synthesis followed General procedure A with compound **3** (0.115 g, 0.8 mmol) and 1,8-dibromooctane **4b** (0.07 ml, 0.4 mmol) as starting materials, giving an orange solid which was sufficiently pure for subsequent steps, 0.121 g, 78% yield. **^{1}H NMR** ($CDCl_3$, 500 MHz): δ = 7.36 (m, 2H, H-7), 7.20-7.16 (m, 4H, H-4 H-6), 3.98 (t, *J* = 6.6 Hz, 4H, C*H*$_2$-1'), 3.06 (m, 4H, C*H*$_2$-1), 2.71 (m, 4H, C*H*$_2$-2), 1.80 (dt, *J* = 6.6, 14.8 Hz, 4H, C*H*$_2$-2'), 1.47 (m, 4H, C*H*$_2$-3'), 1.40 (m, 4H, C*H*$_2$-4'). **^{13}C NMR** ($CDCl_3$, 100.6 MHz): δ = 207.1 (C, C-3), 158.8 (C, C-5), 147.8 (C, C-3a), 138.2 (C, C-7a), 127.3 (CH, C-7), 124.4 (CH, C-6), 105.6 (CH, C-4), 68.3 (CH_2, *C*-1'), 37.0 (CH_2, *C*-2), 29.2 (CH_2, *C*-4'), 29.1 (CH_2, *C*-2'), 25.9 (CH_2, *C*-3'), 25.1 (CH_2, *C*-1). **APCI-MS**: *m/z* calcd. for $C_{26}H_{30}O_4$, $[M+H]^+$: 407; found:407. **UV-vis** (CH_2Cl_2) λ_{max}: 320, 249 nm. Not previously reported.

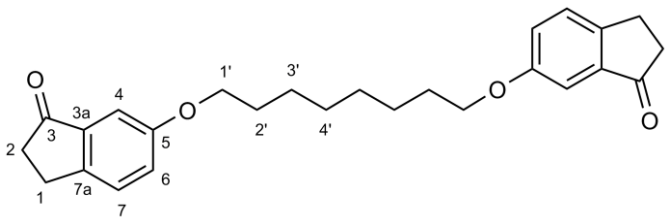

Figure 20.** Product **2b

Alternatively, the synthesis followed General procedure B with compound **3** (0.197 g, 1.3 mmol) and 1,8-dibromooctane **4b** (0.12 ml, 0.7 mmol) as starting materials, giving a black solid which was sufficiently pure for subsequent steps, 0.242 g, 82% yield (calculated from ^{1}H NMR spectrum).

5.2.8 Synthesis of 6-[2-(3-oxoindan-5-yl)oxydecoxy]indan-1-one, 2c

The synthesis followed General procedure A with compound **3** (0.397 g, 2.7 mmol) and 1,10-dibromodecane **4c** (0.405 g, 1.3 mmol) as starting materials, giving a light brown solid which was sufficiently pure for subsequent steps, 0.471 g, 80% yield. **^{1}H NMR** ($CDCl_3$, 500 MHz): δ = 7.34 (m, 2H, H-7), 7.20-7.16 (m, 4H, H-4 H-6), 3.98 (t, *J* = 6.8 Hz, 4H, C*H*$_2$-1'), 3.07 (m, 4H, C*H*$_2$-1), 2.71 (m, 4H, C*H*$_2$-2), 1.79 (dt, *J* = 6.8, 15.0 Hz, 4H, C*H*$_2$-2'), 1.46 (m, 4H, C*H*$_2$-3'), 1.40-1.30 (m, 8H, C*H*$_2$-4' C*H*$_2$-5'). **^{13}C NMR** ($CDCl_3$, 100.6 MHz): δ = 207.1 (C, C-3), 158.9 (C, C-5), 147.8 (C, C-3a), 138.2 (C, C-7a), 127.3 (CH, C-7), 124.4 (CH, C-6), 105.6 (CH, C-4), 68.4 (CH_2, *C*-1'), 37.0 (CH_2, *C*-2), 29.4 (CH_2, *C*-5'), 29.2 (CH_2, *C*-4'), 29.1 (CH_2, *C*-2'), 26.0 (CH_2, *C*-3'), 25.1 (CH_2, *C*-1). **APCI-MS**: *m/z* calcd. for $C_{28}H_{34}O_4$, $[M+H]^+$: 435; found:435. **UV-vis** (CH_2Cl_2) λ_{max}: 320, 248 nm. Not previously reported.

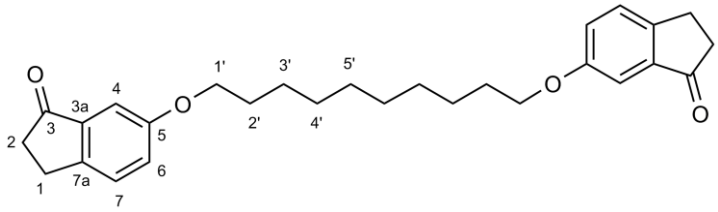

Figure 21. *Product* ***2c***

5.2.9 Synthesis of 6-[2-(3-oxoindan-5-yl)oxydodecoxy]indan-1-one, 2d

The synthesis followed General procedure A with compound **3** (0.102 g, 0.7 mmol) and 1,12-dibromododecane **4d** (0.112 g, $3.5 \cdot 10^{-2}$ mmol) as starting materials, giving a light brown solid which was sufficiently pure for subsequent steps, 0.112 g, 71% yield. **^{1}H NMR** ($CDCl_3$, 500 MHz): δ = 7.36 (m, 2H, H-7), 7.20-7.17 (m, 4H, H-4 H-6), 3.98 (t, *J* = 6.8 Hz, 4H, C*H*$_2$-1'), 3.07 (m, 4H, C*H*$_2$-1), 2.71 (m, 4H, C*H*$_2$-2), 1.79 (dt, *J* = 6.8, 14.8 Hz, 4H, C*H*$_2$-2'), 1.45 (m, 4H, C*H*$_2$-3'), 1.39-1.27 (m, 12H, C*H*$_2$-4' C*H*$_2$-5' C*H*$_2$-6'). **^{13}C NMR** ($CDCl_3$, 100.6 MHz): δ = 207.1 (C, C-3), 158.9 (C, C-5), 147.7 (C, C-3a), 138.2 (C, C-7a), 127.3 (CH, C-7), 124.4 (CH, C-6), 105.6 (CH, C-4), 68.4 (CH_2, *C*-1'), 37.0 (CH_2, *C*-2), 29.5 (CH_2, 4C, *C*-5' *C*-6'), 29.3 (CH_2, *C*-4'), 29.1 (CH_2, *C*-2'), 26.0 (CH_2, *C*-3'), 25.1 (CH_2, *C*-1). **APCI-MS**: *m/z* calcd. for $C_{30}H_{38}O_4$, $[M+H]^+$: 463; found: 463. **UV-vis** (CH_2Cl_2) λ_{max}: 320, 248 nm. Not previously reported.

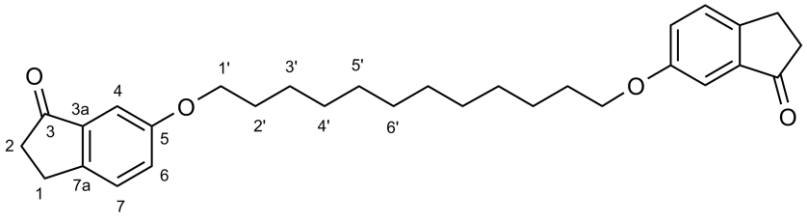

Figure 22. *Product* ***2d***

Alternatively, the synthesis followed General procedure B with compound **3** (0.308 g, 2.1 mmol) and 1,12-dibromododecane **4d** (0.341 g, 1.0 mmol) as starting materials, giving a light brown solid which was sufficiently pure for subsequent steps, 0.437g, 85% yield (calculated from ^{1}H NMR spectrum).

5.2.10 General procedure C: McMurry coupling.

Zinc powder previously grounded (12 eq.) was suspended in dry THF (30 ml). The suspension was cooled to 0ºC in ice bath and $TiCl_4$ (6 eq.) added over 10 minutes. The resulting slurry was refluxed for 1.5 h. A solution of compound **2** in dry THF (50-100 ml) was added over 5-7 h period by syringe pump to the refluxing reaction mixture. The reflux was continued 40 min more after the addition was complete. The reaction mixture was cooled to RT and poured on a saturated aqueous solution of NH_4Cl. The water phase was extracted three times with DCM (3x100 ml). The combined organic phases were washed two times with brine (2x100 ml) dried over $MgSO_4$ and solvent was removed by rotary evaporation. The obtained yellow oil was purified by CC (pentane/DCM 1:0 to 1:1). The obtained product was dried under high vacuum overnight.

5.2.11 Synthesis of product *Z*-1a

The synthesis followed General procedure C with compound **2a** (0.279 g, 0.7 mmol) as starting material and gave the pure product as a light yellow solid, 0.093g, 37% yield. **^{1}H NMR** ($CDCl_3$, 500 MHz): δ = 7.75 (d, *J* = 2.3 Hz, 2H, H-4), 7.19 (d, *J* = 8.0 Hz, 2H, H-7), 6.80 (dd, *J* = 2.3, 8.0 Hz, 2H, H-6), 4.07 (t, *J* = 6.5 Hz, 4H, C*H*$_2$-1'), 2.94 (m, 4H, C*H*$_2$-1), 2.82 (m, 4H, C*H*$_2$-2), 1.80 (m, 4H, C*H*$_2$-2'), 1.59 (m, 4H, C*H*$_2$-3'). **^{13}C NMR** ($CDCl_3$, 100.6 MHz): δ = 157.6 (C, C-5), 141.6 (C, C-7a), 141.1 (C, C-3a), 135.2 (C, C-3), 125.5 (CH, C-7), 116.2 (CH, C-6), 111.9 (CH, C-4), 69.7 (CH_2, *C*-1'), 35.0 (CH_2, *C*-2), 30.0 (CH_2, *C*-1), 28.8 (CH_2, *C*-2'), 24.4 (CH_2, *C*-3'). **APCI-MS**: *m/z* calcd. for $C_{24}H_{26}O_2$, $[M+H]^+$: 347; found: 347. **UV-vis** (CH_2Cl_2) λ_{max}: 350, 298, 253 nm. Not previously reported.

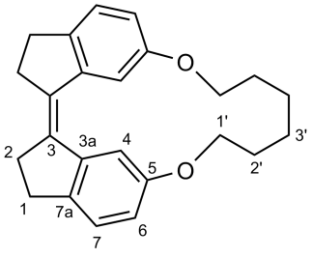

Figure 23. *Product* ***Z-1a***

5.2.12 Synthesis of product *Z*-1b

The synthesis followed General procedure C with compound **2b** (0.105 g, 0.3 mmol) as starting material and gave the pure product as a light yellow solid, 0.038g, 39% yield. **^{1}H NMR** ($CDCl_3$, 500 MHz): δ = 7.69 (d, *J* = 2.5 Hz, 2H, H-4), 7.18 (d, *J* = 8.2 Hz, 2H, H-7), 6.74 (dd, *J* = 2.5, 8.2 Hz, 2H, H-6), 3.97 (t, *J* = 6.1 Hz, 4H, C*H*$_2$-1'), 2.93 (m, 4H, C*H*$_2$-1), 2.82 (m, 4H, C*H*$_2$-2), 1.82 (dt, *J* = 6.1, 12.8 Hz, 4H, C*H*$_2$-2'), 1.56 (m, 4H, C*H*$_2$-3'), 1.45 (m, 4H, C*H*$_2$-4'). **^{13}C NMR** ($CDCl_3$, 100.6 MHz): δ = 157.6 (C, C-5), 141.6 (C, C-7a), 140.5 (C, C-3a), 135.4 (C, C-3), 125.4 (CH, C-7), 113.9 (CH, C-6), 110.0 (CH, C-4), 68.1 (CH_2, *C*-1'), 35.4 (CH_2, *C*-2), 29.8 (CH_2, *C*-1), 28.1 (CH_2, *C*-2'), 27.6 (CH_2, *C*-4'), 25.3 (CH_2, *C*-3'). **APCI-MS**: *m/z* calcd. for $C_{26}H_{30}O_2$, $[M+H]^+$: 375; found: 375. **UV-vis** (CH_2Cl_2) λ_{max}: 361, 349, 300, 253 nm. Not previously reported.

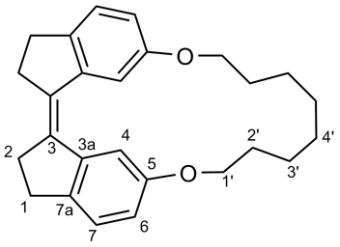

Figure 24*. Product* ***Z-1b***

5.2.13 Synthesis of product *Z*-1c

The synthesis followed General procedure C with compound **2c** (0.350 g, 0.8 mmol) as starting material and gave the pure product as a light yellow solid, 0.171g, 53% yield. **^{1}H NMR** ($CDCl_3$, 500 MHz): δ = 7.66 (d, *J* = 2.4 Hz, 2H, H-4), 7.19 (d, *J* = 8.3 Hz, 2H, H-7), 6.75 (dd, *J* = 2.4, 8.3 Hz, 2H, H-6), 3.92 (t, *J* = 5.9 Hz, 4H, C*H*$_2$-1'), 2.93 (m, 4H, C*H*$_2$-1), 2.82 (m, 4H, C*H*$_2$-2), 1.79 (dt, *J* = 5.9, 12.6 Hz, 4H, C*H*$_2$-2'), 1.55 (dt, *J* = 5.9, 12.6 Hz, 4H, C*H*$_2$-3'), 1.45-1.37 (m, 8H, C*H*$_2$-4' C*H*$_2$-5'). **^{13}C NMR** ($CDCl_3$, 100.6 MHz): δ = 157.7 (C, C-5), 141.7 (C, C-7a), 140.4 (C, C-3a), 135.5 (C, C-3), 125.4 (CH, C-7), 113.6 (CH, C-6), 109.5 (CH, C-4), 67.1 (CH_2, *C*-1'), 35.6 (CH_2, *C*-2), 29.8 (CH_2, *C*-1), 28.4 (CH_2, *C*-2'), 26.9 (CH_2, *C*-4'), 26.4 (CH_2, *C*-5'), 24.8 (CH_2, *C*-3'). **APCI-MS**: *m/z* calcd. for $C_{28}H_{34}O_2$, $[M+H]^+$: 403; found: 403. **UV-vis** (CH_2Cl_2) λ_{max}: 361, 349, 301, 252 nm. Not previously reported.

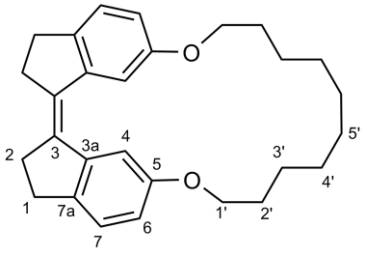

Figure 25. *Product* ***Z-1c***

5.2.14 Synthesis of product *Z*-1d

The synthesis followed General procedure C with compound **2d** (0.312 g, 0.7 mmol) as starting material and gave the pure product as a light yellow solid, 0.152g, 52% yield. **^{1}H NMR** ($CDCl_3$, 500 MHz): δ = 7.64 (d, *J* = 2.4 Hz, 2H, H-4), 7.19 (d, *J* = 8.3 Hz, 2H, H-7), 6.76 (dd, *J* = 2.4, 8.3 Hz, 2H, H-6), 3.91 (t, *J* = 6.3 Hz, 4H, C*H*$_2$-1'), 2.93 (m, 4H, C*H*$_2$-1), 2.82 (m, 4H, C*H*$_2$-2), 1.76 (dt, *J* = 6.3, 15.0 Hz, 4H, C*H*$_2$-2'), 1.49 (m, 4H, C*H*$_2$-3'), 1.44-1.26 (m, 12H, C*H*$_2$-4' C*H*$_2$-5' C*H*$_2$-6'). **^{13}C NMR** ($CDCl_3$, 100.6 MHz): δ = 157.8 (C, C-5), 141.6 (C, C-7a), 140.5 (C, C-3a), 135.4 (C, C-3), 125.4 (CH, C-7), 114.1 (CH, C-6), 109.3 (CH, C-4), 68.4 (CH_2, *C*-1'), 35.5 (CH_2, *C*-2), 29.8 (CH_2, *C*-1), 29.6 (CH_2, *C*-2'), 27.4 (CH_2, *C*-4'), 27.1 (CH_2, *C*-5'), 26.2 (CH_2, *C*-6'), 25.1 (CH_2, *C*-3'). **APCI-MS**: *m/z* calcd. for $C_{30}H_{38}O_2$, $[M+H]^+$: 431; found: 431. **UV-vis** (CH_2Cl_2) λ_{max}: 359, 349, 298, 252 nm. Not previously reported.

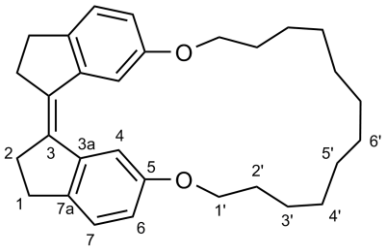

Figure 26. *Product* ***Z-1d***

5.2.15 Synthesis of 1,8-dibromooctane, 4b

1,8-octanediol **8b** (4.023 g, 27.5 mmol) was dissolved in HBr (48%, 50 ml) and refluxed for 48h. The reaction was cooled to RT. DCM (50 ml) was added and the organic phase collected. The water phase was extracted two times with DCM (2x50 ml). The combined organic phases were washed two times with brine (2x50 ml) and saturated $NaHCO_3$ aqueous solution (2x50 ml) and dried over $MgSO_4$. The solvent was removed by rotary evaporation, giving a brown oil which was sufficiently pure for subsequent steps, 6.449g, 86% yield. **^{1}H NMR** ($CDCl_3$, 500 MHz): δ = 3.42 (t, *J* = 7.0 Hz, 4H, BrC*H*$_2$), 1.86 (m, 4H, $BrCH_2C\underline{H_2}$), 1.44 (m, 4H, $Br(CH_2)_2C\underline{H_2}$) 1.34 (m, 4H, $Br(CH_2)_3C\underline{H_2}$). **^{13}C NMR** ($CDCl_3$,

100.6 MHz): δ = 33.9 (Br*C*H_2), 32.7 (BrCH_2*C*H_2), 28.6 (Br$(CH_2)_3$*C*H_2), 28.0 (Br$(CH_2)_2$*C*H_2). In agreement with literature.[80]

5.2.16 Conversion study of the last step: McMurry coupling.

The synthesis followed General procedure C without with compounds **2a** (0.112 g, 0.3 mmol), **2b** (0.100 g, 0.2 mmol), **2c** (0.102 g, 0.2 mmol) and **2d** (0.101 g,0.2 mmol) as starting materials and gave a mixture of products ***Z*-1a**, ***Z*-1b**, ***Z*-1c** and ***Z*-1d**, which was analyzed without purification by NMR spectroscopy (DOSY).

5.2.17 Photo-isomerizations

$CDCl_3$ solutions of products ***Z*-1a**, ***Z*-1b**, ***Z*-1c** and ***Z*-1d** were irradiated after they were degassed by argon bubbling for 15 min. As reaction vessels, 5mm NMR-tubes, Type 5Hp, 178 mm were used. Isomerization course were assessed by NMR spectroscopy (Varian Unity Inova 500 MHz NMR spectrometer, ^1H at 499.94 MHz.).

6. ACKNOWLEDGEMENTS

I would like to thank the people who made this Erasmus exchange and my first research project an extraordinary experience. Thanks, Tack, gràcies.

First of all, I wish to thank my supervisor Prof. Adolf Gogoll. Thanks for accepting me in your group giving me such an interesting project. I learnt a lot every time we met. I wish I had come into your office more times. I also want to thank you for reviewing my report and for each advice you have given me.

Sandra, you can't imagine how much you have helped me and made me grow as a chemist. I can't write down everything you have made for me because I would need several pages and we are environmentally friendly, you know… The only advise you gave me and I didn't follow was 'quit bikes!' and you know what happened afterwards…Jag känner mig mycket lycklig att jag har haft dig som handledare. Tack så mycket!

Magnus, I could only share lab with you a couple of weeks but those days I learnt a lot. Your doctoral dissertation defense was an inspiration for me. I felt really motivated to work on this project after that. Tack!

Michael, thank you for fixing all the problems I have had, not all of them related with chemistry… Also thanks for helping me in the lab when Sandra was doing what she loves: teaching. Thanks for keeping me motivated when I got to the first downhill of the camel back. Jag är glad att jag träffade dig.

I would also like to thank the other members of the AGHG group: Prof. Helena Grennberg, Anna, Hao, Leili and Xiao. Thank you for adopting me not only as a student but also as a friend and made these months amazing. I wish you all the best.

I want to thank Prof. Lars Engman for reviewing and examining this thesis.

Gràcies Prof. Paul Lloyd-Williams, per aquests quatre anys de consells i obrir-me la porta del teu despatx sempre que ho he necessitat. Espero que puguem seguir treballant junts molt aviat.

Alèria, mil gràcies per aquets 'cafès' eterns de mitjanit. Has aconseguit que aquests últims dies de report passessin molt millor. Recorda sempre que quan he dit que vals molt i tens un futur brillant ho he dit perquè ho penso de veritat.

Vull donar les gràcies també a la meva família, més preocupada per mi que jo mateix.

A les meves àvies, Demetria i Antonia, que tant m'han ensenyat.

Carina, gràcies per sempre ser allà.

7. REFERENCES

1. Coxon, J. M.; Halton, B., *Organic Photochemistry*. Cambridge University Press: London, 1974.

2. Knowles, J. P.; Elliott, L. D.; Booker-Milburn, K. I. Flow photochemistry: Old light through new windows. *Beilstein J. Org. Chem.* **2012,** *8*, 2025-2052.

3. Natarajan, A.; Tsai, C. K.; Khan, S. I.; McCarren, P.; Houk, K. N.; Garcia-Garibay, M. A. The Photoarrangement of α-Santonin is a Single-Crystal-to-Single-Crystal Reaction: A Long Kept Secret in Solid-State Organic Chemistry Revealed. *J. Am. Chem. Soc.* **2007,** *129* (32), 9846-9847.

4. Trommsdorff, H. Ueber Santonin. *Ann. Pharm.* **1834,** *11* (2), 190-207.

5. Paniagua, J. C.; Alemany, P., *Química quàntica*. 3rd ed.; Llibres De L'Index. Universitat: Barcelona, 1999; Vol. 1.

6. Ciamician, G.; Silber, P. Chemische Lichtwirkungen. *Ber. Dtsch. Chem. Ges.* **1901,** *34* (2), 2040-2046.

7. Yonemitsu, O.; Cerutti, P.; Witkop, B. Photoreductions and Photocyclizations of Tryptophan. *J. Am. Chem. Soc.* **1966,** *88* (17), 3941-3945.

8. Rawal, V. H.; Fabré, A.; Iwasa, S. Photocyclization-fragmentation route to linear triquinanes: Stereocontrolled synthesis of (±)-endo-hirsutene. *Tetrahedron Lett.* **1995,** *36* (38), 6851-6854.

9. Corey, E. J.; Nozoe, S. The Total Synthesis of α-Caryophyllene Alcohol. *J. Am. Chem. Soc.* **1965,** *87* (24), 5733-5735.

10. Lévesque, F.; Seeberger, P. H. Continuous-Flow Synthesis of the Anti-Malaria Drug Artemisinin. *Angew. Chem. Int. Ed.* **2012,** *51* (7), 1706-1709.

11. Hall, D. O.; Rao, K. K., *Photosynthesis*. 6th ed.; Cambridge University Press: Cambridge, 1972.

12. Pessarakli, M., *Handbook of Photosynthesis*. 2nd ed.; Marcel Dekker, Inc.: New York, 1996.

13. Atkins, P. W.; De Paula, J., *Atkins' Physical Chemistry*. 9th ed.; Oxford University Press: Oxford, 2010.

14. Franck, J.; Dymond, E. G. Elementary processes of photochemical reactions. *T. Faraday Soc.* **1926,** *21* (February), 536-542.

15. Condon, E. U. Nuclear Motions Associated with Electron Transitions in Diatomic Molecules. *Phys. Rev.* **1928,** *32* (6), 858-872.

16. Tavarone, R.; Charbonneau, P.; Stark, H. Kinetic Monte Carlo simulations for birefringence relaxation of photo-switchable molecules on a surface. *J. Chem. Phys.* **2016,** *144* (10), 104703.

17. Ko, C.-C.; Wing-Wah Yam, V., Photoswitching Materials. In *Supramol. Chem.*, John Wiley & Sons, Ltd: New York, 2012.

18. Einaga, Y. Photo-switching magnetic materials. *J. Photochem. Photobiol. C* **2006,** *7* (2–3), 69-88.

19. Szymański, W.; Beierle, J. M.; Kistemaker, H. A. V.; Velema, W. A.; Feringa, B. L. Reversible Photocontrol of Biological Systems by the Incorporation of Molecular Photoswitches. *Chem. Rev.* **2013,** *113* (8), 6114-6178.

20. Velema, W. A.; Szymanski, W.; Feringa, B. L. Photopharmacology: Beyond Proof of Principle. *J. Am. Chem. Soc.* **2014,** *136* (6), 2178-2191.

21. Shimasaki, T.; Kato, S.-i.; Ideta, K.; Goto, K.; Shinmyozu, T. Synthesis and Structural and Photoswitchable Properties of Novel Chiral Host Molecules: Axis Chiral 2,2‘-Dihydroxy-1,1‘-binaphthyl-Appended stiff-Stilbene1. *J. Org. Chem.* **2007,** *72* (4), 1073-1087.

22. Xu, J.-F.; Chen, Y.-Z.; Wu, D.; Wu, L.-Z.; Tung, C.-H.; Yang, Q.-Z. Photoresponsive Hydrogen-Bonded Supramolecular Polymers Based on a Stiff Stilbene Unit. *Angew. Chem. Int. Ed.* **2013,** *52* (37), 9738-9742.

23. Rothenberger, G.; Negus, D. K.; Hochstrasser, R. M. Solvent influence on photoisomerization dynamicsa). *J. Chem. Phys.* **1983,** *79* (11), 5360-5367.

24. Doany, F. E.; Heilweil, E. J.; Moore, R.; Hochstrasser, R. M. Picosecond study of an intermediate in the trans to cis isomerization pathway of stiff stilbene. *J. Chem. Phys.* **1984,** *80* (1), 201-206.

25. Saltiel, J.; D'Agostino, J. T. Separation of viscosity and temperature effects on the singlet pathway to stilbene photoisomerization. *J. Am. Chem. Soc.* **1972,** *94* (18), 6445-6456.

26. Improta, R.; Santoro, F. Excited-State Behavior of trans and cis Isomers of Stilbene and Stiff Stilbene: A TD-DFT Study. *J. Phys. Chem. A* **2005,** *109* (44), 10058-10067.

27. Quick, M.; Berndt, F.; Dobryakov, A. L.; Ioffe, I. N.; Granovsky, A. A.; Knie, C.; Mahrwald, R.; Lenoir, D.; Ernsting, N. P.; Kovalenko, S. A. Photoisomerization Dynamics of Stiff-Stilbene in Solution. *J. Phys. Chem. B* **2014,** *118* (5), 1389-1402.

28. Kondo, K.; Hirose, T.; Yasutake, M. Development of liquid crystal material having Stiff-stilbene unit as a core and their photoisomerization behavior. *Proceedings of Japanese Liquid Crystal Society Annual meeting* **2011,** *2011*, 176-176.

29. Huang, Z.; Yang, Q.-Z.; Boulatov, R., Macrocyclic disulfides for model studies of tryptophan-sensitized homolysis of disulfides in proteins. In *The 237th ACS National Meeting*, Salt Lake City, UT, 2009.

30. Yan, X.; Xu, J.-F.; Cook, T. R.; Huang, F.; Yang, Q.-Z.; Tung, C.-H.; Stang, P. J. Photoinduced transformations of stiff-stilbene-based discrete metallacycles to metallosupramolecular polymers. *Proc. Natl. Acad. Sci. U. S. A.* **2014,** *111* (24), 8717-8722.

31. Blom, M.; Norrehed, S.; Andersson, C.-H.; Huang, H.; Light, M.; Bergquist, J.; Grennberg, H.; Gogoll, A. Synthesis and Properties of Bis-Porphyrin Molecular Tweezers: Effects of Spacer Flexibility on Binding and Supramolecular Chirogenesis. *Molecules* **2016,** *21* (1), 16.

32. Yang, Q.-Z.; Huang, Z.; Kucharski, T. J.; Khvostichenko, D.; ChenJoseph; BoulatovRoman A molecular force probe. *Nat. Nanotechnol.* **2009,** *4* (5), 302-306.

33. Huang, Z.; Yang, Q.-Z.; Khvostichenko, D.; Kucharski, T. J.; Chen, J.; Boulatov, R. Method to Derive Restoring Forces of Strained Molecules from Kinetic Measurements. *J. Am. Chem. Soc.* **2009,** *131* (4), 1407-1409.

34. Lenhardt, J. M.; Craig, S. L. Mechanochemistry: Force probes in a bottle. *Nat. Nanotechnol.* **2009,** *4* (5), 284-285.

35. Kean, Z. S.; Akbulatov, S.; Tian, Y.; Widenhoefer, R. A.; Boulatov, R.; Craig, S. L. Photomechanical Actuation of Ligand Geometry in Enantioselective Catalysis. *Angew. Chem. Int. Ed.* **2014,** *53* (52), 14508-14511.

36. Neuman, K. C.; Nagy, A. Single-molecule force spectroscopy: optical tweezers, magnetic tweezers and atomic force microscopy. *Nat. Methods* **2008,** *5* (6), 491-505.

37. Bruice, P. Y., *Organic Chemistry*. 6th ed.; Pearson Education, Inc.: 2004.

38. Lambert, J. B.; Mazzola, E. P., Nuclear Magnetic Resonance Spectroscopy. An introduction to principles, applications, and experimental methods. Pearson Education, Inc.: New Jersey, 2004.

39. Wokaun, A.; Ernst, R. R. Selective detection of multiple quantum transitions in NMR by two-dimensional spectroscopy. *Chem. Phys. Lett.* **1977,** *52* (3), 407-412.

40. Shaka, A. J.; Freeman, R. Simplification of NMR spectra by filtration through multiple-quantum coherence. *Journal of Magnetic Resonance (1969)* **1983,** *51* (1), 169-173.

41. Braunschweiler, L.; Ernst, R. R. Coherence transfer by isotropic mixing: Application to proton correlation spectroscopy. *Journal of Magnetic Resonance (1969)* **1983,** *53* (3), 521-528.

42. Davis, A. L.; Keeler, J.; Laue, E. D.; Moskau, D. Experiments for recording pure-absorption heteronuclear correlation spectra using pulsed field gradients. *Journal of Magnetic Resonance (1969)* **1992,** *98* (1), 207-216.

43. Hurd, R. E.; John, B. K. Gradient-enhanced proton-detected heteronuclear multiple-quantum coherence spectroscopy. *Journal of Magnetic Resonance (1969)* **1991,** *91* (3), 648-653.

44. Sabatini, V.; Farina, H.; Ortenzi, M. A. Functional end-capped conducting poly (3,4-ethylenedioxythiophene). *AIP Conf. Proc.* **2016,** *1736* (1), 020082.

45. Liu, Y.; Meng, G.; Liu, R.; Szostak, M. Sterically-controlled intermolecular Friedel-Crafts acylation with twisted amides via selective N-C cleavage under mild conditions. *Chem. Commun.* **2016,** *52* (41), 6841-6844.

46. Tran, P. H.; Nguyen, H. T.; Hansen, P. E.; Le, T. N. An efficient and green method for regio- and chemo-selective Friedel-Crafts acylations using a deep eutectic solvent ([CholineCl][ZnCl2]3). *RSC Adv.* **2016,** *6* (43), 37031-37038.

47. McOmie, J. F. W.; West, D. E. 3,3'-Dihydroxybiphenyl. *Org. Synth.* **1969,** *49*, 50-52.

48. McOmie, J. F. W.; Watts, M. L.; West, D. E. Demethylation of aryl methyl ethers by boron tribromide. *Tetrahedron* **1968,** *24* (5), 2289-2292.

49. Ingold, C. K., *Structure and Mechanism in Organic Chemistry*. 2nd ed.; Cornell University Press, Ithaca: New York, 1969.

50. Uggerud, E. Reactivity trends and stereospecificity in nucleophilic substitution reactions. *J. Phys. Org. Chem.* **2006,** *19* (8-9), 461-466.

51. Gokel, G. W.; Ugi, I. K. The Retentive Nucleophilic Substitution of (R)α-Ferrocenylethyl Acetate. *Angew. Chem. Int. Ed.* **1971,** *10* (3), 191-191.

52. Williamson, A. XLV. Theory of ætherification. *Philosophical Magazine Series 3* **1850,** *37* (251), 350-356.

53. McMurry, J. E.; Fleming, M. P. New method for the reductive coupling of carbonyls to olefins. Synthesis of .beta.-carotene. *J. Am. Chem. Soc.* **1974,** *96* (14), 4708-4709.

54. Mukaiyama, T.; Sato, T.; Hanna, J. Reductive coupling of carbonyl compounds to pinacols and olefins by using $TiCl_4$ and Zn. *Chem. Lett.* **1973,** *2* (10), 1041-1044.

55. Tyrlik, S.; Wolochowicz, I. Application of transition metal complexes with low oxidation states in organic synthesis. I. New synthesis of olefins from carbonyl compounds. *Bull. Soc. Chim. Fr.* **1973,** *6*, 2147-2148.

56. McMurry, J. E. Carbonyl-coupling reactions using low-valent titanium. *Chem. Rev.* **1989,** *89* (7), 1513-1524.

57. McMurry, J. E.; Fleming, M. P.; Kees, K. L.; Krepski, L. R. Titanium-induced reductive coupling of carbonyls to olefins. *J. Org. Chem.* **1978,** *43* (17), 3255-3266.

58. Nagaraju, K.; Chegondi, R.; Chandrasekhar, S. Expanding Diversity without Protecting Groups: (+)-Sclareolide to Indolosesquiterpene Alkaloid Mycoleptodiscin A and Analogues. *Org. Lett.* **2016**.

59. Rehahn, M.; Schlüter, A.-D. Soluble poly(p-phenylenevinylene)s from 2,5-dihexylterephthalaldehyde using the improved McMurry reagent. *Makromol. Chem., Rapid Commun.* **1990,** *11* (8), 375-379.

60. Ephritikhine, M. A new look at the McMurry reaction. *Chem. Commun.* **1998,** (23), 2549-2554.

61. Villiers, C.; Ephritikhine, M. New Insights into the Mechanism of the McMurry Reaction. *Angew. Chem. Int. Ed.* **1997,** *36* (21), 2380-2382.

62. Kucharski, T. J.; Huang, Z.; Yang, Q.-Z.; Tian, Y.; Rubin, N. C.; Concepcion, C. D.; Boulatov, R. Kinetics of Thiol/Disulfide Exchange Correlate Weakly with the Restoring Force in the Disulfide Moiety. *Angew. Chem.* **2009,** *121* (38), 7174-7177.

63. Tong, Y.; Przytulinska, M.; Tao, Z.-F.; Bouska, J.; Stewart, K. D.; Park, C.; Li, G.; Claiborne, A.; Kovar, P.; Chen, Z.; Merta, P. J.; Bui, M.-H.; Olson, A.; Osterling, D.; Zhang, H.; Sham, H. L.;

Rosenberg, S. H.; Sowin, T. J.; Lin, N.-h. Cyanopyridyl containing 1,4-dihydroindeno[1,2-c]pyrazoles as potent checkpoint kinase 1 inhibitors: Improving oral biovailability. *Bioorg. Med. Chem. Lett.* **2007,** *17* (20), 5665-5670.

64. Lowe, J.; Drozda, S.; Qian, W.; Peakman, M. C.; Liu, J.; Gibbs, J.; Harms, J.; Schmidt, C.; Fisher, K.; Strick, C.; Schmidt, A.; Vanase, M.; Lebel, L. A novel, non-substrate-based series of glycine type 1 transporter inhibitors derived from high-throughput screening. *Bioorg. Med. Chem. Lett.* **2007,** *17* (6), 1675-1678.

65. Raja, E. K.; DeSchepper, D. J.; Nilsson Lill, S. O.; Klumpp, D. A. Friedel–Crafts Acylation with Amides. *J. Org. Chem.* **2012,** *77* (13), 5788-5793.

66. Polo, E. C.; Silva-Filho, L. C. d.; Silva, G. V. J. d.; Constantino, M. G. Síntese de 1-indanonas através da reação de acilação de Friedel-Crafts intramolecular utilizando NbCl5 como ácido de Lewis. *Quim. Nova* **2008,** *31*, 763-766.

67. Mohrschladt, R.; Schroeder, J.; Troe, J.; Voehringer, P.; Votsmeier, M. Solvent influence on barrier crossing in the S1 state of cis- and trans-"stiff"-stilbene. *Springer Ser. Chem. Phys.* **1994,** *60*, 499-500.

68. Doany, F. E.; Hochstrasser, R. M. Isomerization intermediates in the photochemistry of stilbenes. *Springer Ser. Chem. Phys.* **1984,** *38*, 326-328.

69. Chen, C.; Zhang, R.; Lin, L.; Yang, G.-F.; Wu, Q.-Y. Brønsted acid promoted one-pot synthesis of 4-aryl-3,4-dihydrocoumarins. *Tetrahedron*.

70. Wu, Q.; Ma, C.; Du, X.-h.; Chen, Y.; Huang, T.-z.; Shi, X.-q.; Tu, S.-j.; Cai, P.-j. Chiral Brønsted acid-catalyzed alkylation of C3-substituted indoles with o-hydroxybenzyl alcohols: highly enantioselective synthesis of diarylindol-2-ylmethanes and evaluation on their cytotoxicity. *Tetrahedron: Asymmetry* **2016,** *27* (7–8), 307-316.

71. Oliverio, M.; Nardi, M.; Costanzo, P.; Cariati, L.; Cravotto, G.; Giofrè, S.; Procopio, A. Non-Conventional Methodologies in the Synthesis of 1-Indanones. *Molecules* **2014,** *19* (5), 5599.

72. Roberts, R. M. G.; Sadri, A. R. Studies in trifluoromethanesulphonic acid—IV. *Tetrahedron* **1983,** *39* (1), 137-142.

73. Wang, B.; Zhang, L.; Fu, K.; Luo, Y.; Lu, W.; Tang, J. An Efficient Synthesis of 1,2,6,7-Tetrahydro-8H-indeno[5,4-b]furan-8-one. *Org. Prep. Proced. Int.* **2009,** *41* (4), 309-314.

74. Oelgemöller, M.; Frank, R.; Lemmen, P.; Lenoir, D.; Lex, J.; Inoue, Y. Synthesis, structural characterization and photoisomerization of cyclic stilbenes. *Tetrahedron* **2012,** *68* (21), 4048-4056.

75. McMurry, J. E.; Lectka, T.; Rico, J. G. An optimized procedure for titanium-induced carbonyl coupling. *J. Org. Chem.* **1989,** *54* (15), 3748-3749.

76. Vladimir, G. G. Influence of Ring Size on Properties and Reactivity of Cyclic Systems. *Russ. Chem. Rev.* **1982,** *51* (2), 119.

77. Zhao, K.-Q.; Chen, C.; Monobe, H.; Hu, P.; Wang, B.-Q.; Shimizu, Y. Three-chain truxene discotic liquid crystal showing high charged carrier mobility. *Chem. Commun.* **2011,** *47* (22), 6290-6292.

78. De, S.; Aswal, V. K.; Ramakrishnan, S. Phenyl-Ring-Bearing Cationic Surfactants: Effect of Ring Location on the Micellar Structure. *Langmuir* **2010,** *26* (23), 17882-17889.

79. Vautravers, N. R.; Regent, D. D.; Breit, B. Inter- and intramolecular hydroacylation of alkenes employing a bifunctional catalyst system. *Chem. Commun.* **2011,** *47* (23), 6635-6637.

80. Mekala, S.; Hahn, R. C. Process intensification-assisted conversion of α,ω-alkanediols to dibromides. *Tetrahedron Lett.* **2015,** *56* (4), 630-632.

8. Popular Summary

Photochemistry is the field of Chemistry that studies the relationship between light and chemical reactions. Light is energy as electromagnetic radiation. Some chemical reactions can be initiated by the energy provided by light. Quantum mechanics describes that electromagnetic radiation, like light, has a dual nature. On the one hand, it behaves as a wave which explains how it propagates through space. On the other hand, it also behaves as discrete particles called photons. When we say that molecules absorb light we mean that they absorb photons and these photons give extra energy to these molecules letting them, sometimes, undergo chemical reactions.

One type of photochemical reactions is photo-isomerizations. Some molecules have different isomers. Isomers are molecules with the same molecular formula (the proportion of atoms that constitute the molecule) but with different structures. In our project a kind of isomers, stereoisomers, are involved. In addition to have the same proportion of atoms, stereoisomers have the same connectivity between the atoms but they differ in the way their atoms are arranged in space. In Figure A, the two stereoisomers of stiff-stilbene are shown.

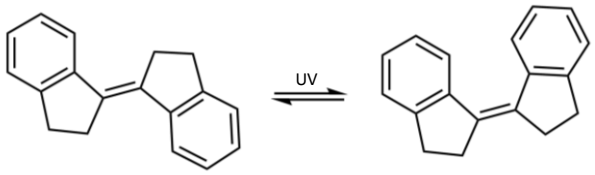

Figure A. *Stiff-stilbene isomers, E or trans (left) and Z or cis (right).*

Isomerization is a chemical process where a molecule change its shape from one isomer to the other but this process requires energy. If a molecule gets this energy from light (it absorbs a photon) the process is called photo-isomerization. It has many applications in science, basically because it allows us to control molecule shapes with light, an easy and clean way. Sometimes, these photo-switchable molecules are only the backbone of more complex molecular system what can be used in a wide range of fields from material science to biology. Some of these systems are cyclic molecules and when they undergo isomerization they twisted themselves as it can be seen in figure B.

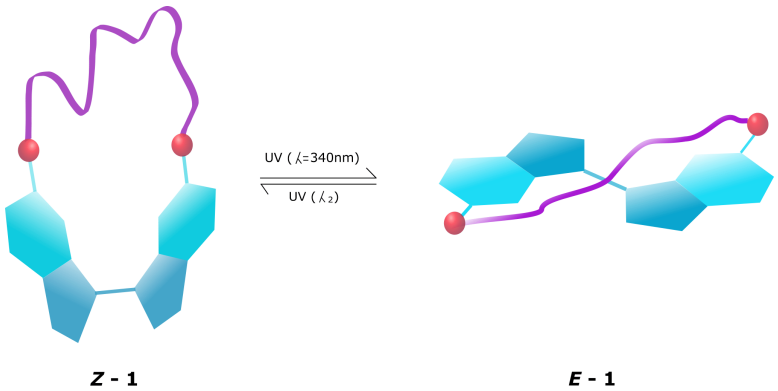

Figure B. *Photo-isomerization of a model compound.*

Now, we set out this question: Does the ring size affect the photo-isomerization process? In other words, is there a minimum size to let these systems overcome the strain caused when they twist themselves during the photo-isomerization process? To answer these questions, we designed a small library of cyclic molecules composed by a stiff-stilbene backbone (photo-switchable unit) and different linkers with different lengths (Figure C). They aim to be model systems of those more complex ones described above. A photo-switching study of these molecules would let us establish the limit, in term of length, of the linker to make the molecule able to undergo photo-isomerization processes.

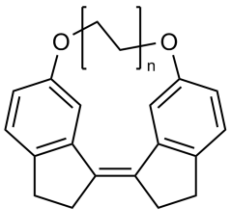

***Z* - 1a**, n=3
***Z* - 1b**, n=4
***Z* - 1c**, n=5
***Z* - 1d**, n=6

Figure C. *Target molecules.*

The target molecules were synthesized successfully and a good synthetic route was found from starting materials available in our lab. Then, we tested all the molecules exposing them to UV light. We used a characterization technique called NMR spectroscopy to follow the isomerization course. This technique gives us a signals pattern unique and different for each molecule and also different for each isomer, so we knew how the isomerization process was going studying the differences in NMR signal patterns. The molecules with the shortest linkers (6 and 8 carbons) showed quite low conversion from the relaxed to the twisted isomer whereas the molecule with 10 carbons linker showed moderate conversion and the molecule with 12 carbon linker showed the best conversion rate. These are the expected results since the shorter the linker was, the more strained the molecule were in its twisted isomer so isomerization was less favorable and lower conversion rates were obtained.

Coming to the initial questions, the ring size (which depends on the linker length) affects the photo-switching properties of this kind of molecules and it was determined that a minimum of ten carbons length is necessary to get appreciable photo-isomerization.

In future projects, an in-depth photo-switching study of these systems will be performed together with a conformational analysis of both isomers. Conformational analysis will describe how the atoms of both isomers are arranged in space and structural energies of the different conformers.

9. APPENDICES

Index

NMR:

MS:

UV-vis:

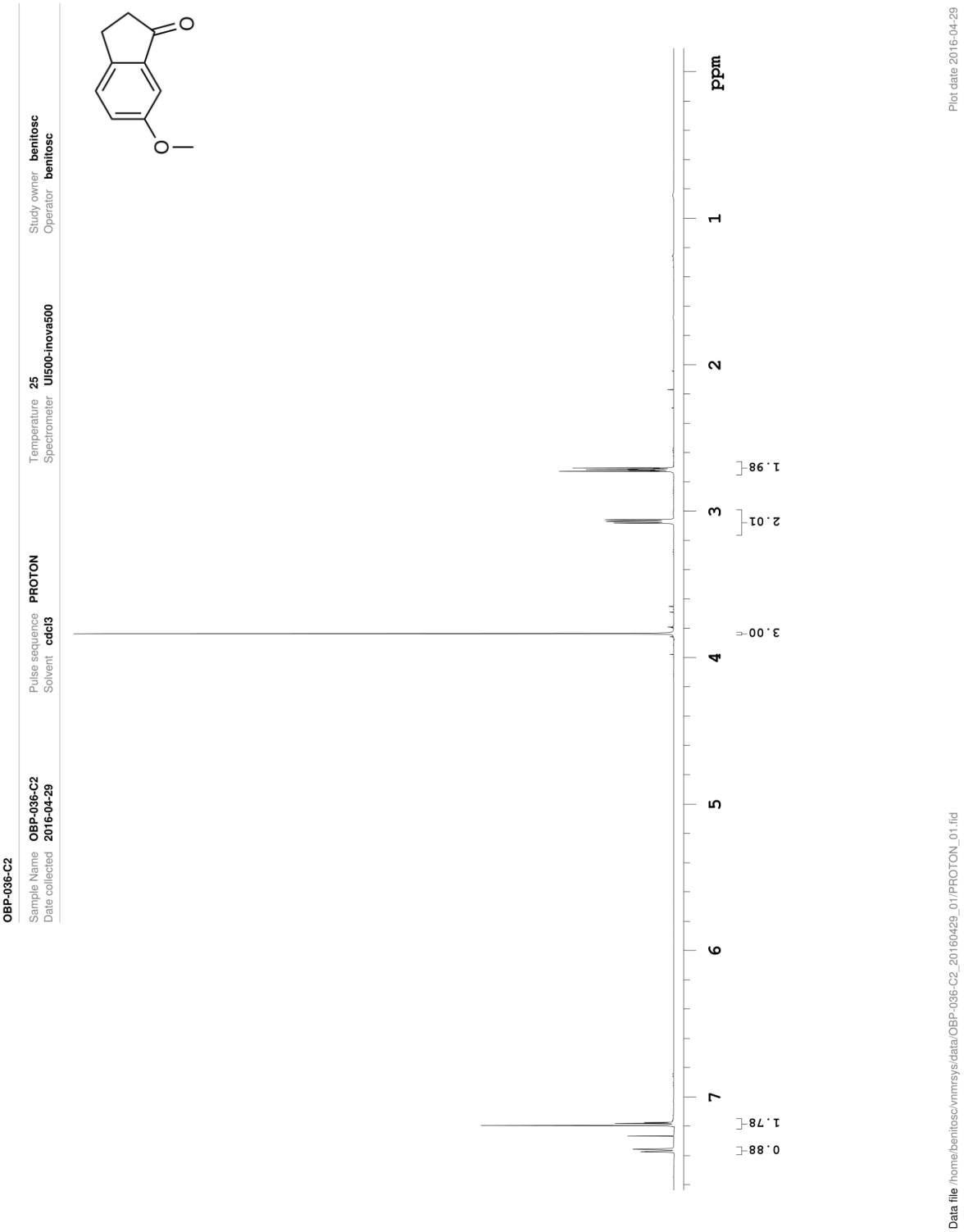

Figure 27. ^{1}H-NMR spectrum of compound 5.

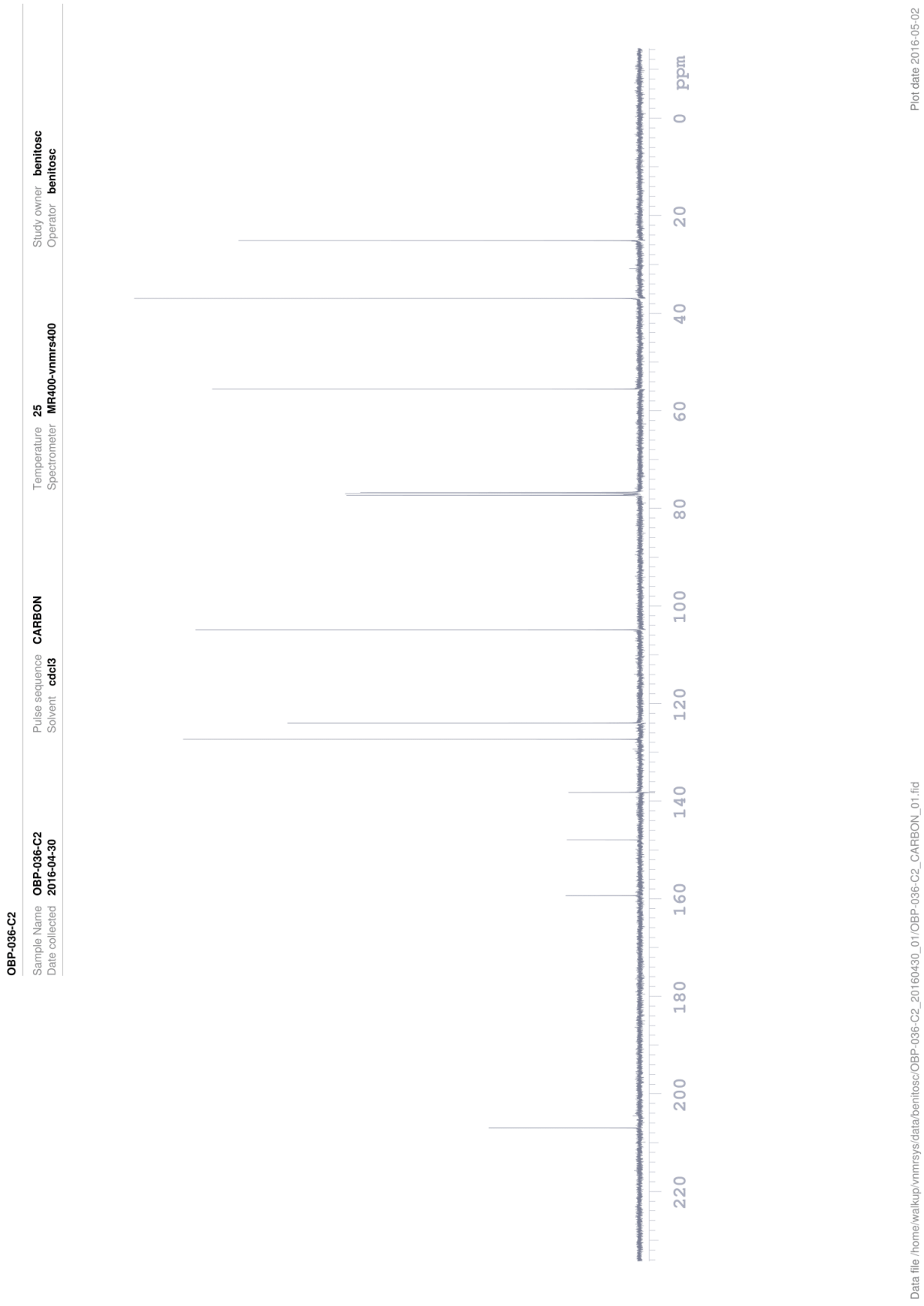

Figure 28. ^{13}C-NMR spectrum of compound 5.

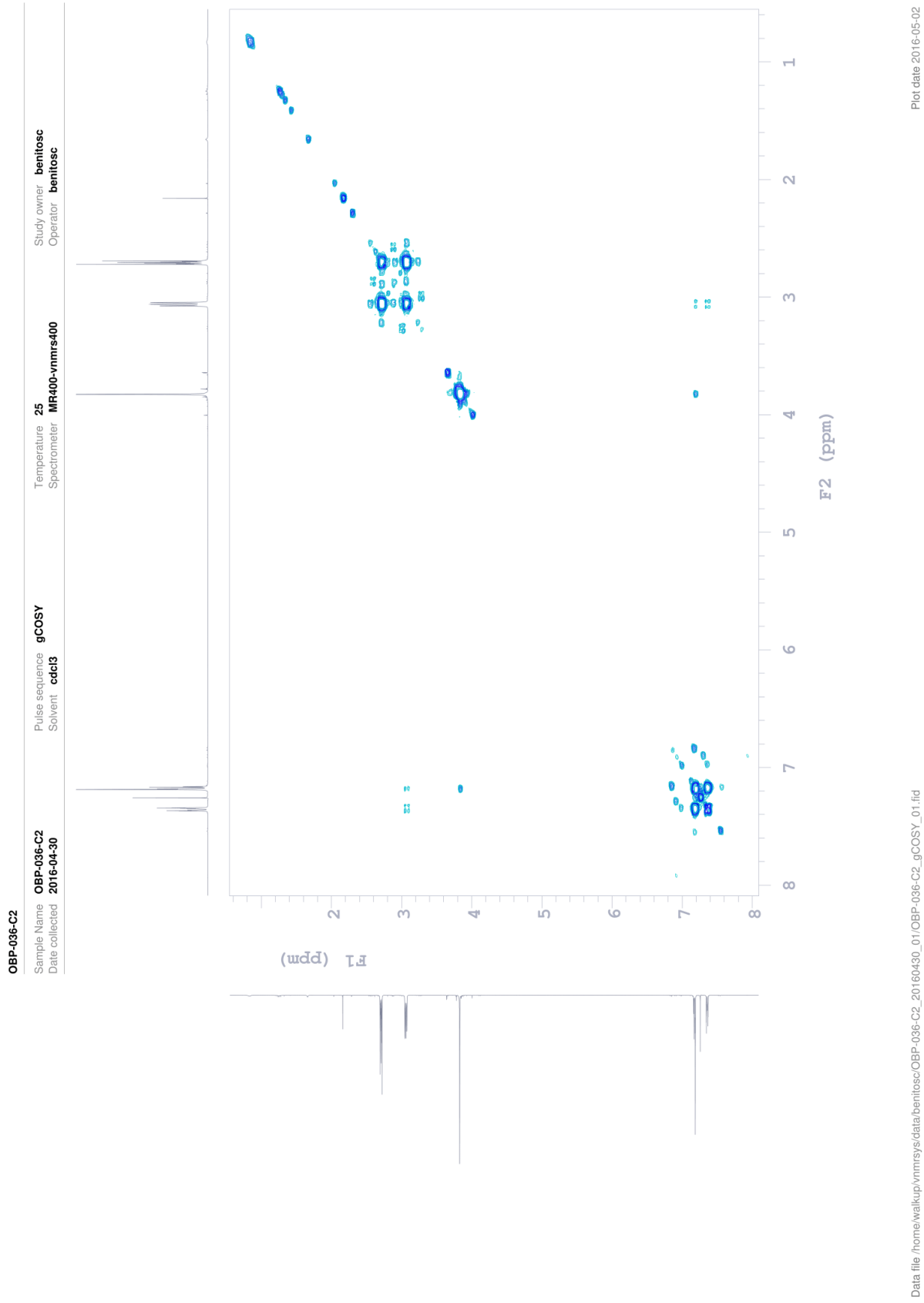

Figure 29. COSY NMR spectrum of compound 5.

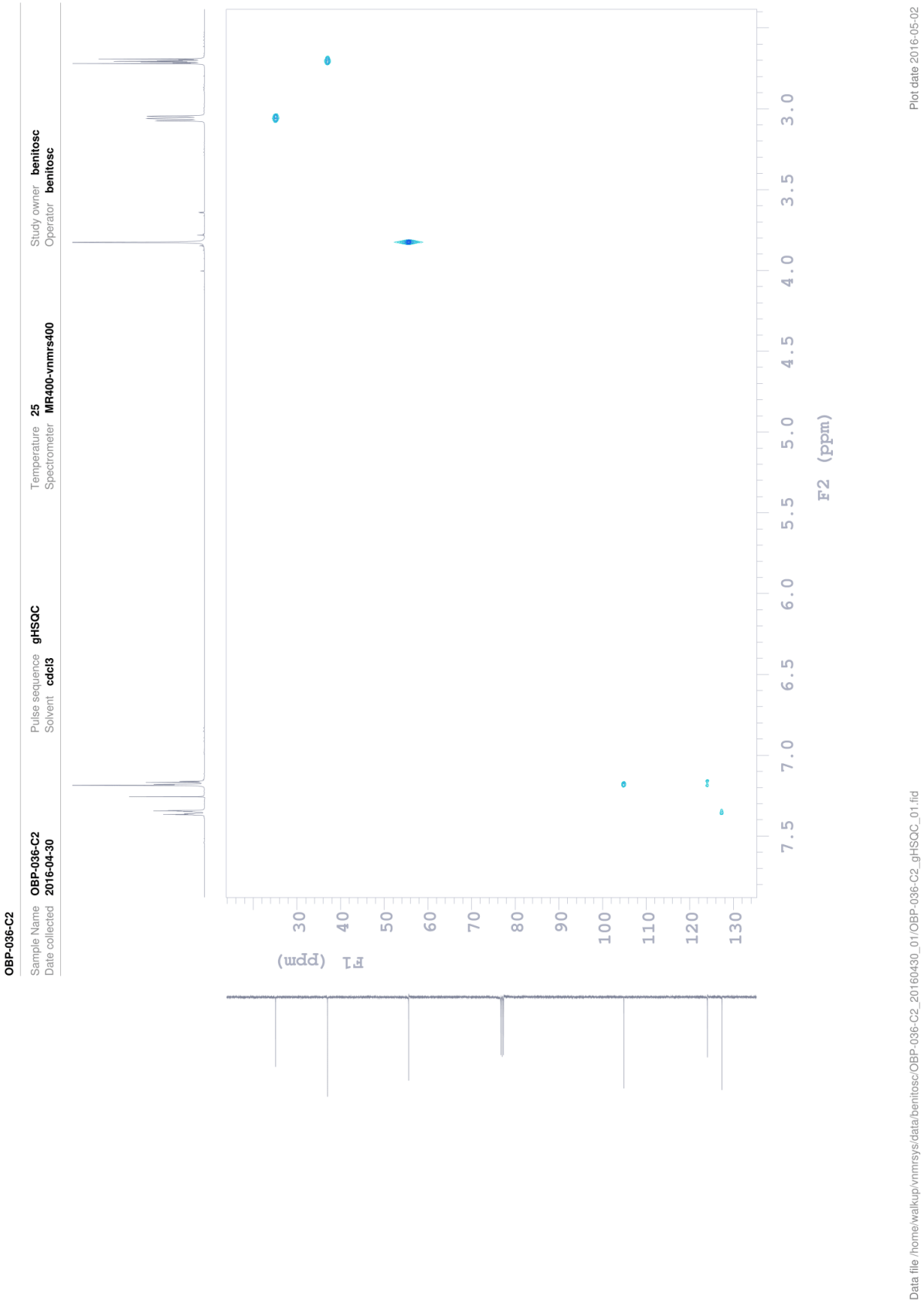

Figure 30. HSQC NMR spectrum of compound 5.

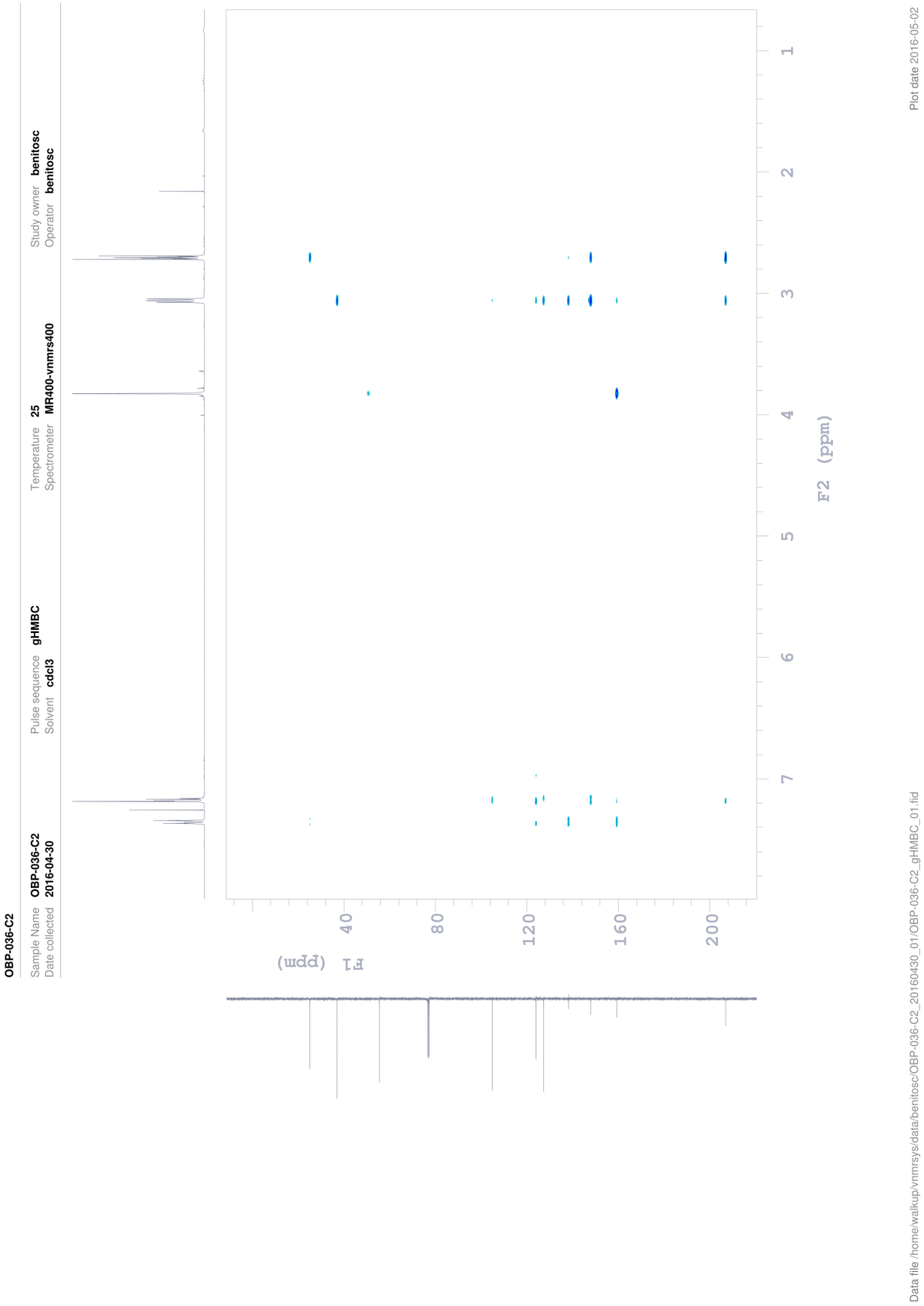

Figure 31. HMBC NMR spectrum of compound 5.

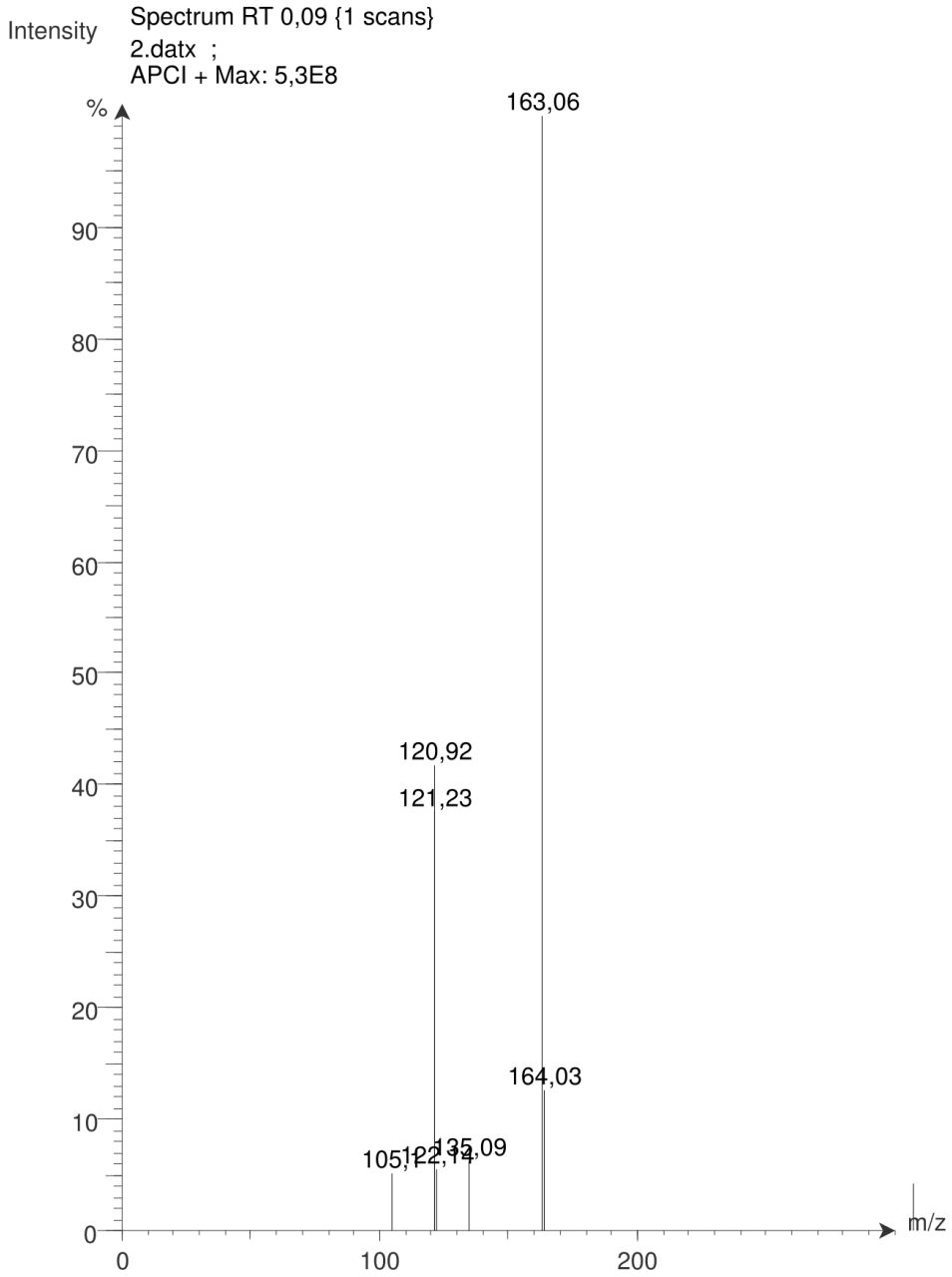

Figure 32. MS spectrum of compound 5.

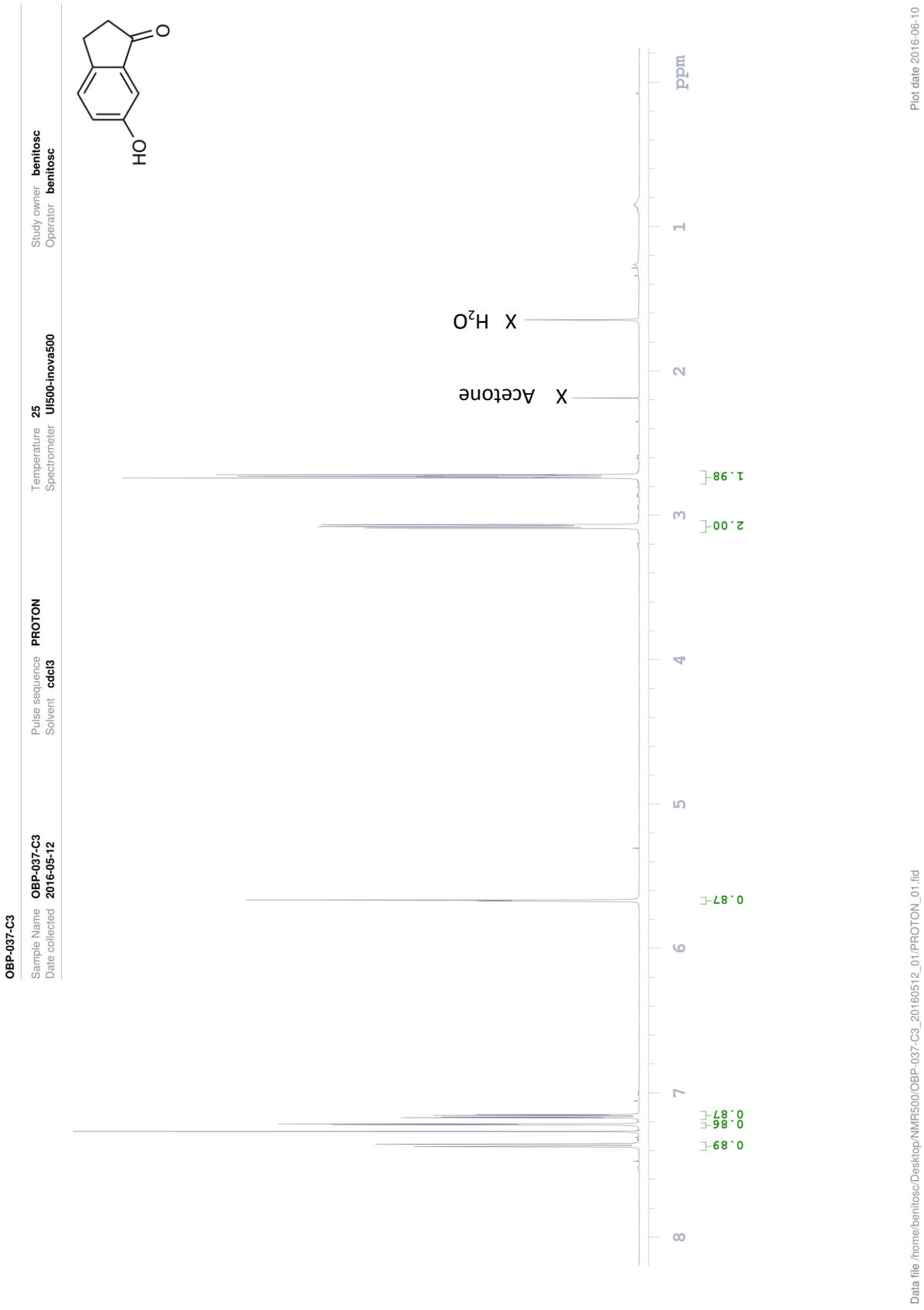

Figure 33. ^{1}H-NMR spectrum of compound 3.

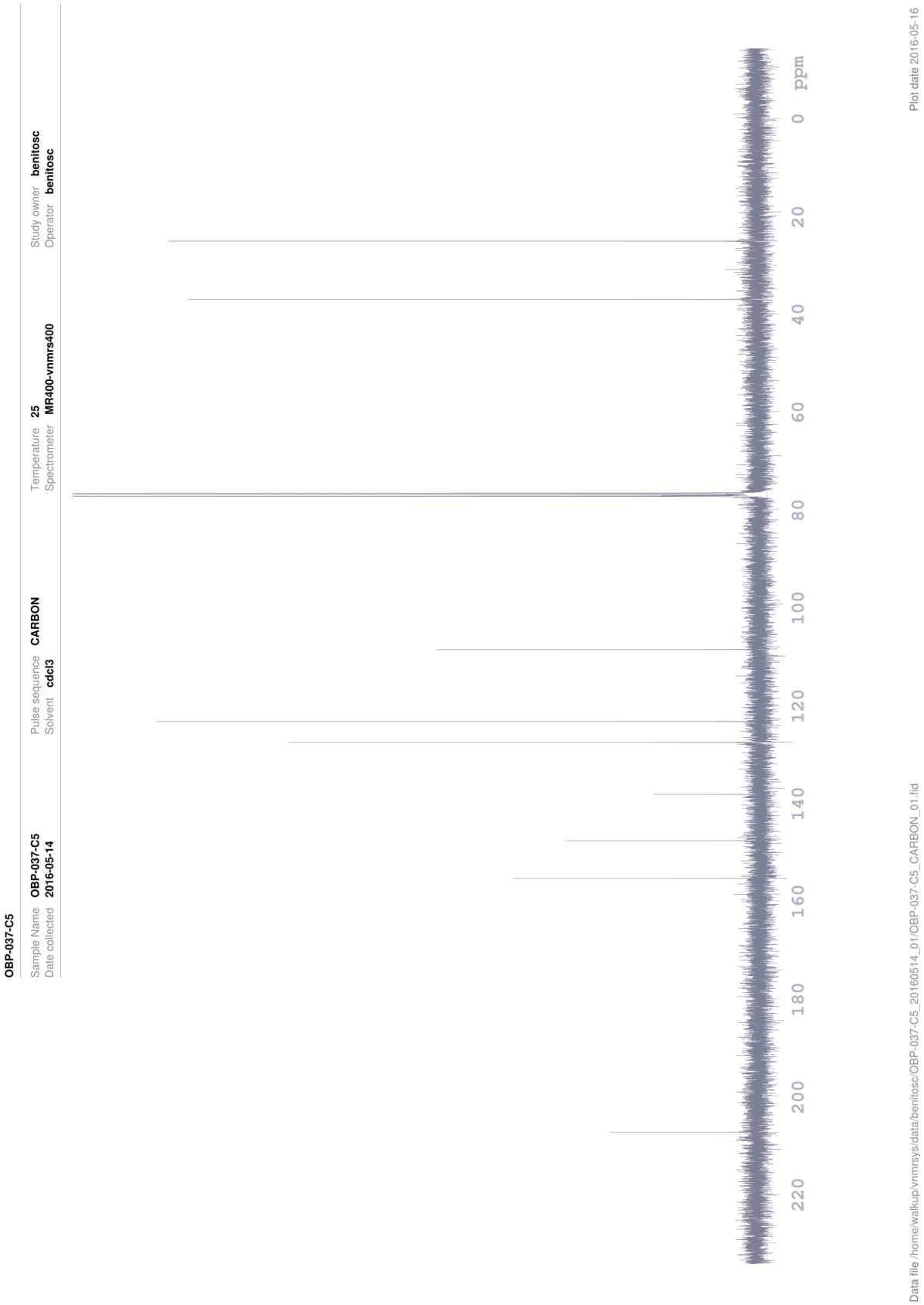

Figure 34. ^{13}C-NMR spectrum of compound 3.

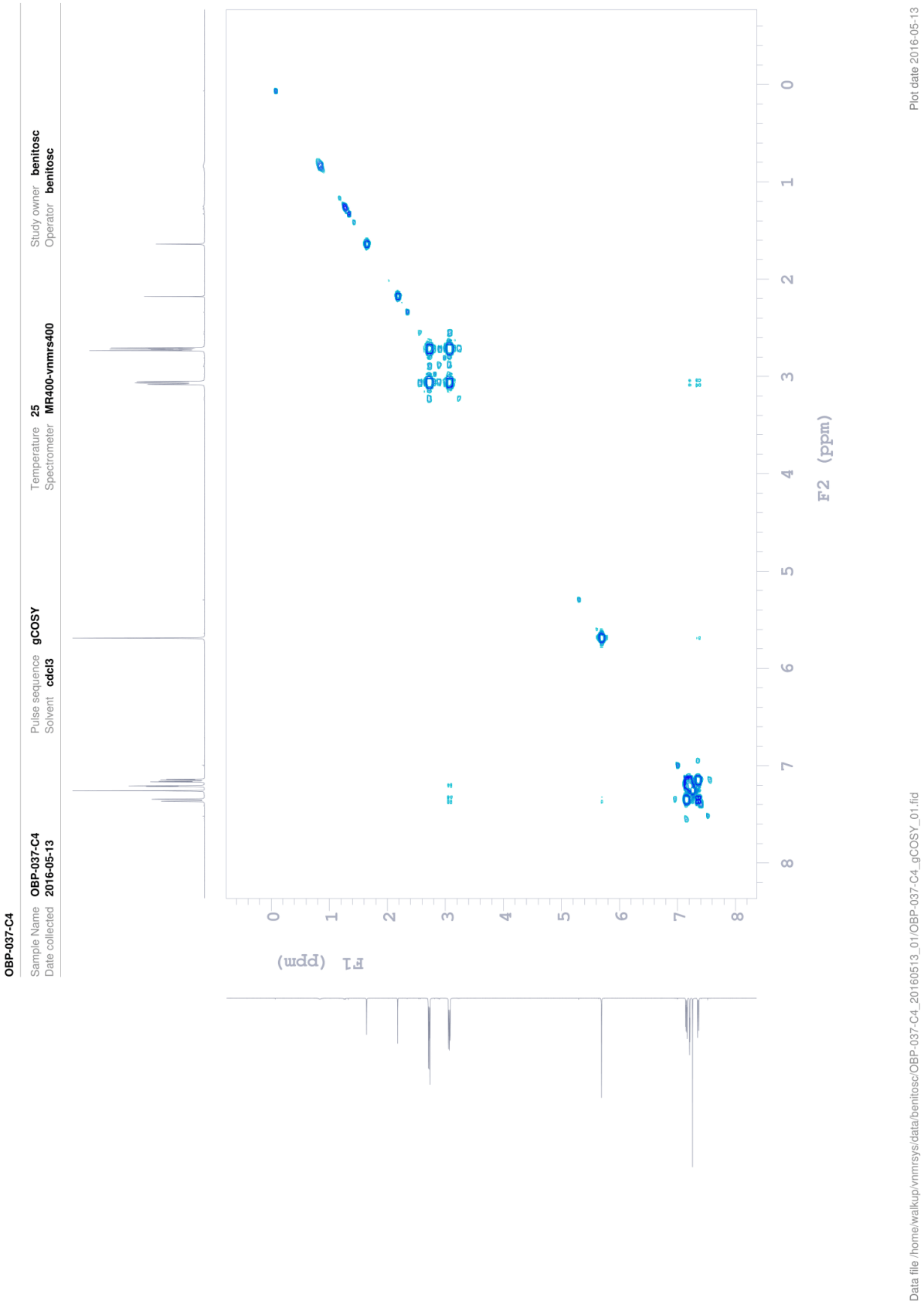

Figure 35. COSY NMR spectrum of compound 3.

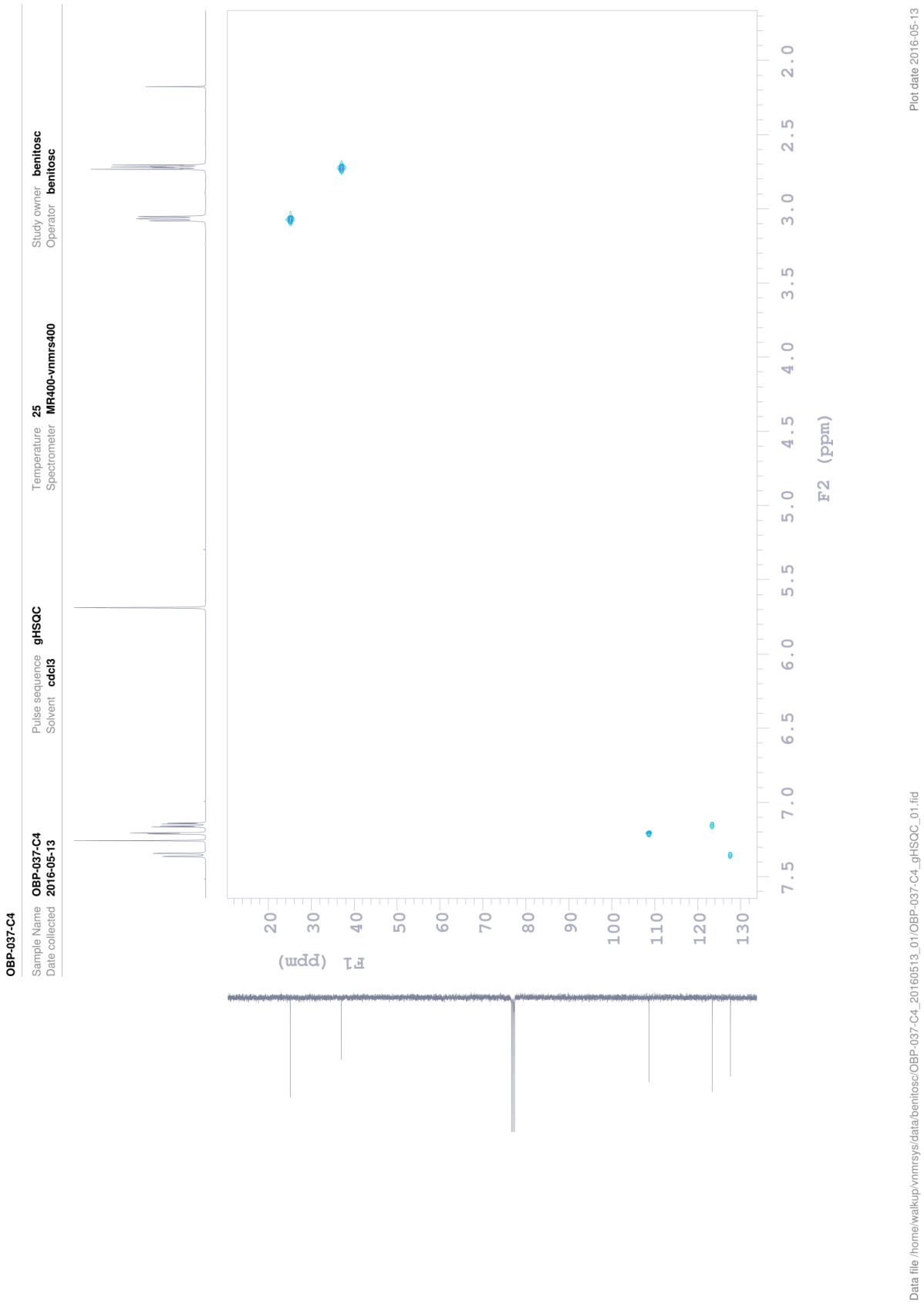

Figure 36. HSQC NMR spectrum of compound 3.

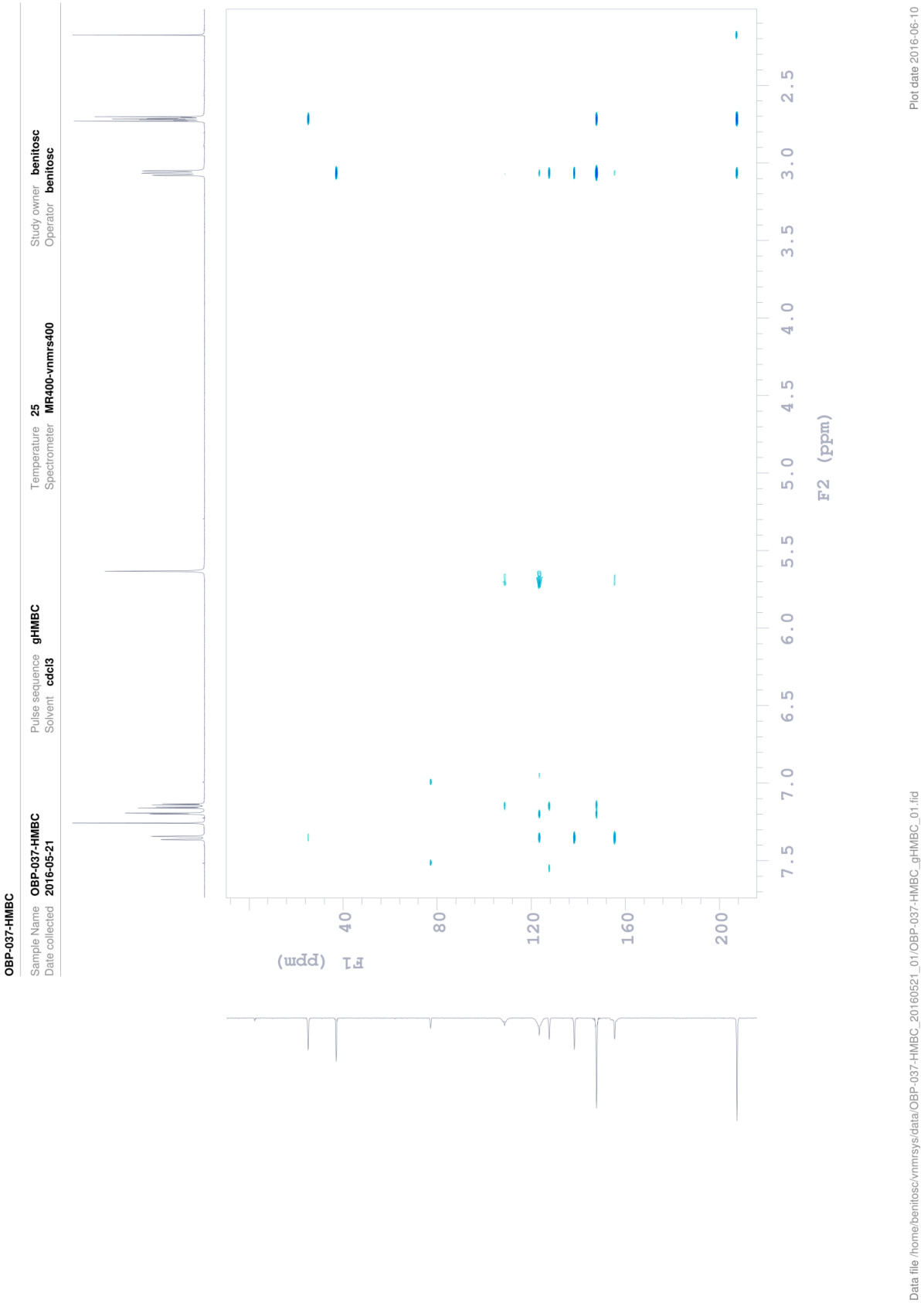

Figure 37. HMBC NMR spectrum of compound 3.

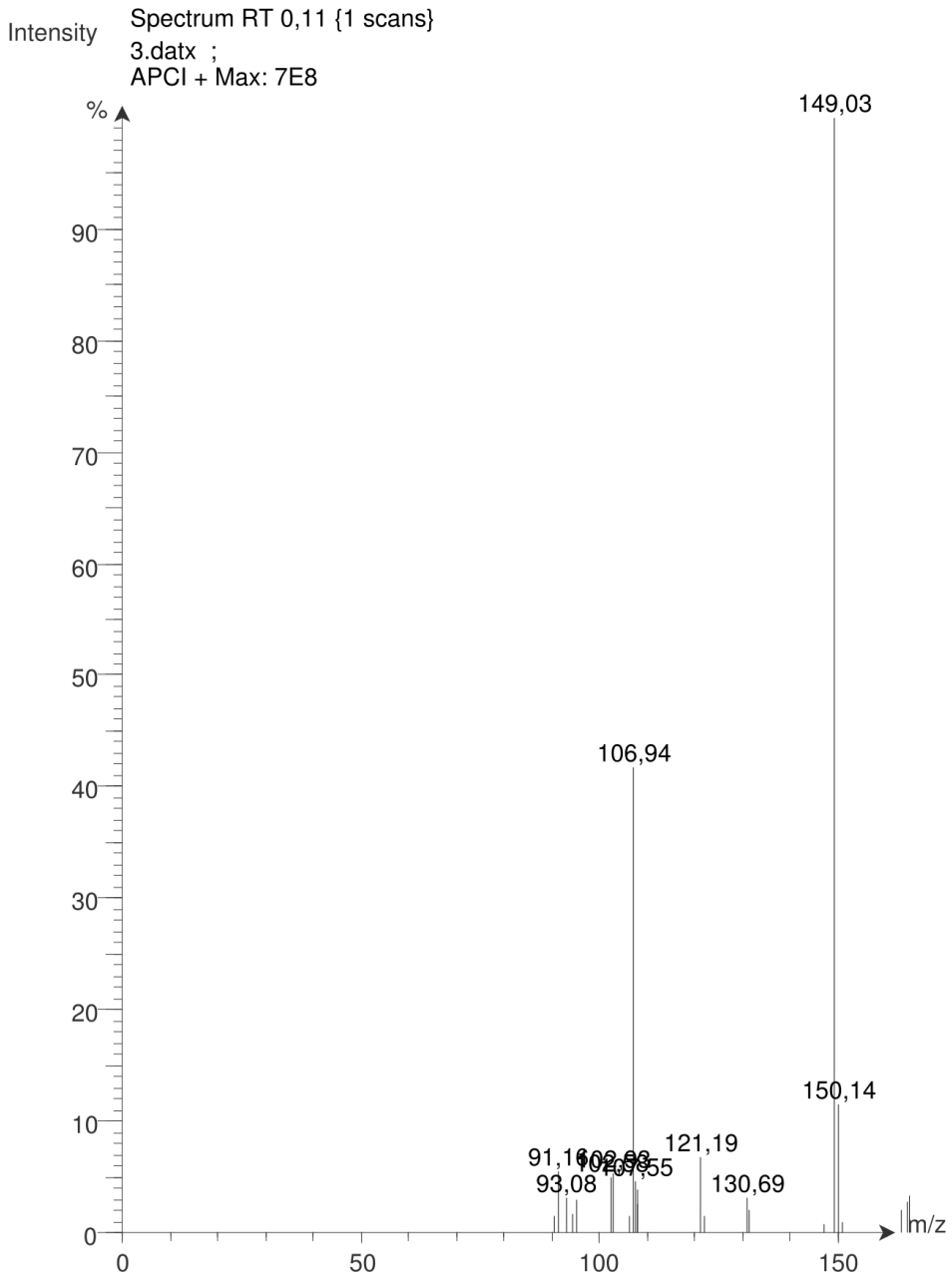

Figure 38. MS spectrum of compound 3.

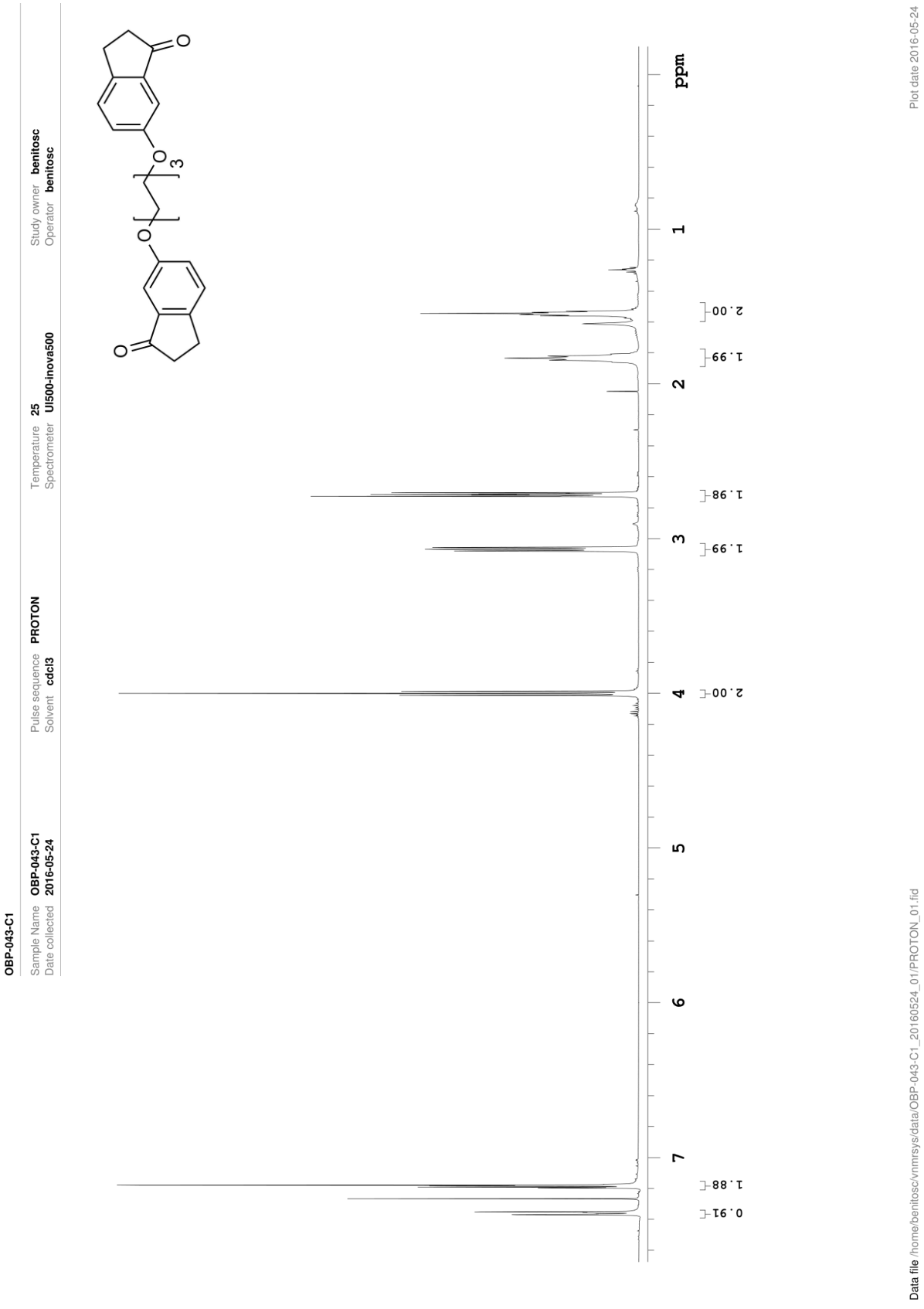

Figure 39. ^{1}H-NMR spectrum of compound 2a.

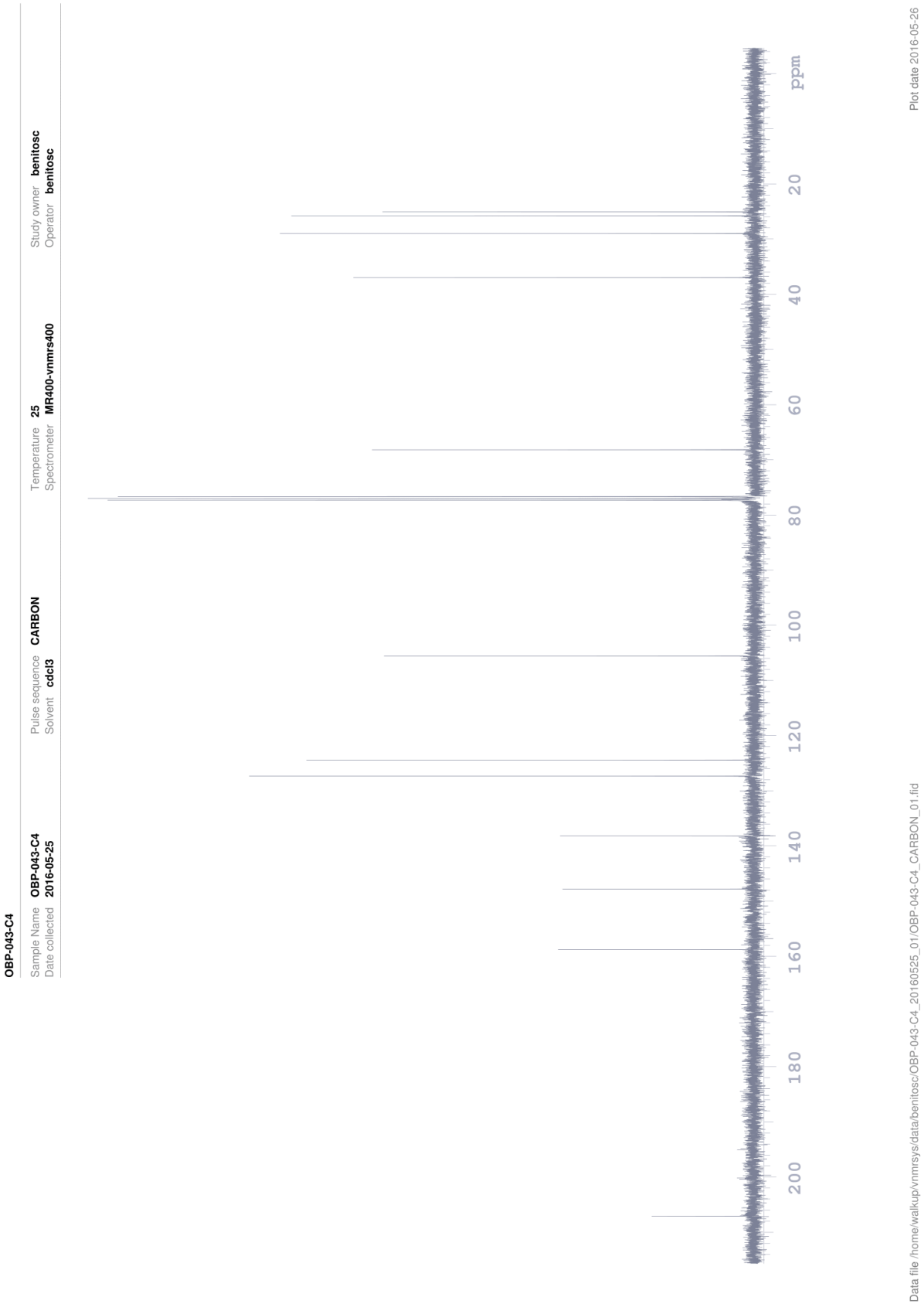

Figure 40. ^{13}C-NMR spectrum of compound 2a.

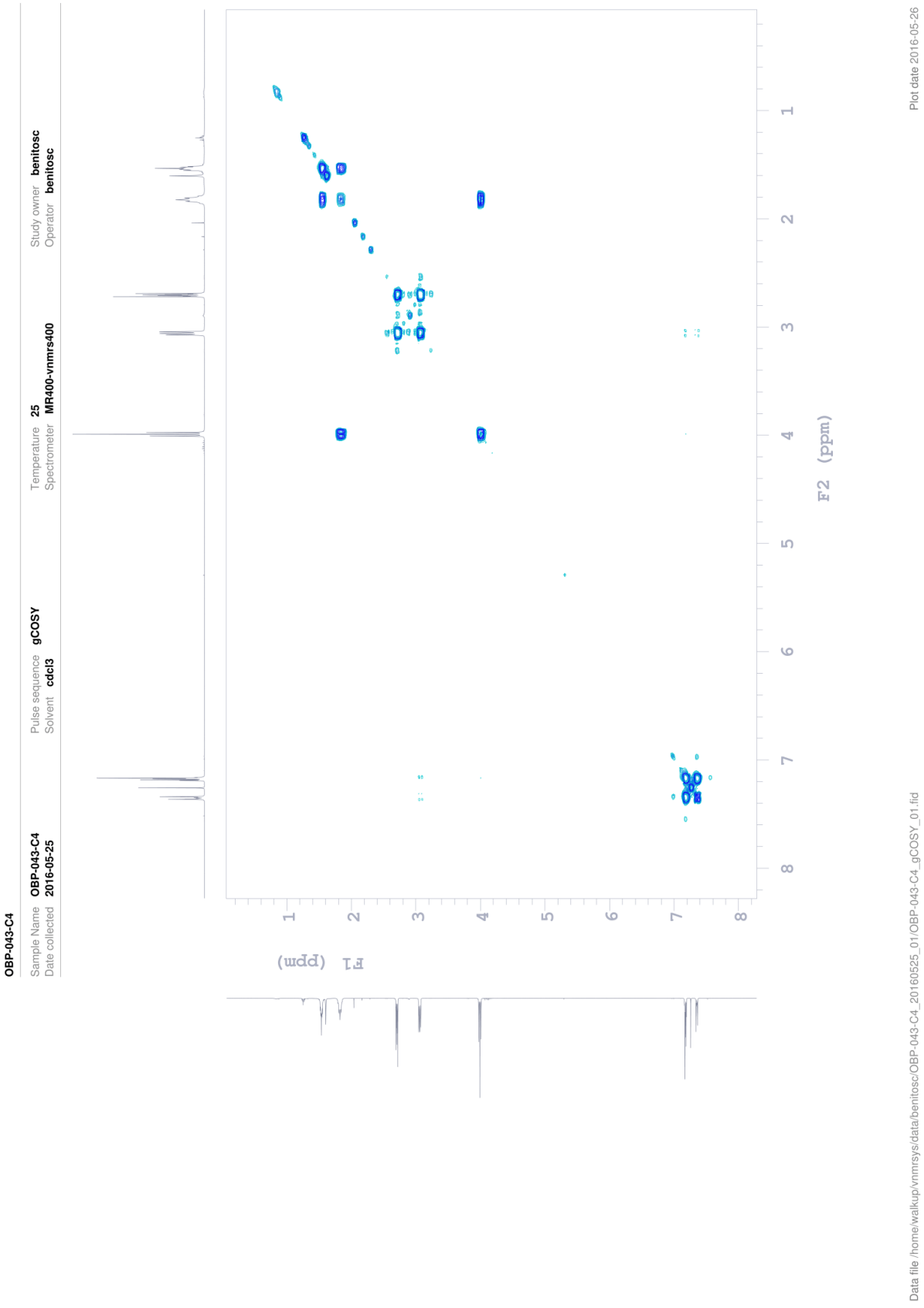

Figure 41. COSY NMR spectrum of compound 2a.

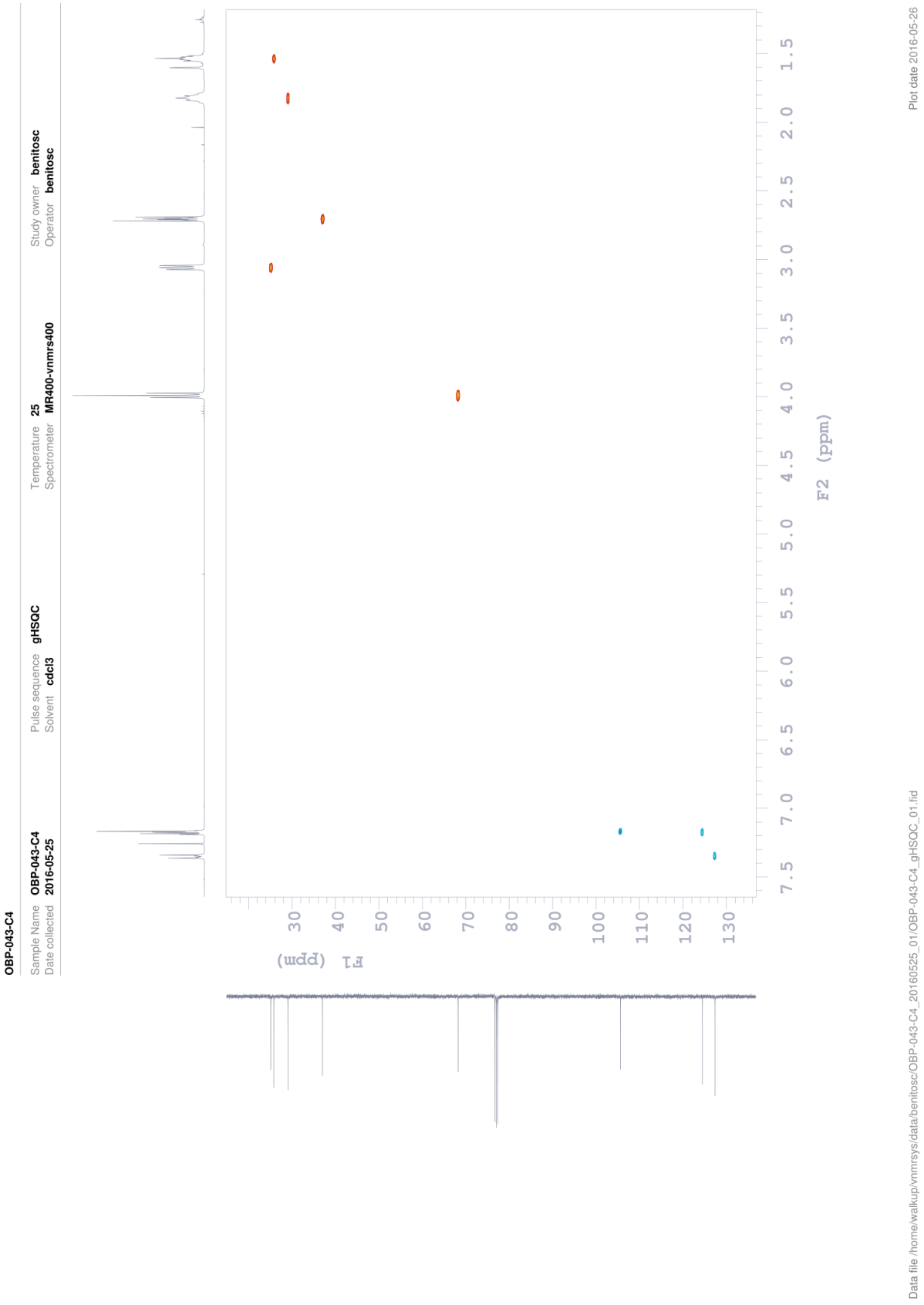

Figure 42. HSQC NMR spectrum of compound 2a.

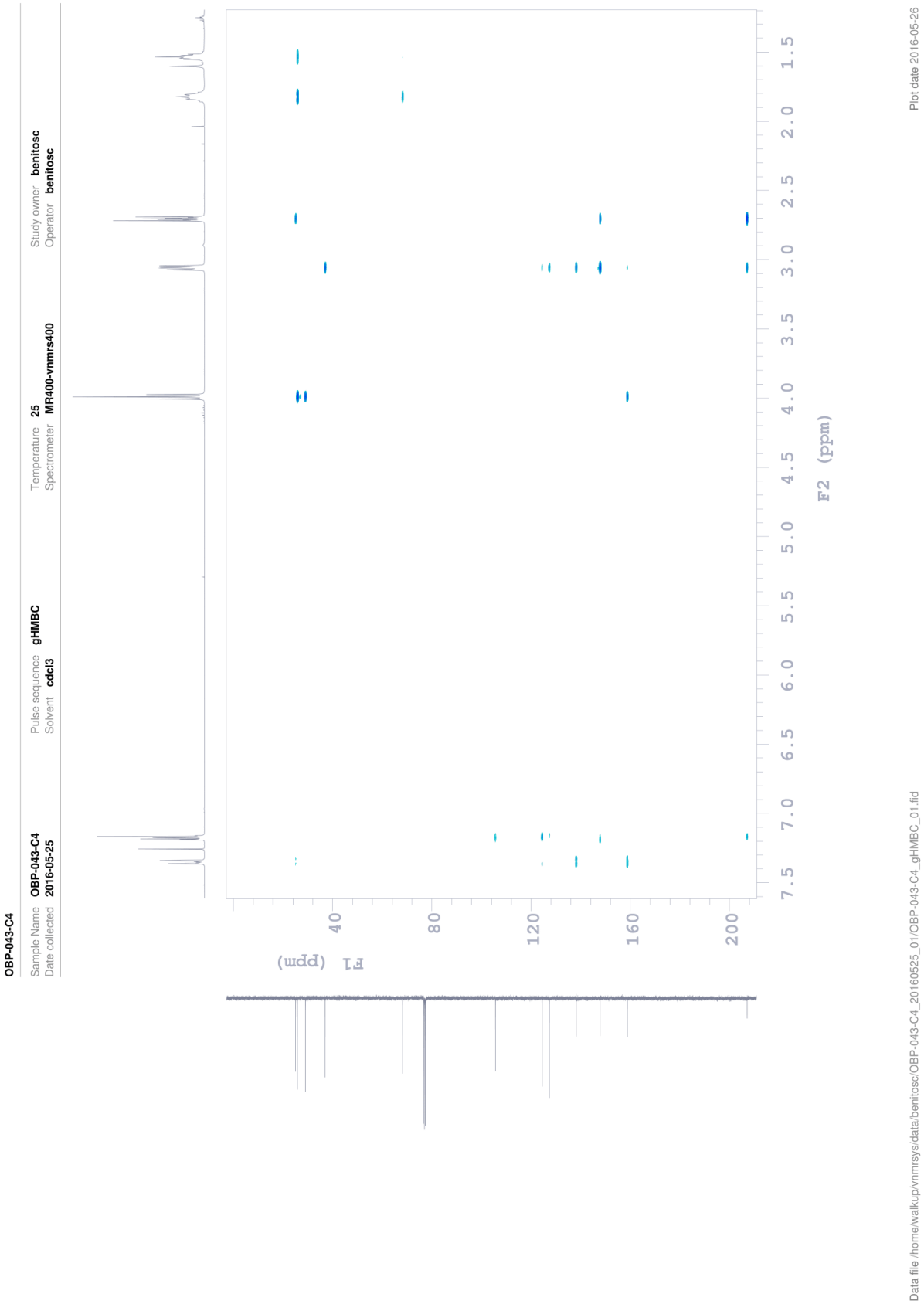

Figure 43. HMBC NMR spectrum of compound 2a.

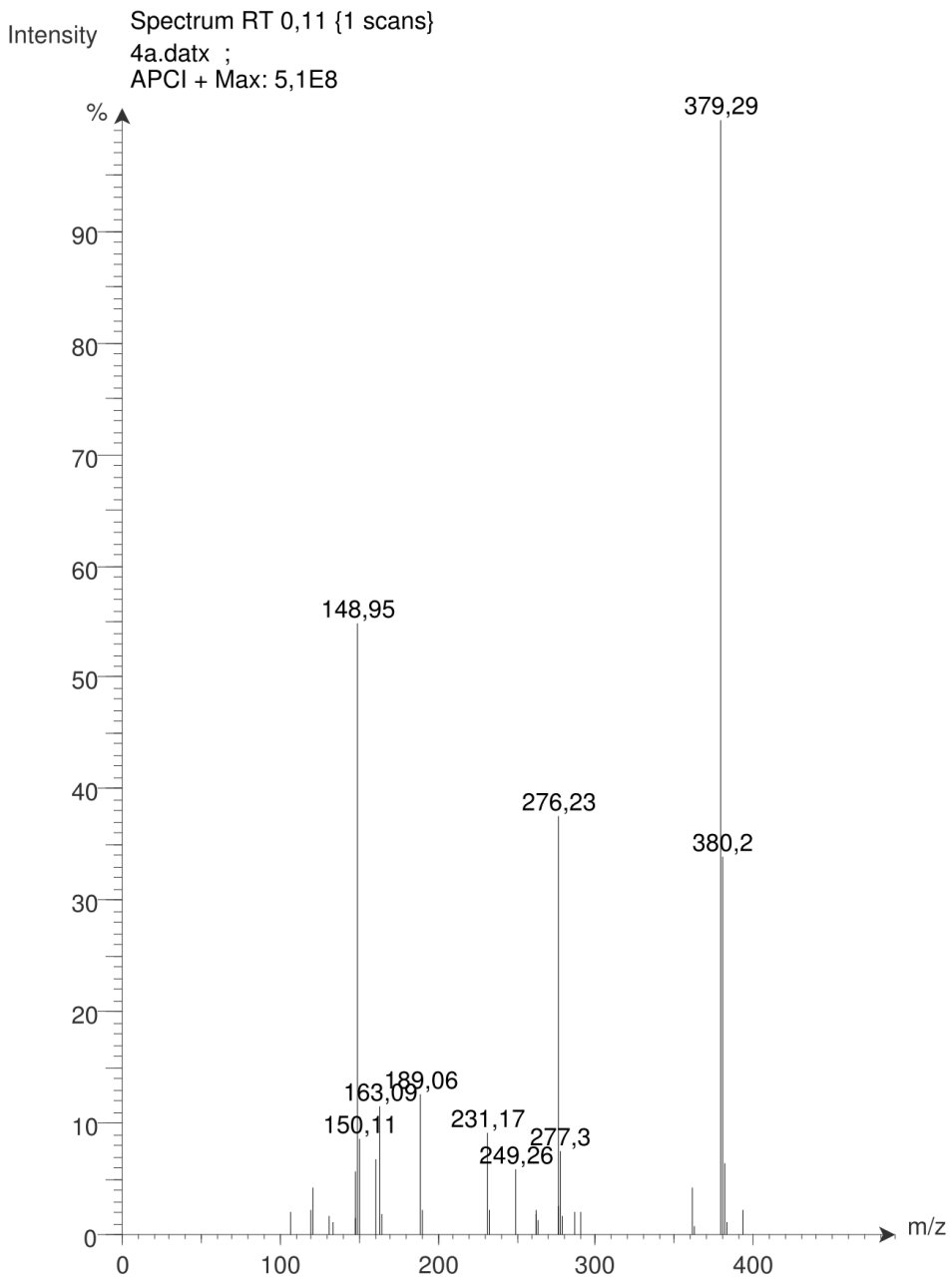

Figure 44. MS spectrum of compound 2a.

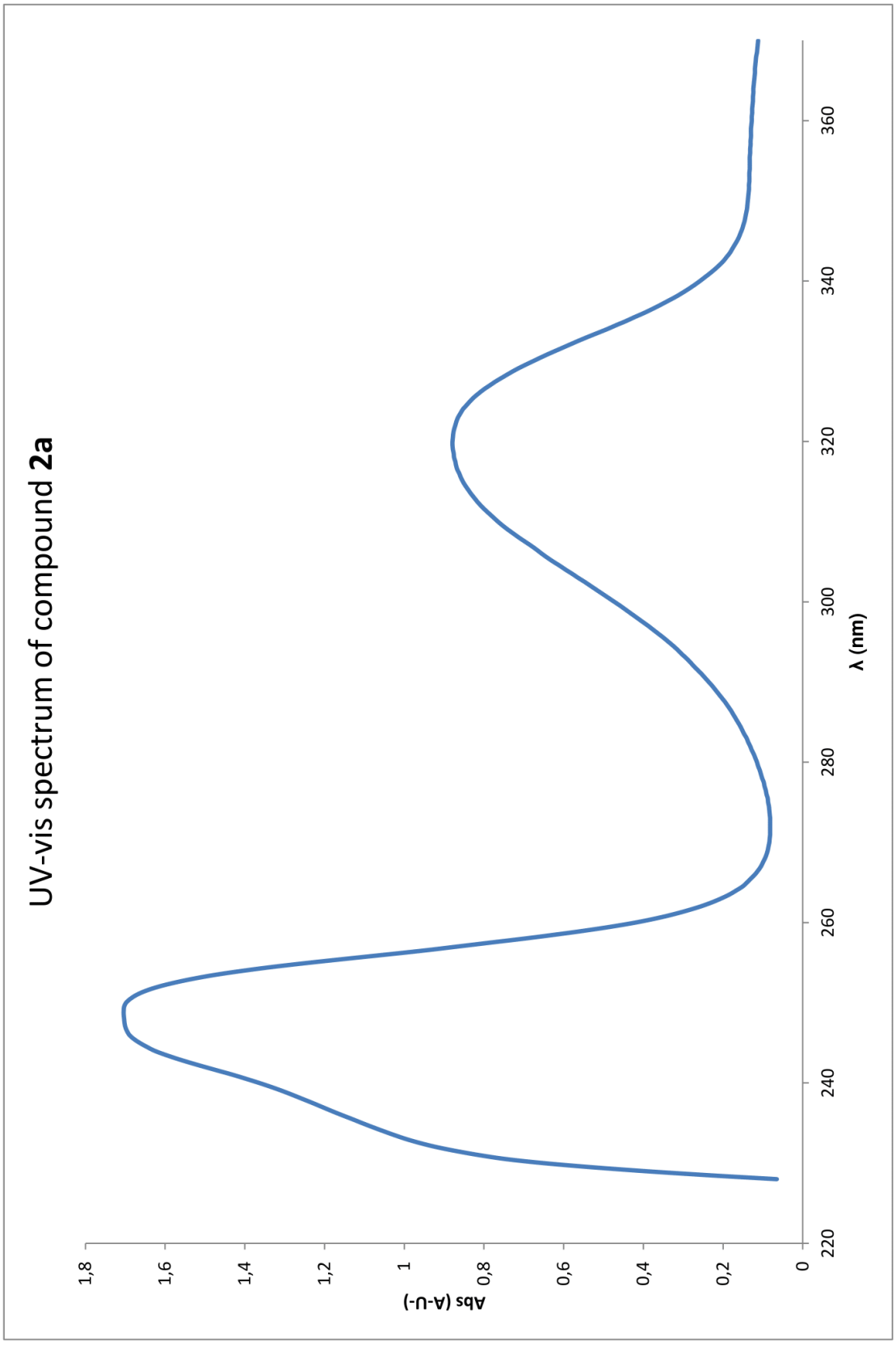

Figure 45. UV-vis spectrum of compound 2a.

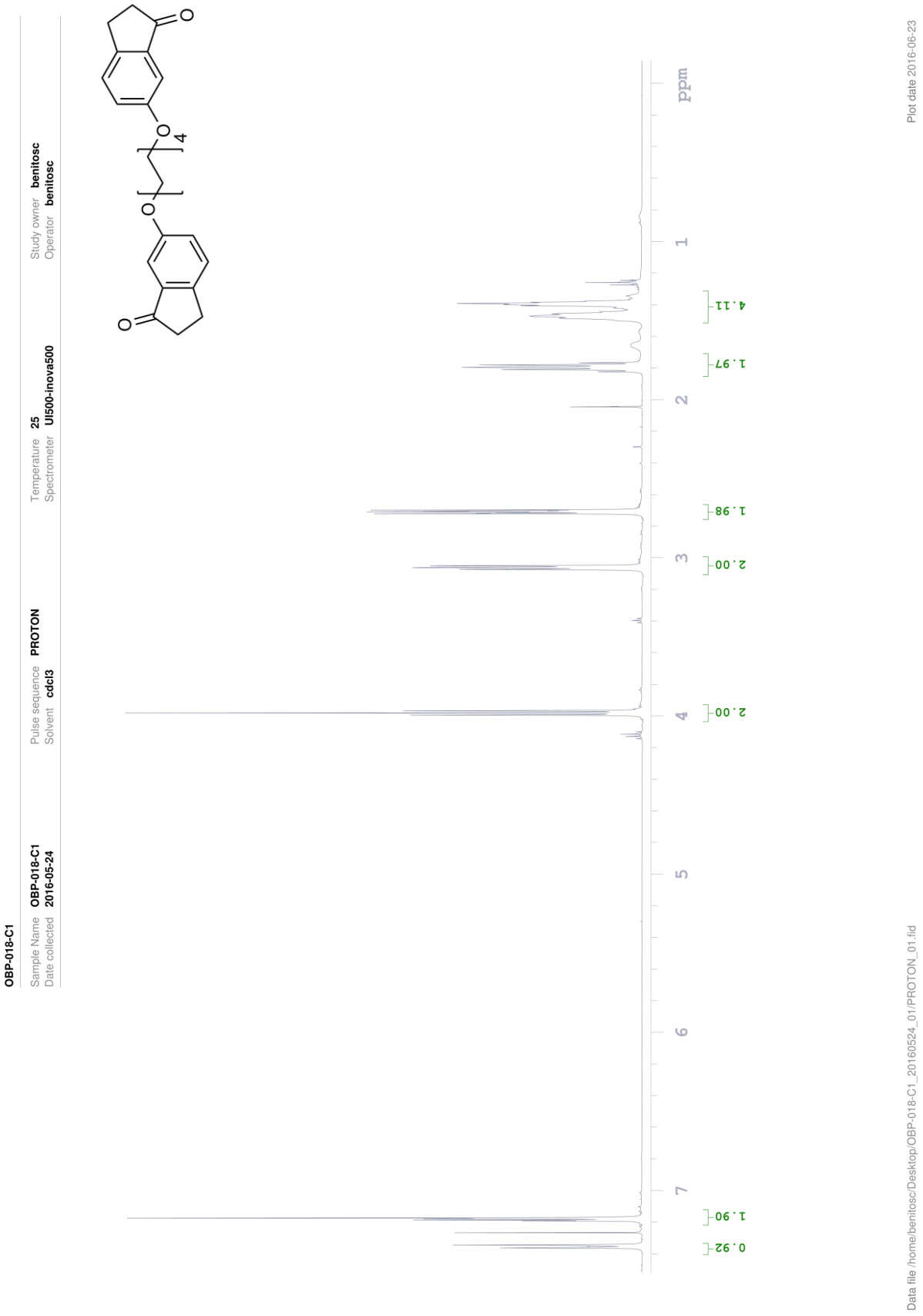

Figure 46. ^{1}H-NMR spectrum of compound 2b.

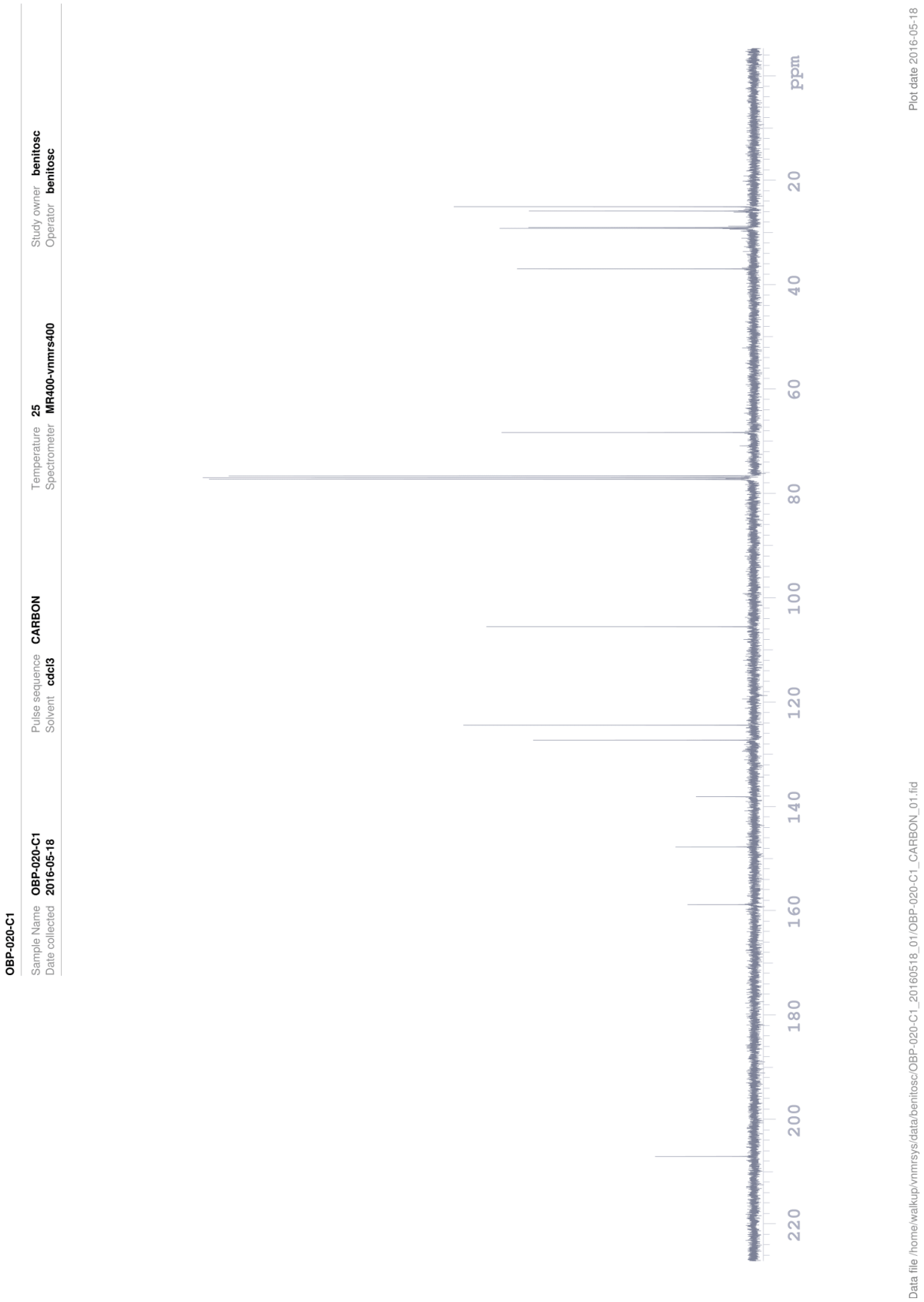

Figure 47. ^{13}C-NMR spectrum of compound 2b.

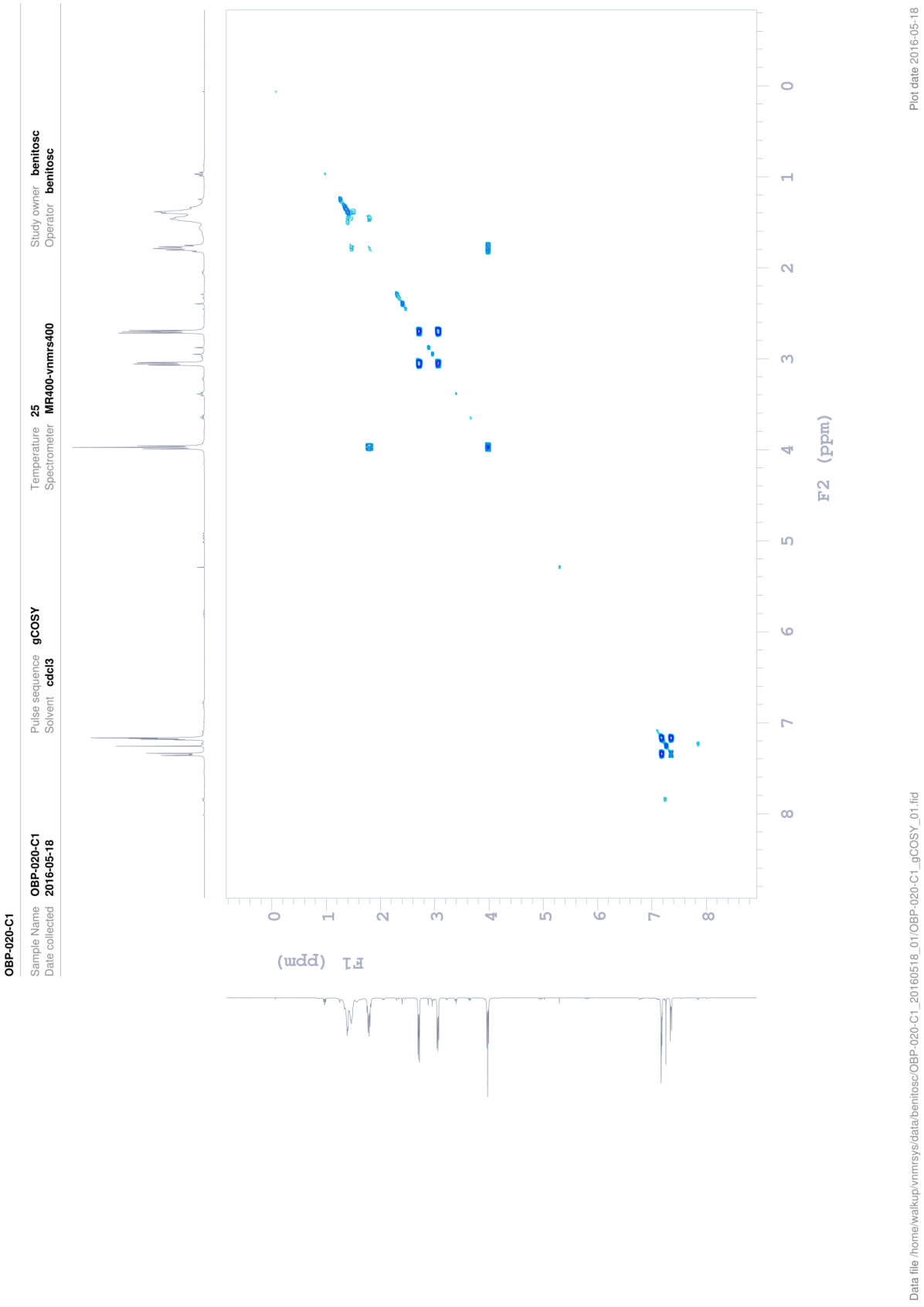

Figure 48. COSY NMR spectrum of compound 2b.

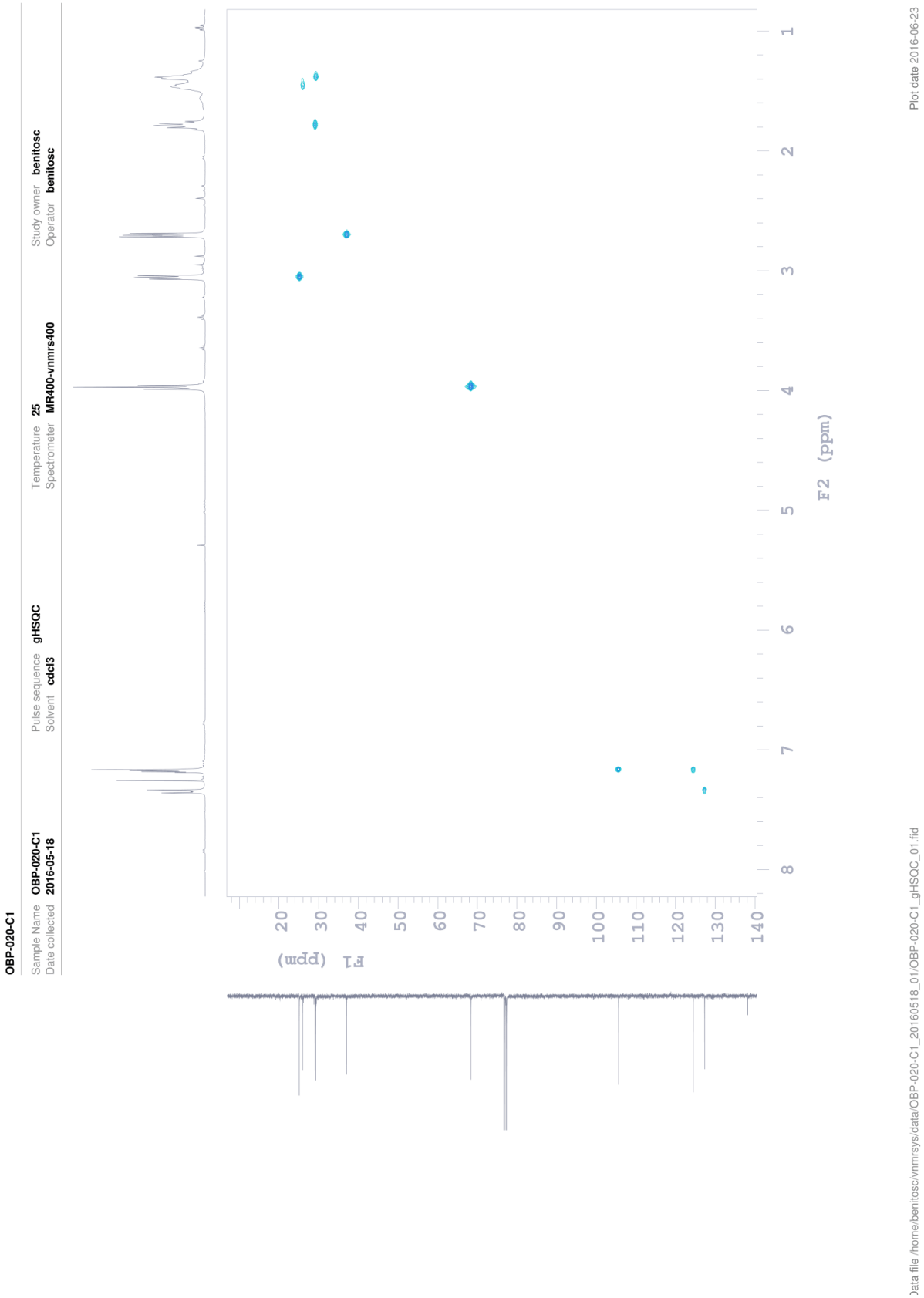

Figure 49. HSQC NMR spectrum of compound 2b.

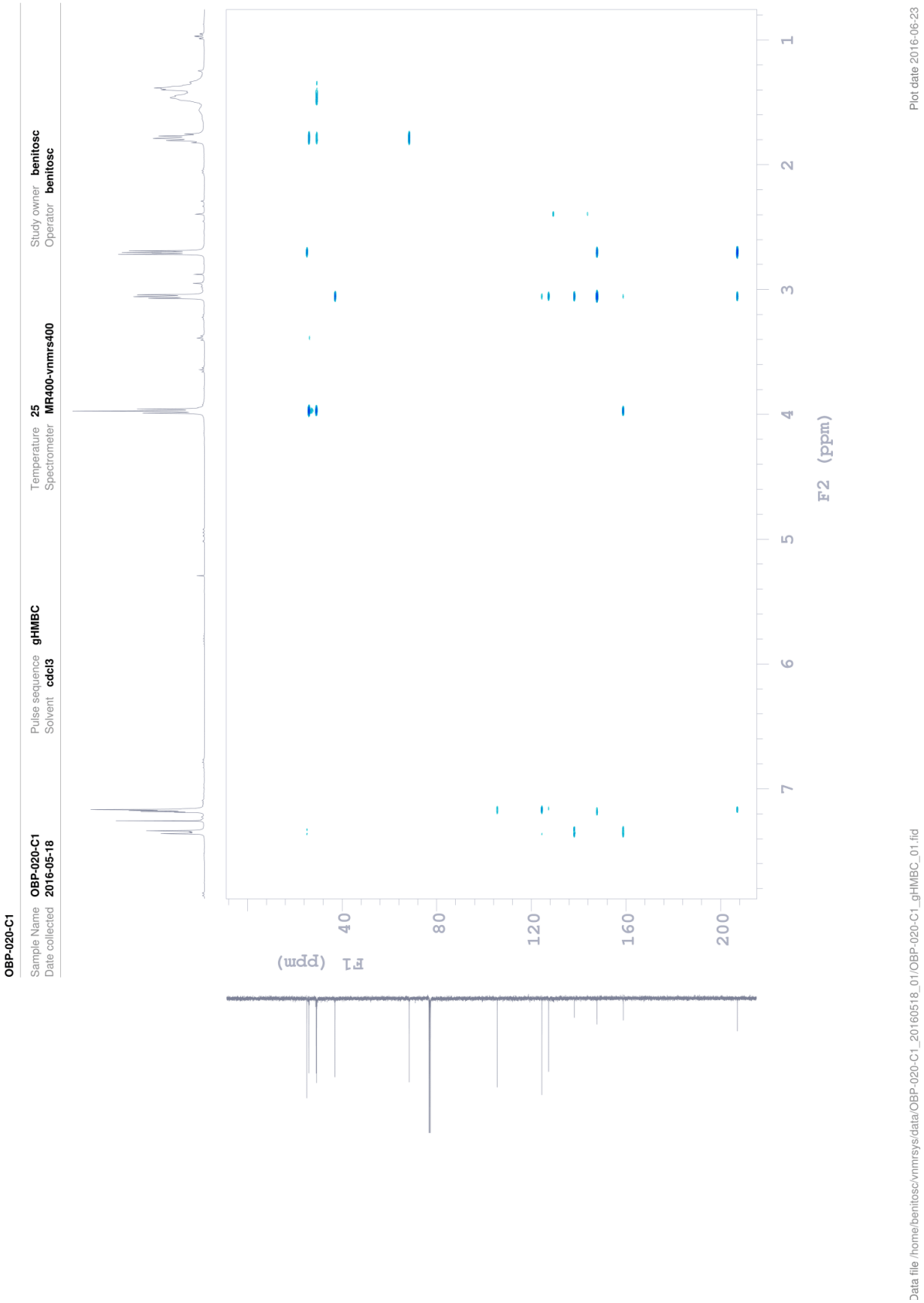

Figure 50. HMBC NMR spectrum of compound 2b.

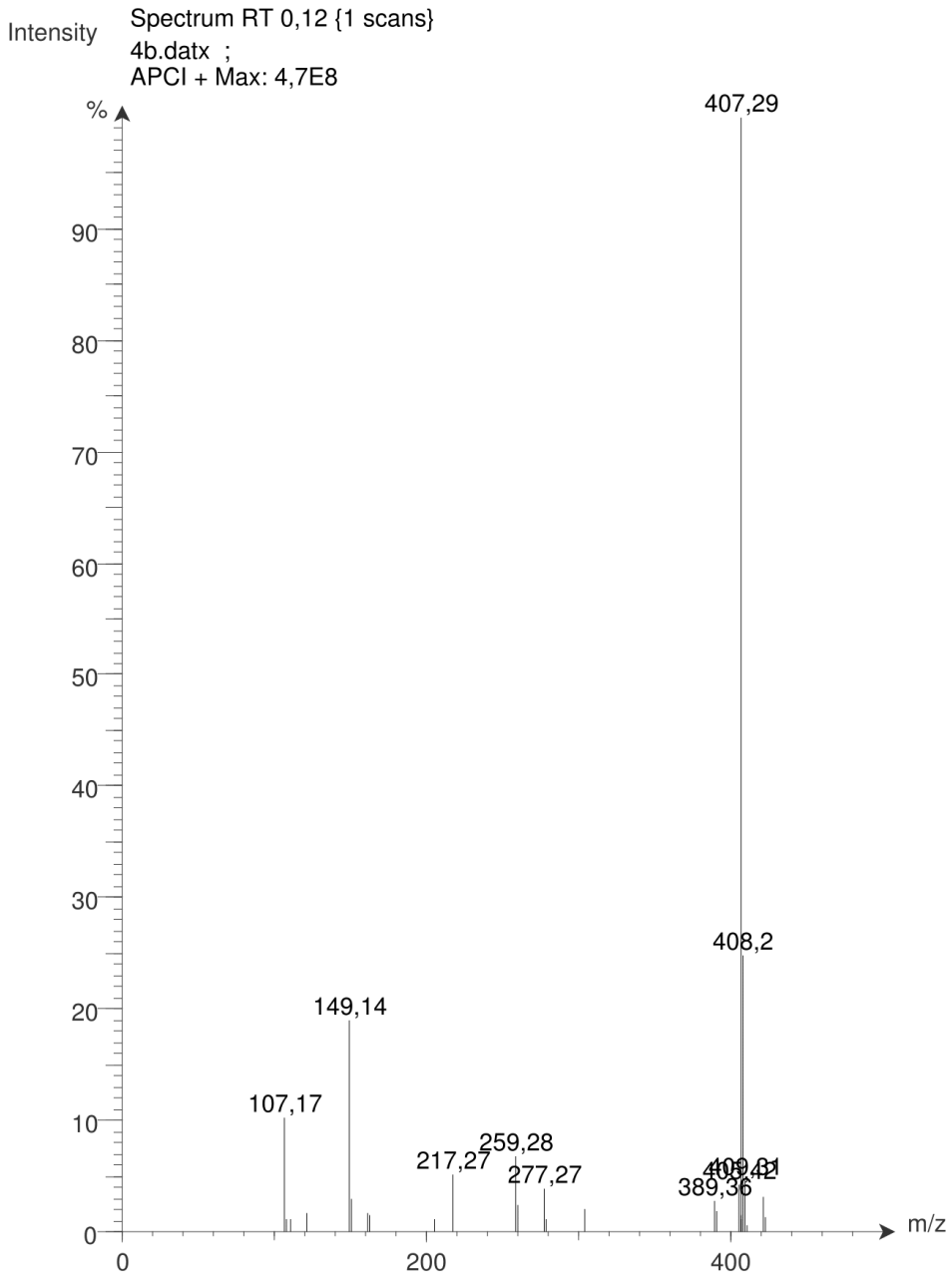

Figure 51. MS spectrum of compound 2b.

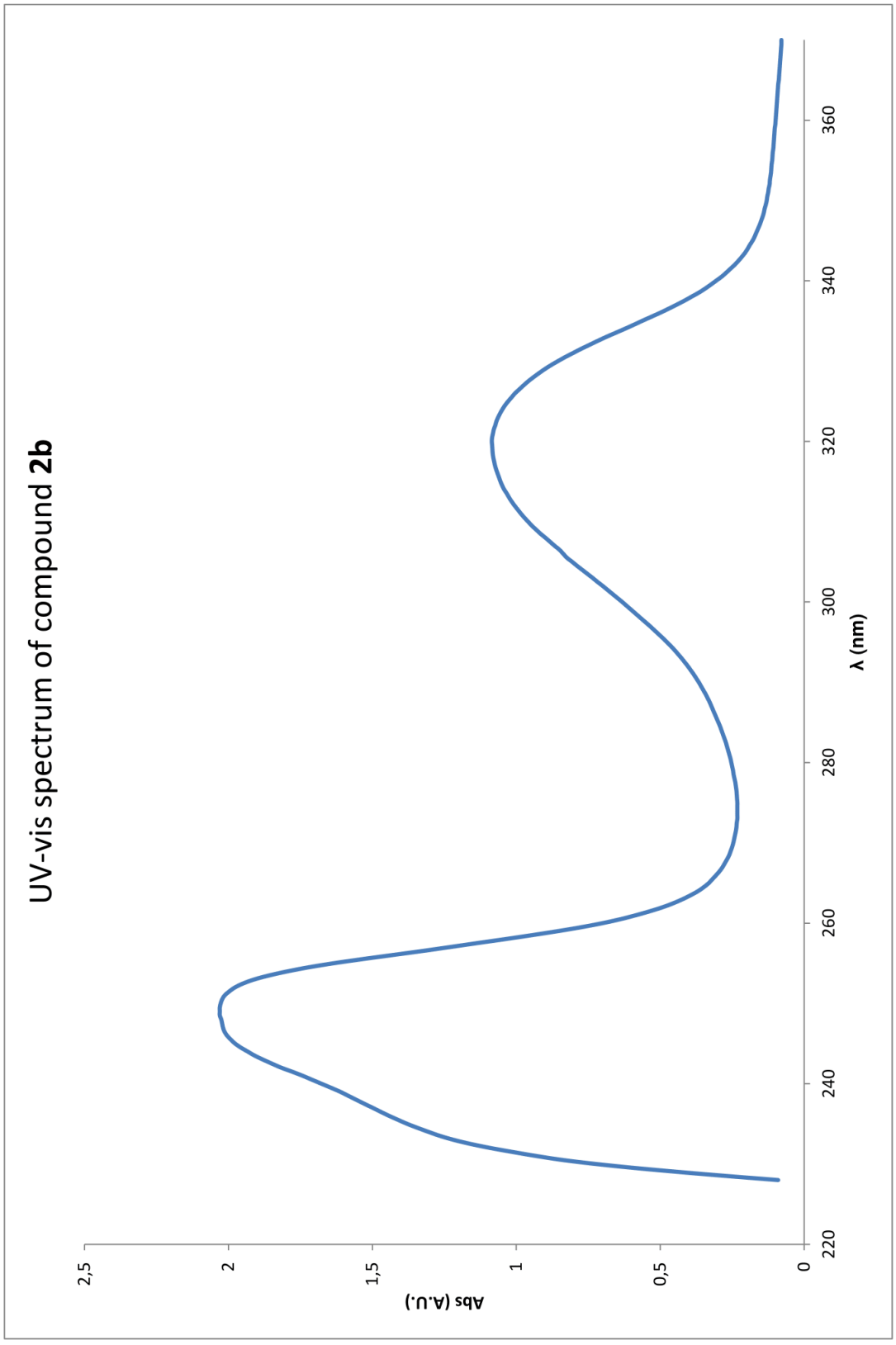

Figure 52. UV-vis spectrum of compound 2b.

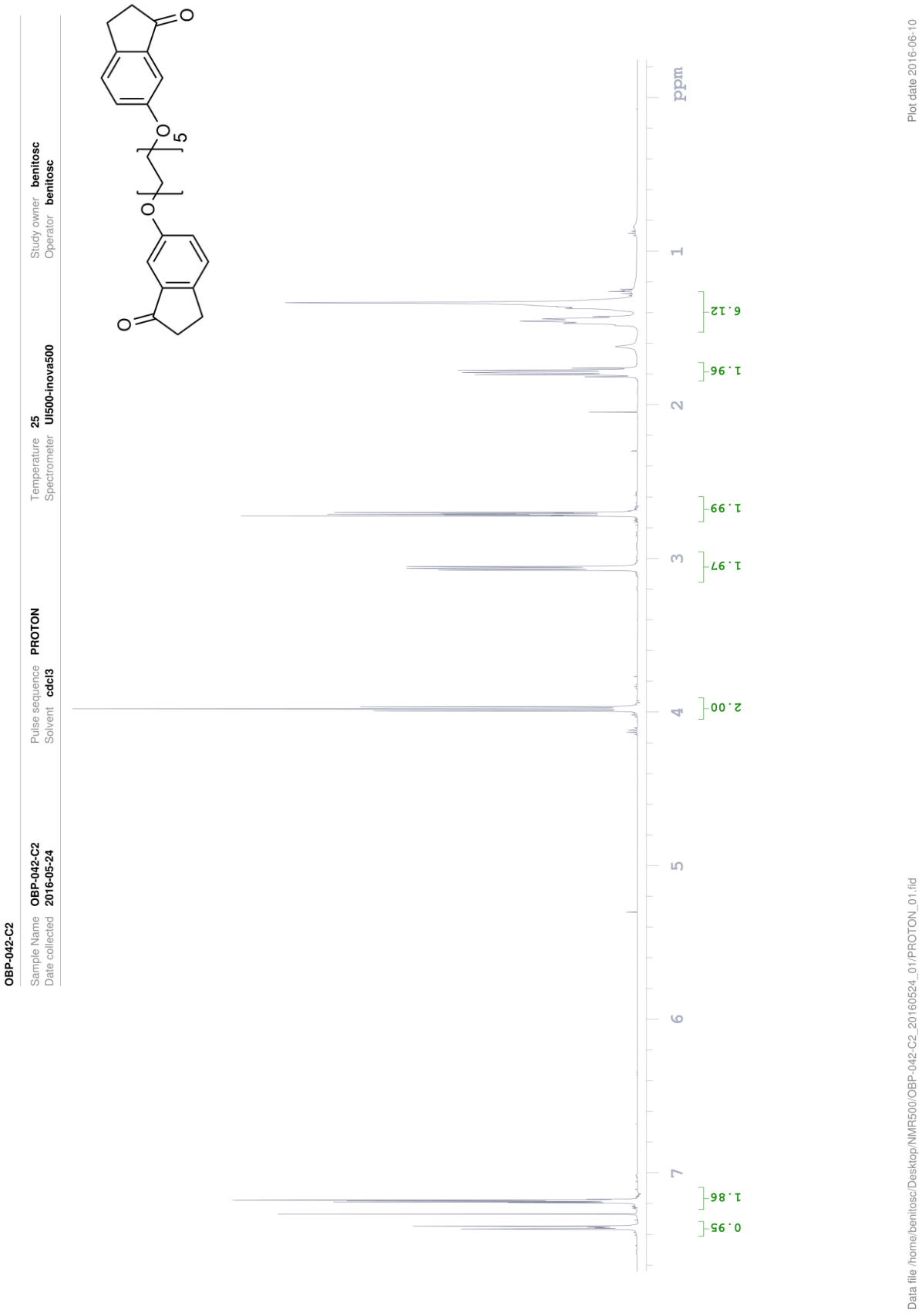

Figure 53. ^{1}H-NMR spectrum of compound 2c.

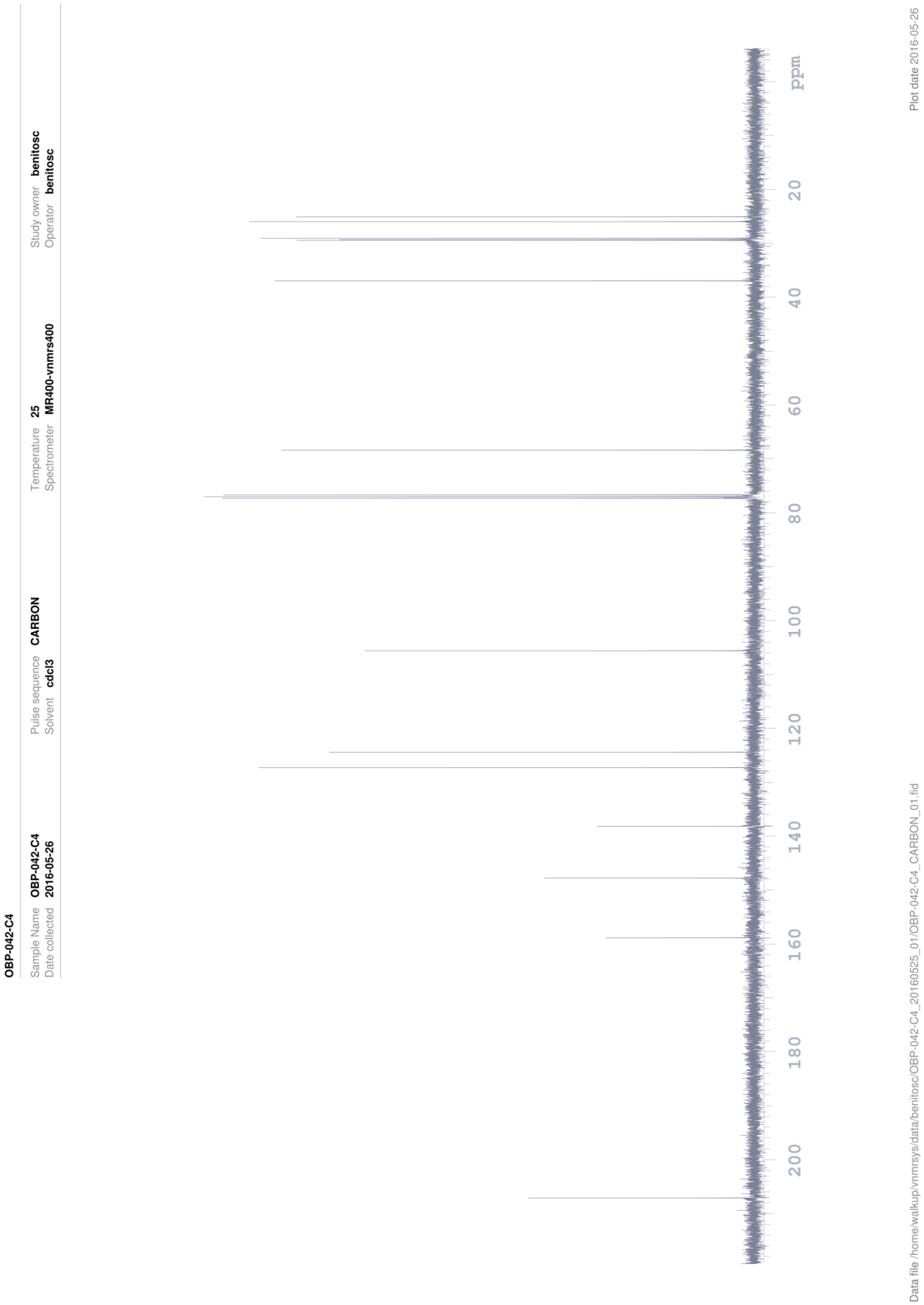

Figure 54. ^{13}C-NMR spectrum of compound 2c.

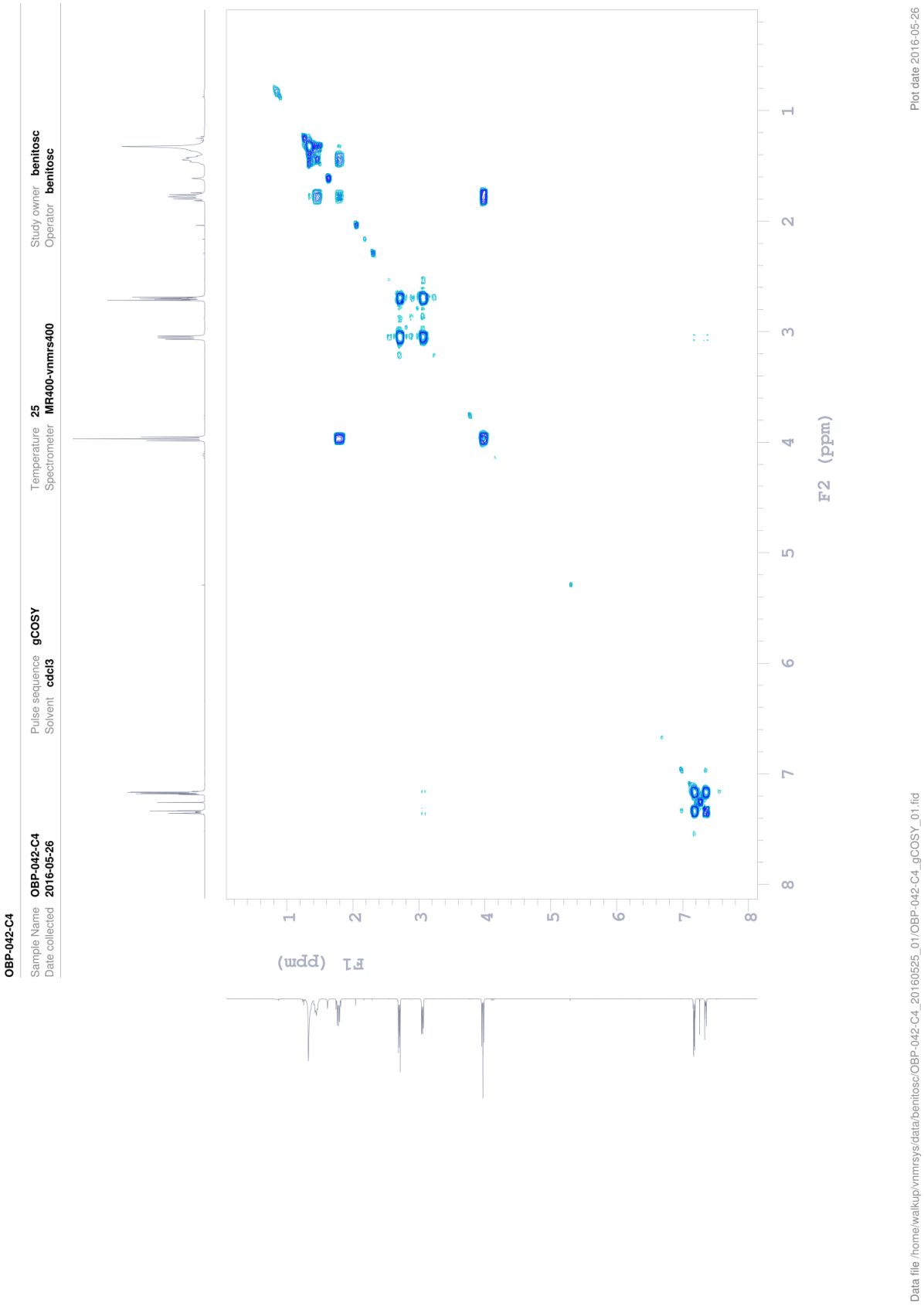

Figure 55. COSY NMR spectrum of compound 2c.

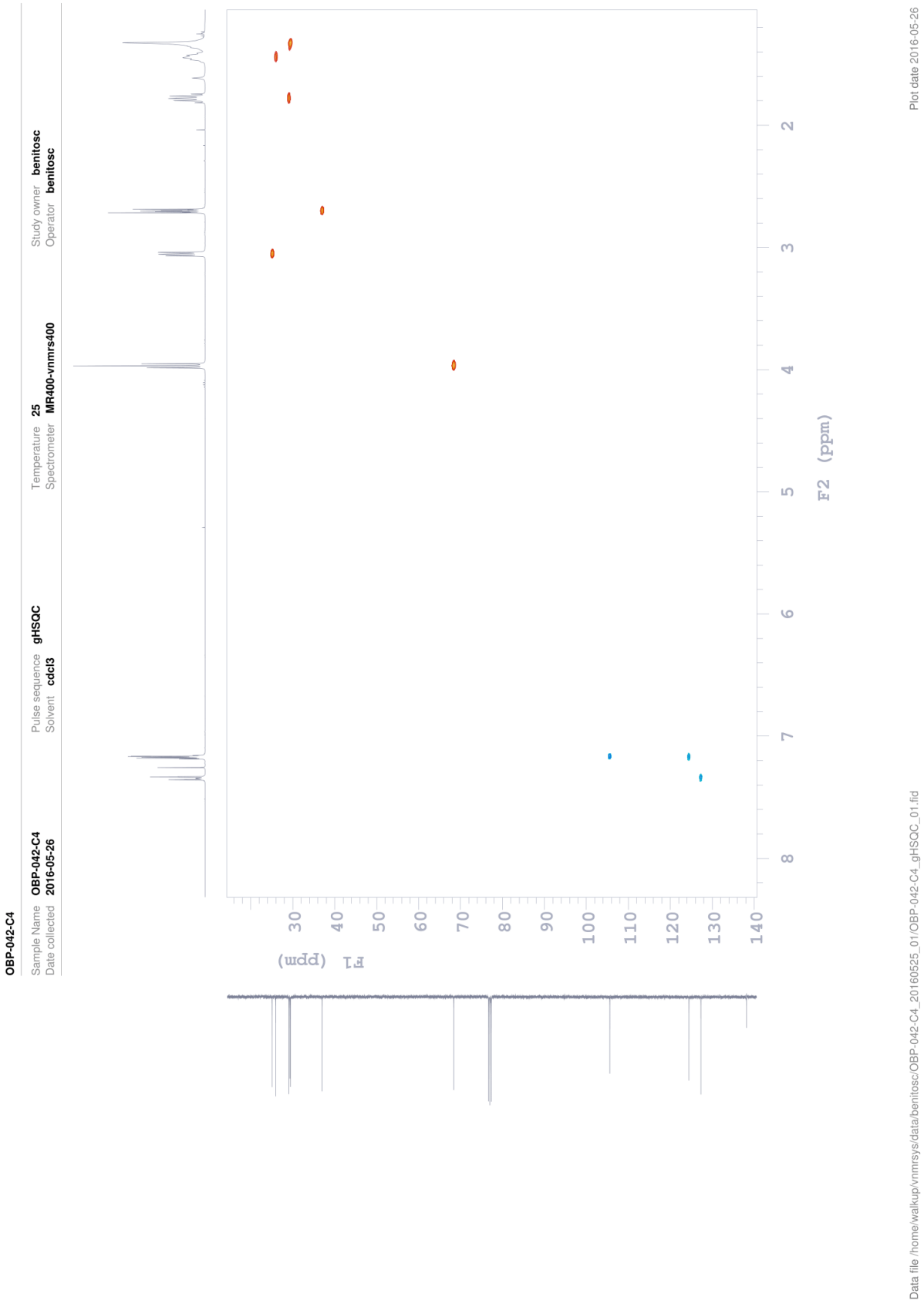

Figure 56. HSQC NMR spectrum of compound 2c.

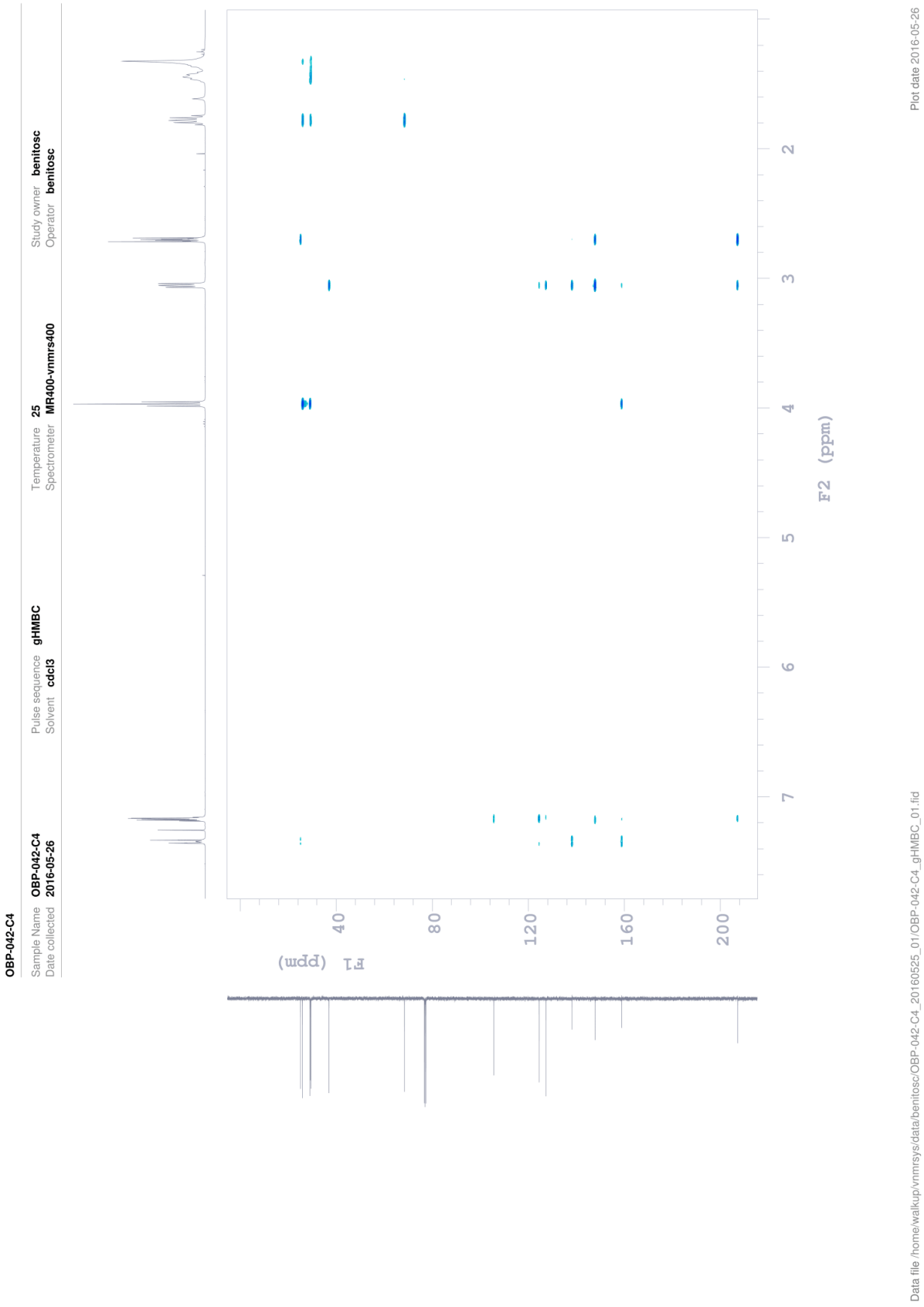

Figure 57. HMBC NMR spectrum of compound 2c.

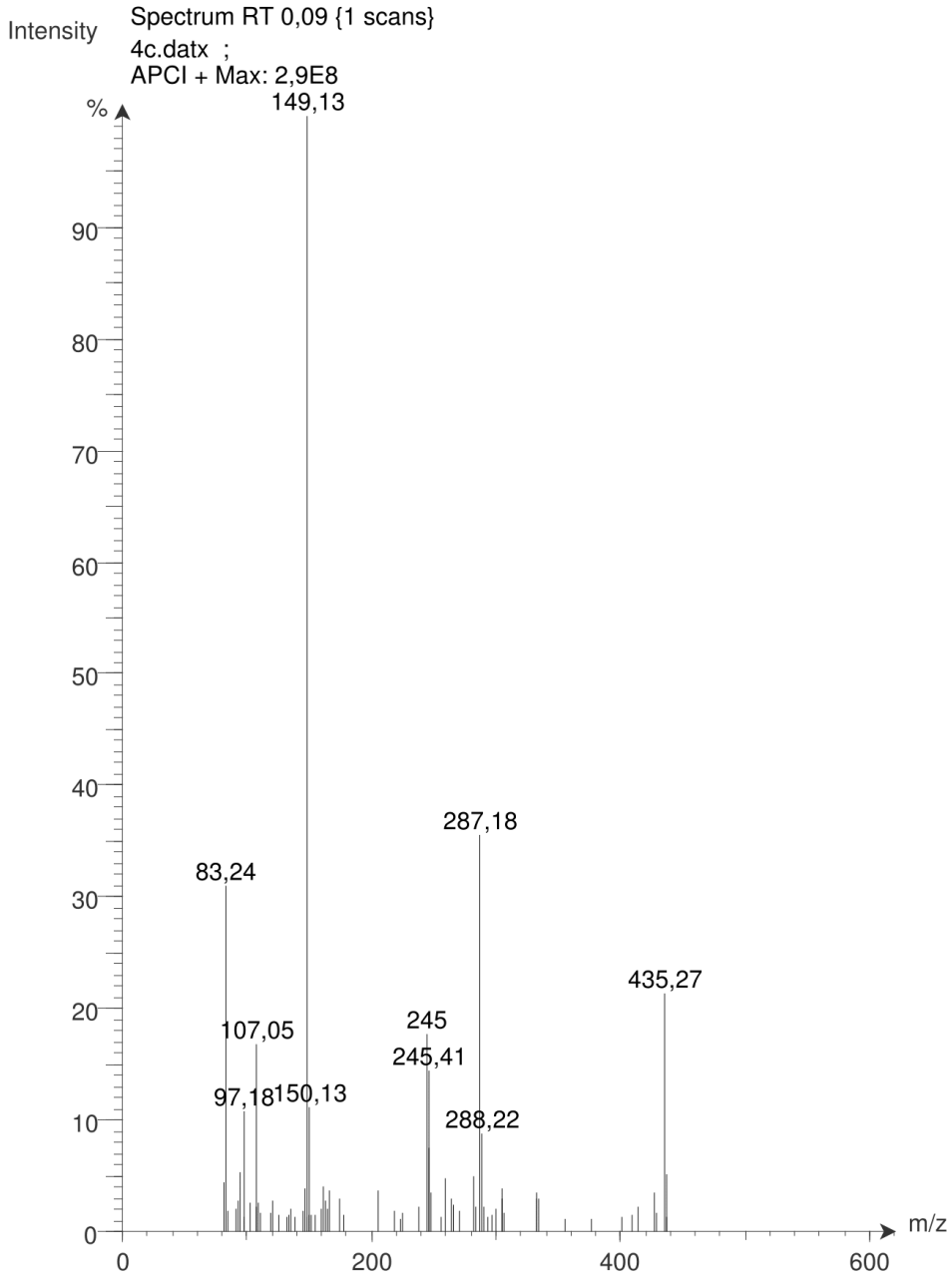

Figure 58. MS spectrum of compound 2c.

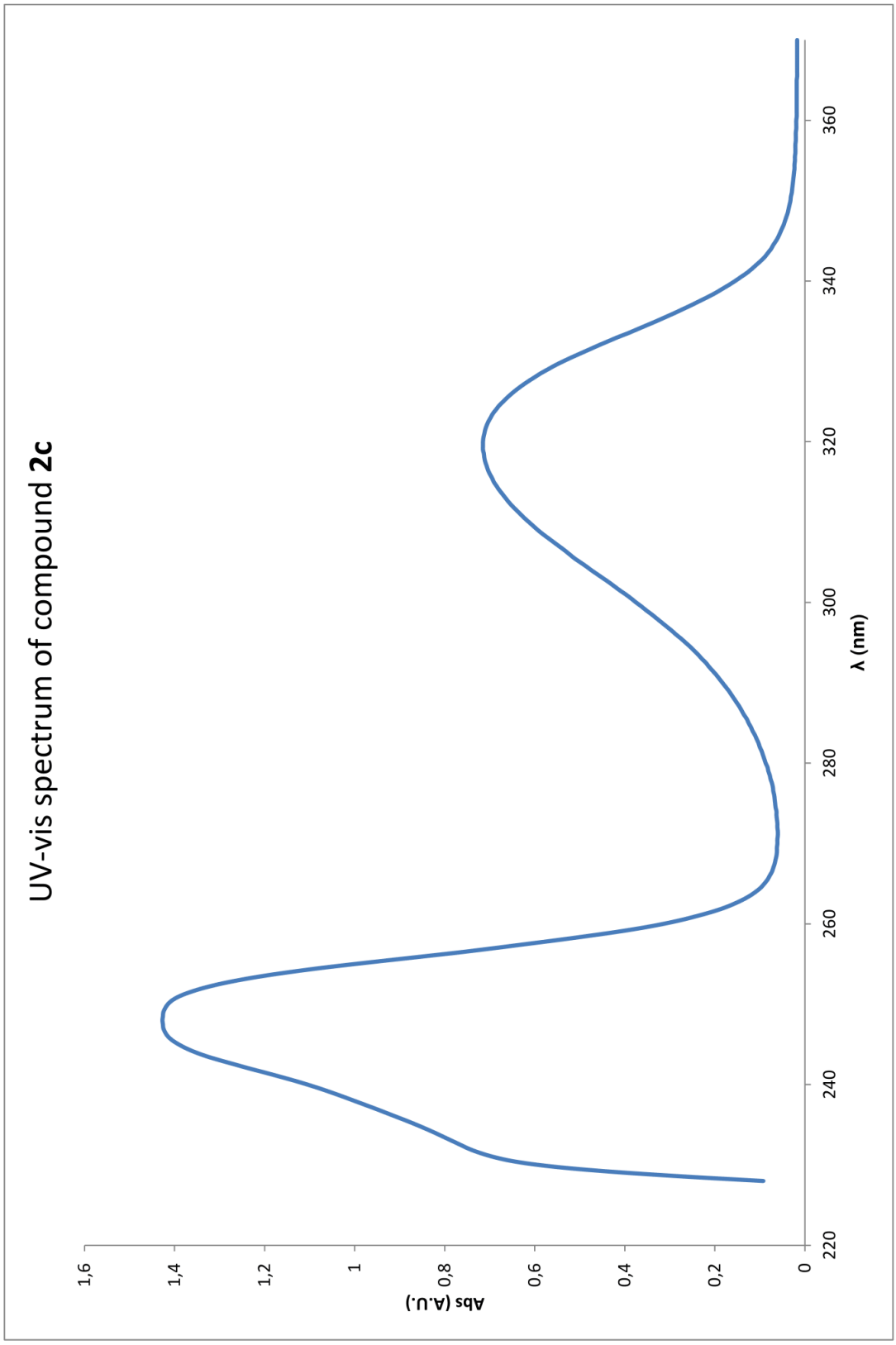

Figure 59. UV-vis spectrum of compound 2c.

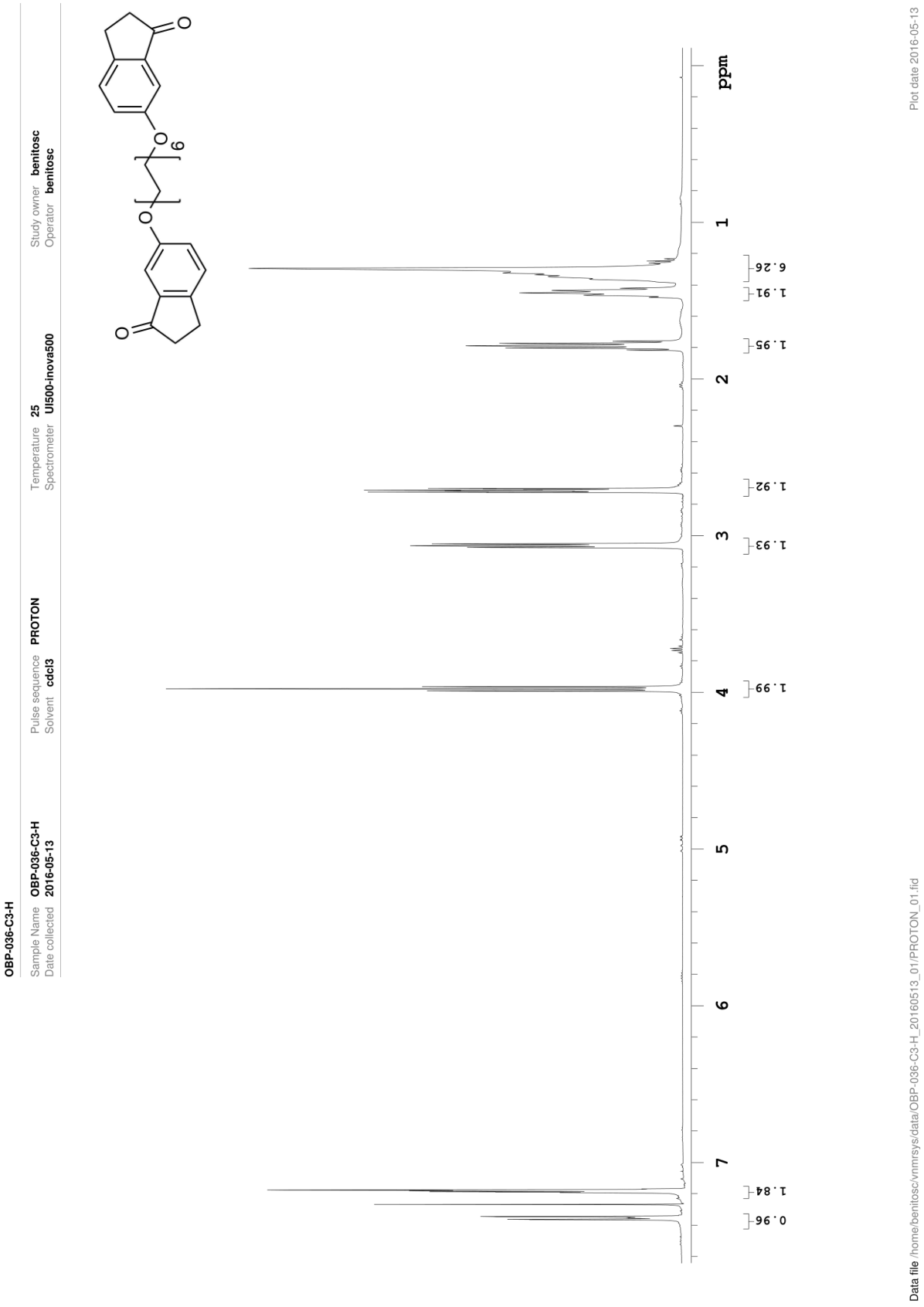

Figure 60. ^{1}H-NMR spectrum of compound 2d.

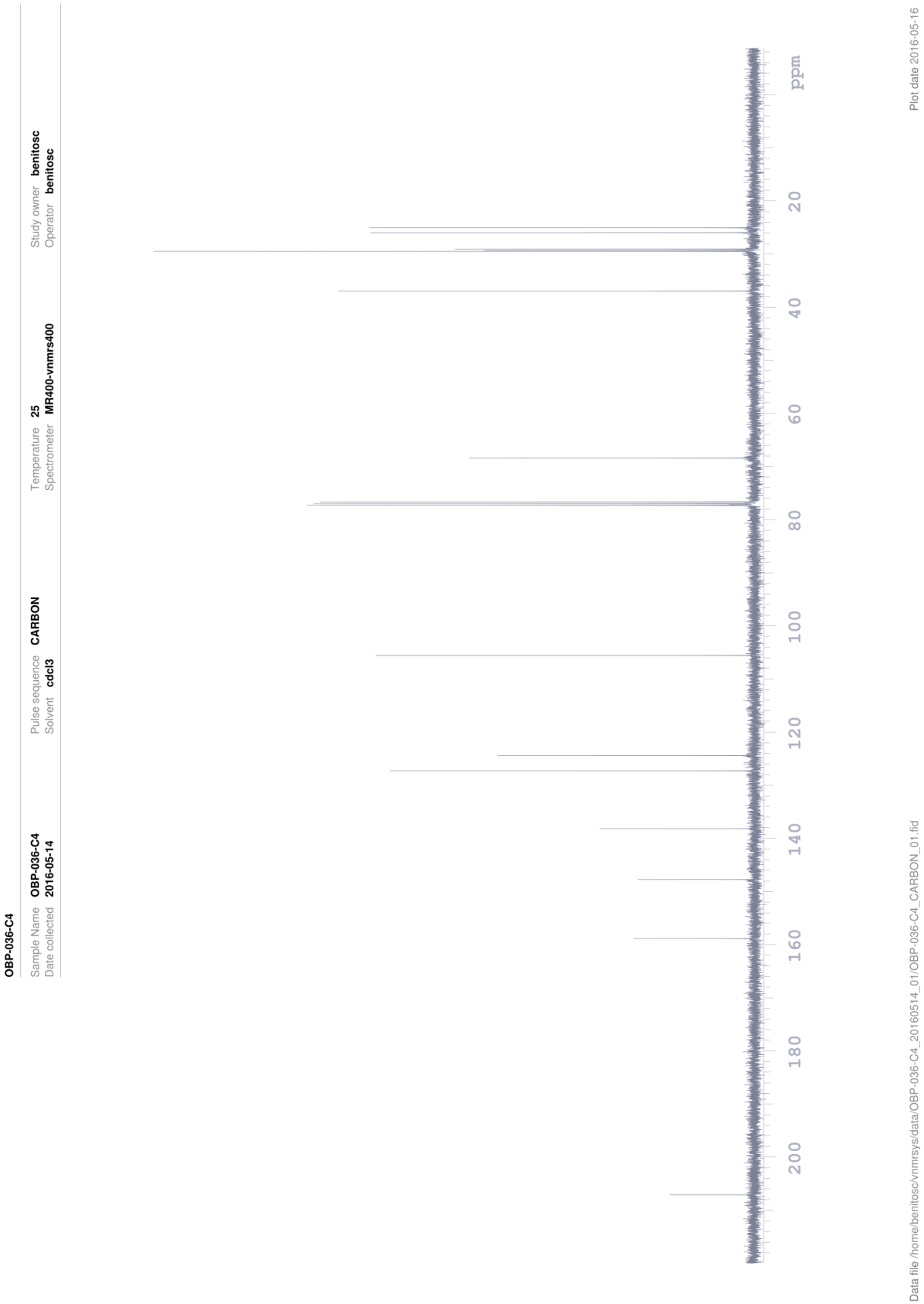

Figure 61. ^{13}C-NMR spectrum of compound 2d.

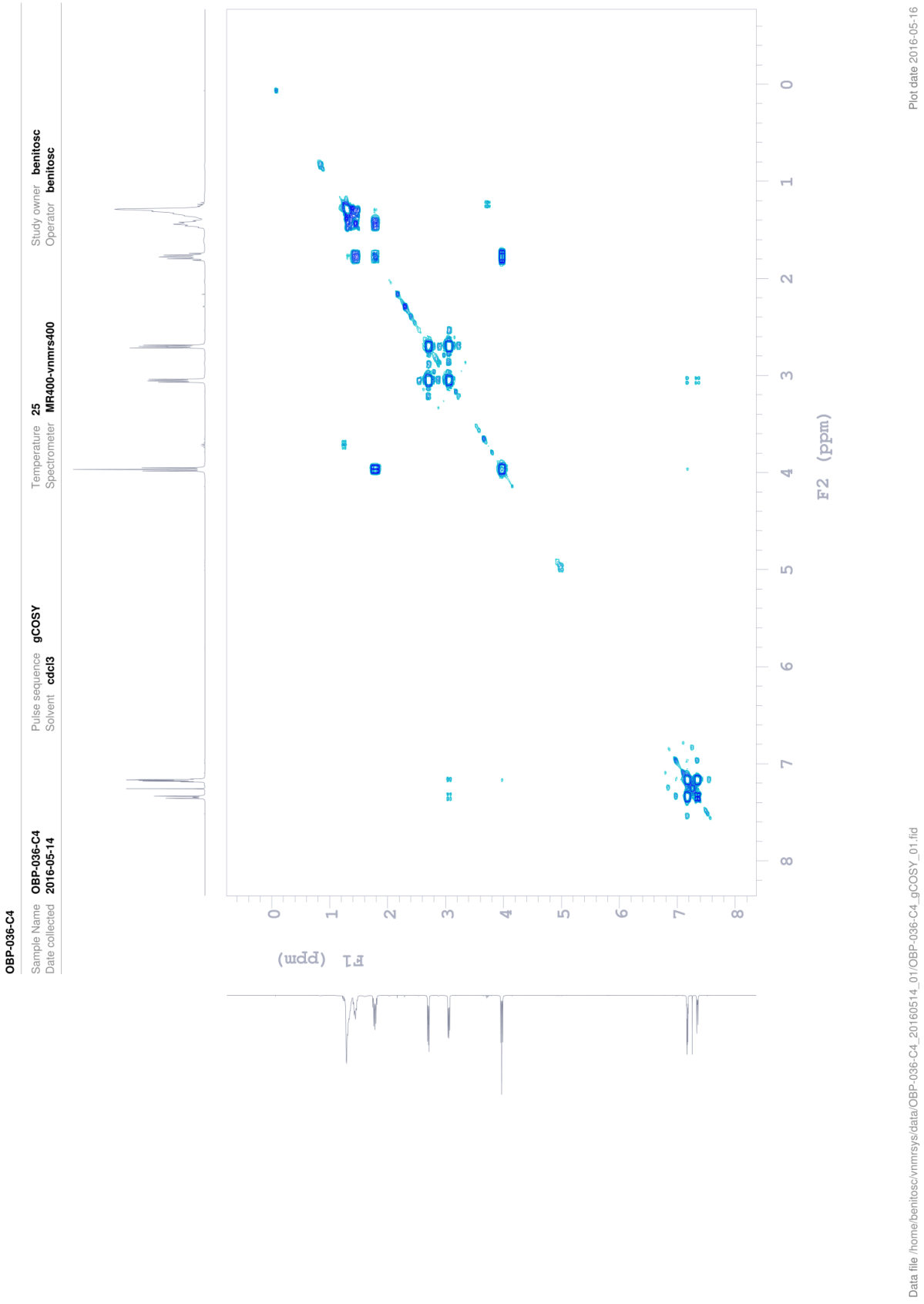

Figure 62. COSY NMR spectrum of compound 2d.

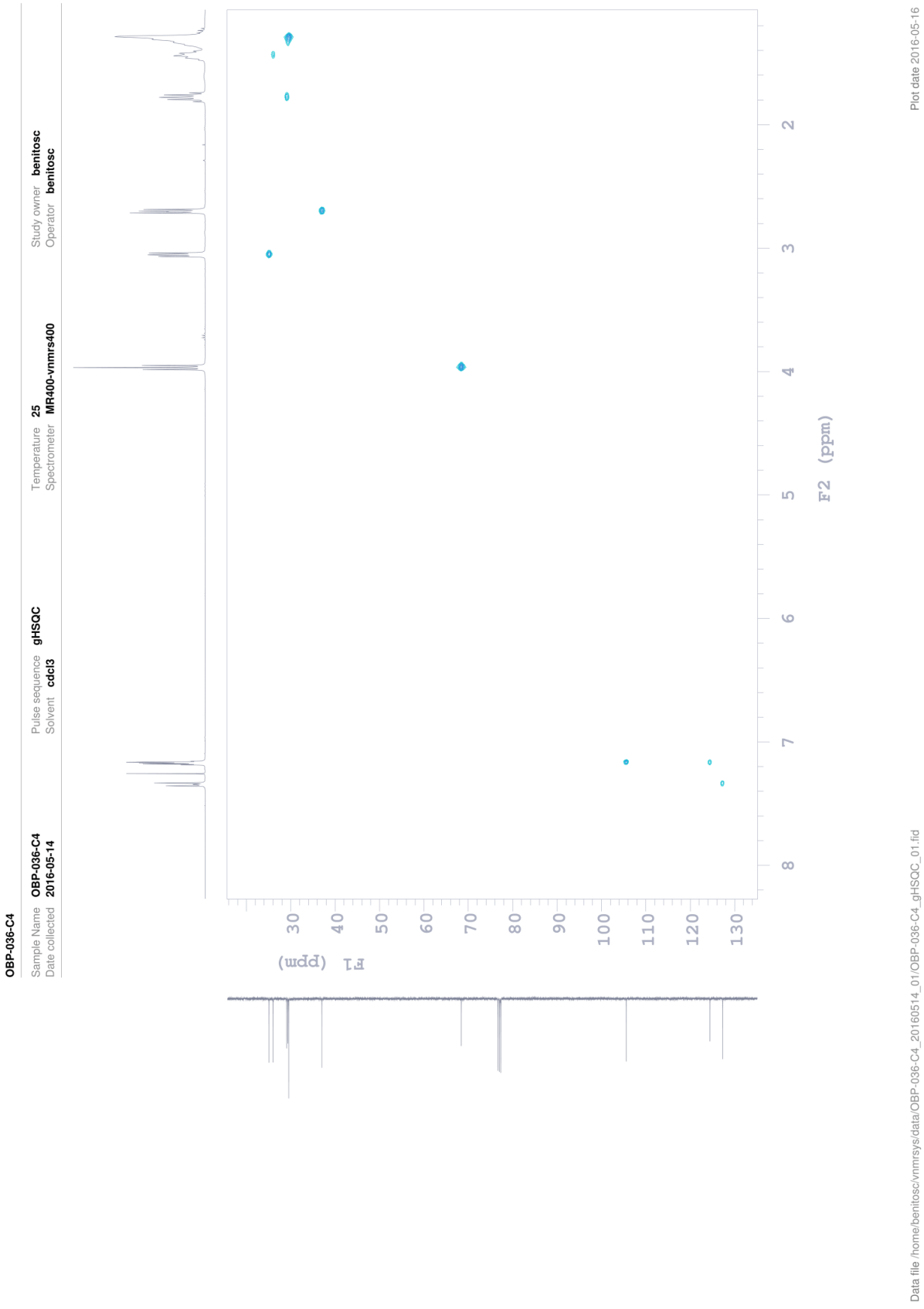

Figure 63. HSQC NMR spectrum of compound 2d.

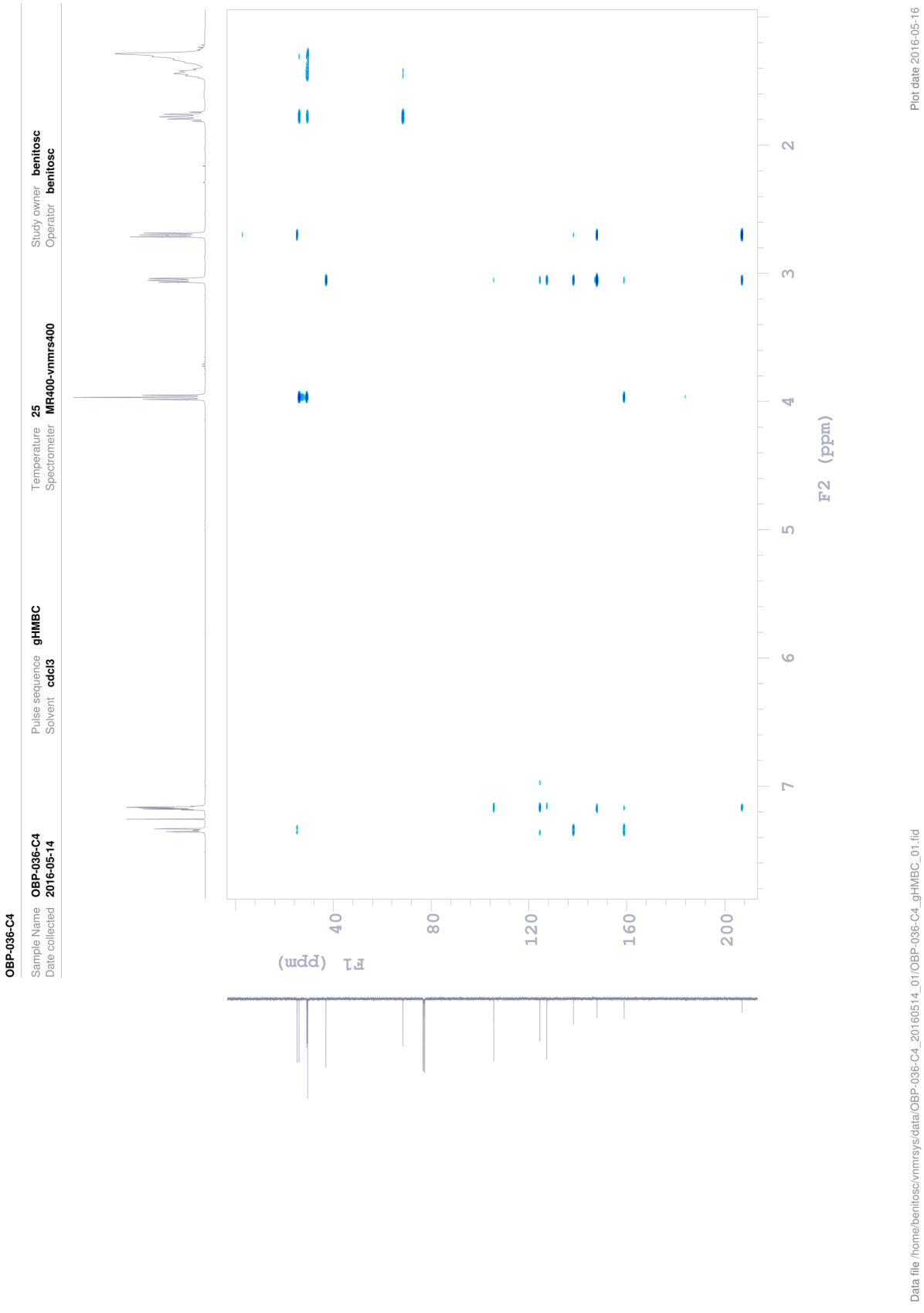

Figure 64. HMBC NMR spectrum of compound 2d.

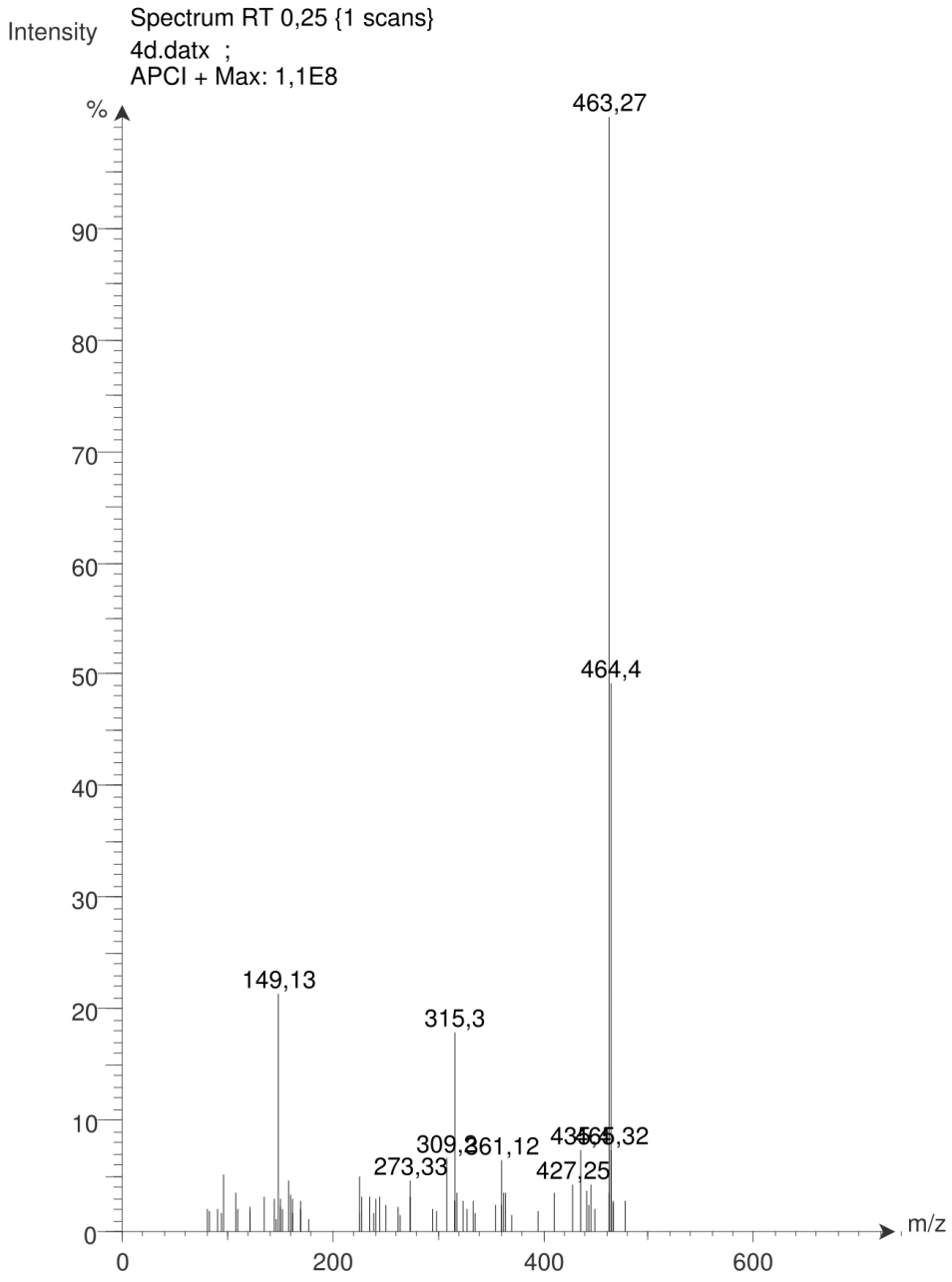

Figure 65. MS spectrum of compound 2d.

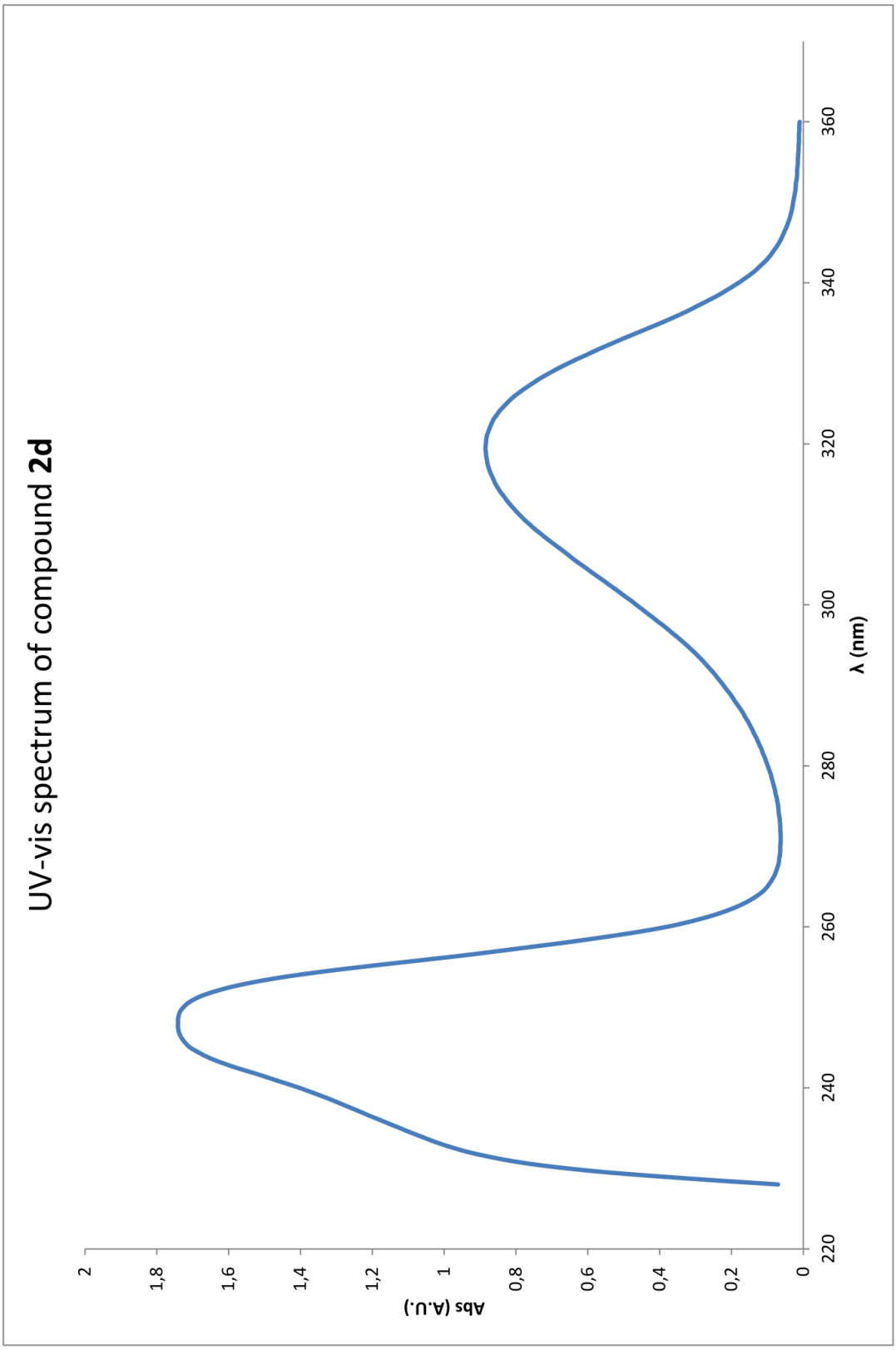

Figure 66. UV-vis spectrum of compound 2d.

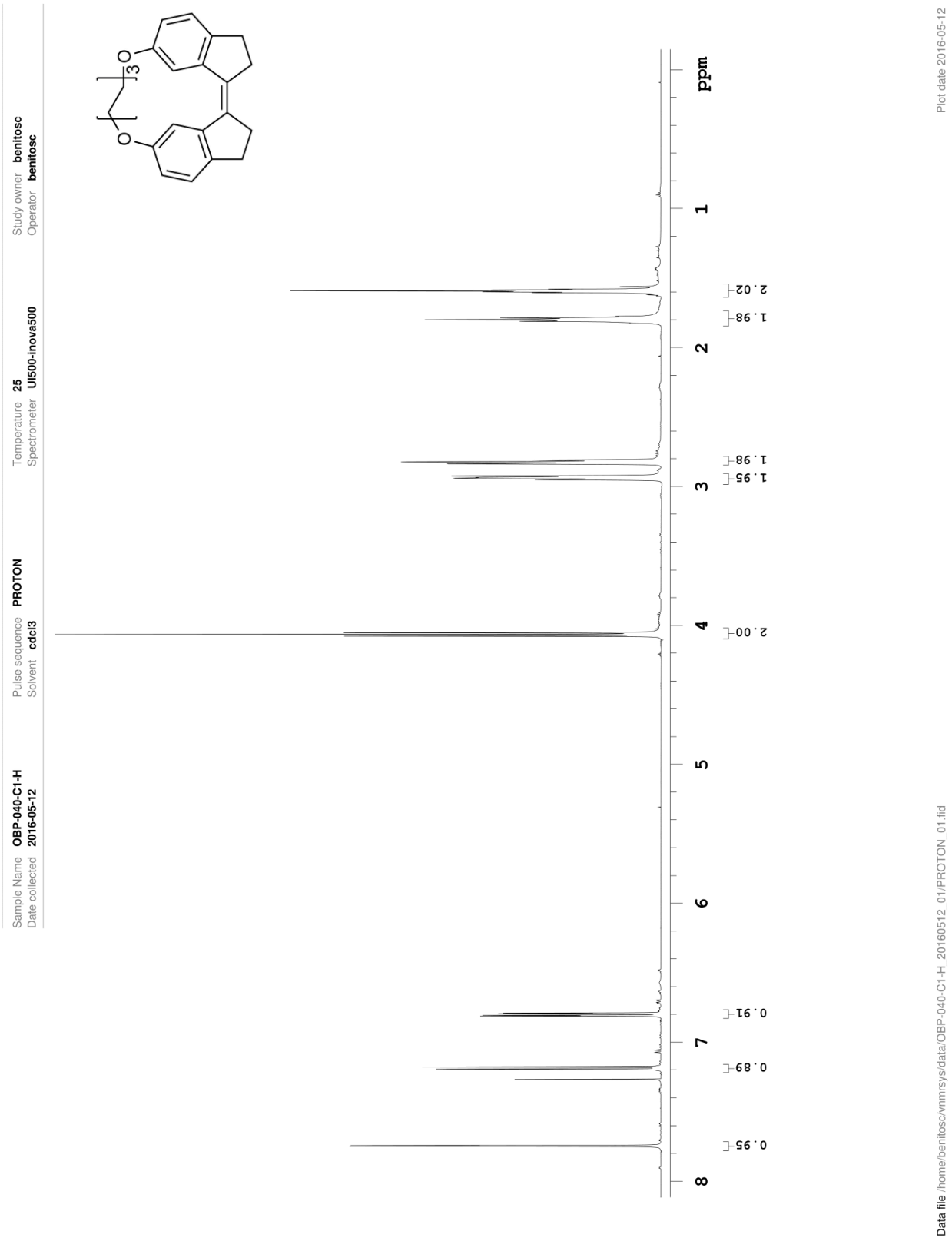

Figure 67. ^{1}H-NMR spectrum of compound *Z*-1a.

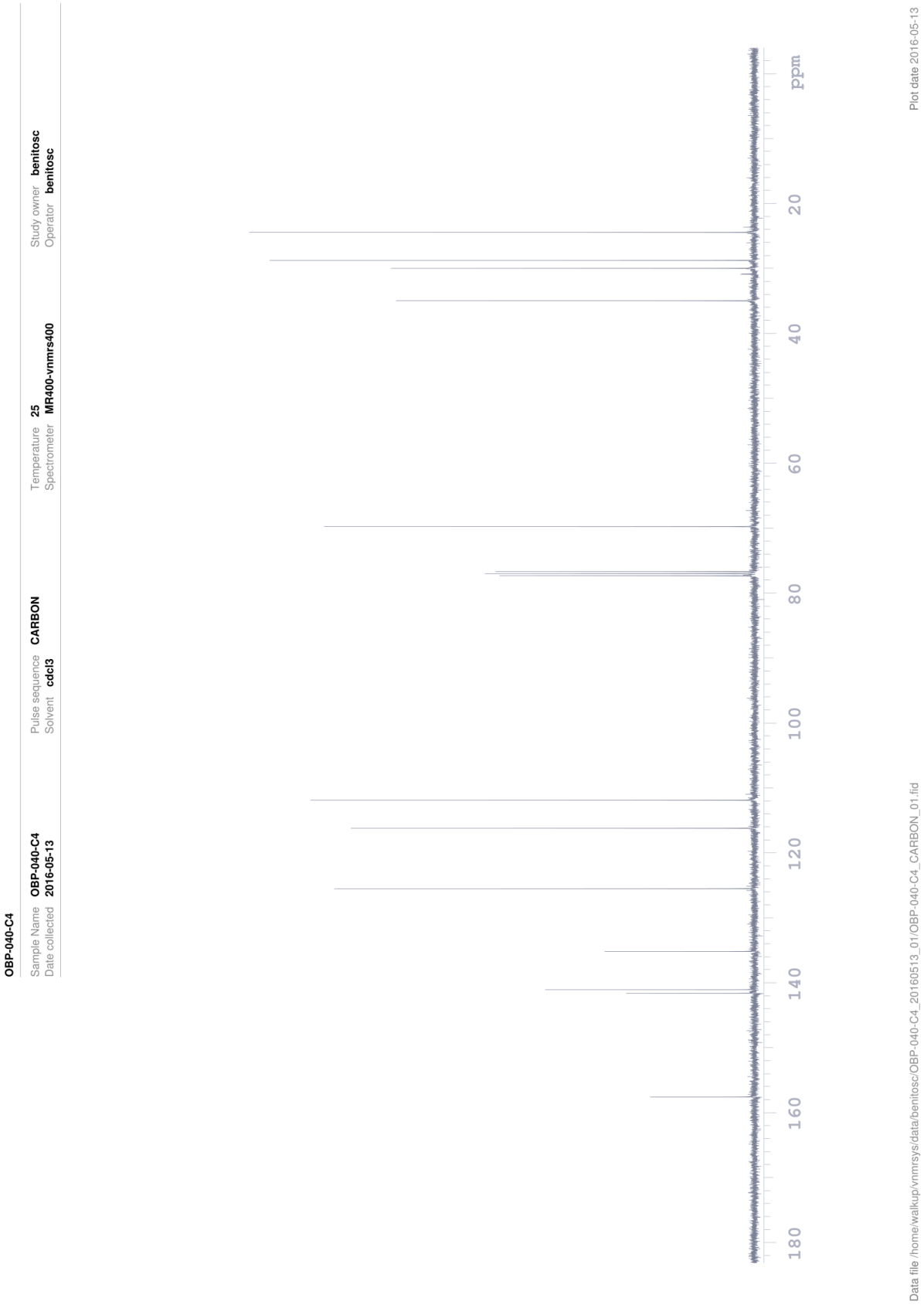

Figure 68. ^{13}C-NMR spectrum of compound *Z*-1a.

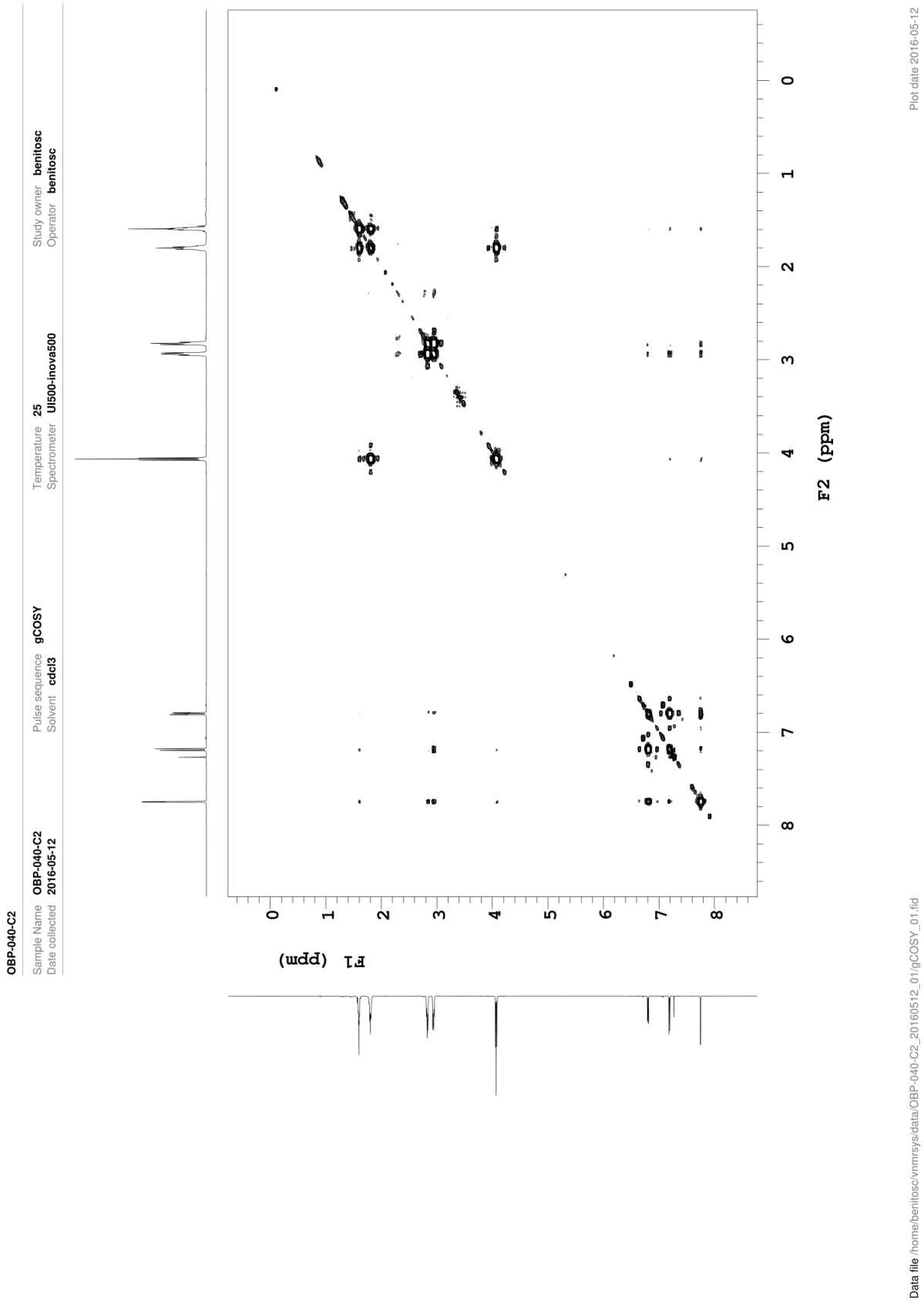

Figure 69. COSY NMR spectrum of compound *Z*-1a.

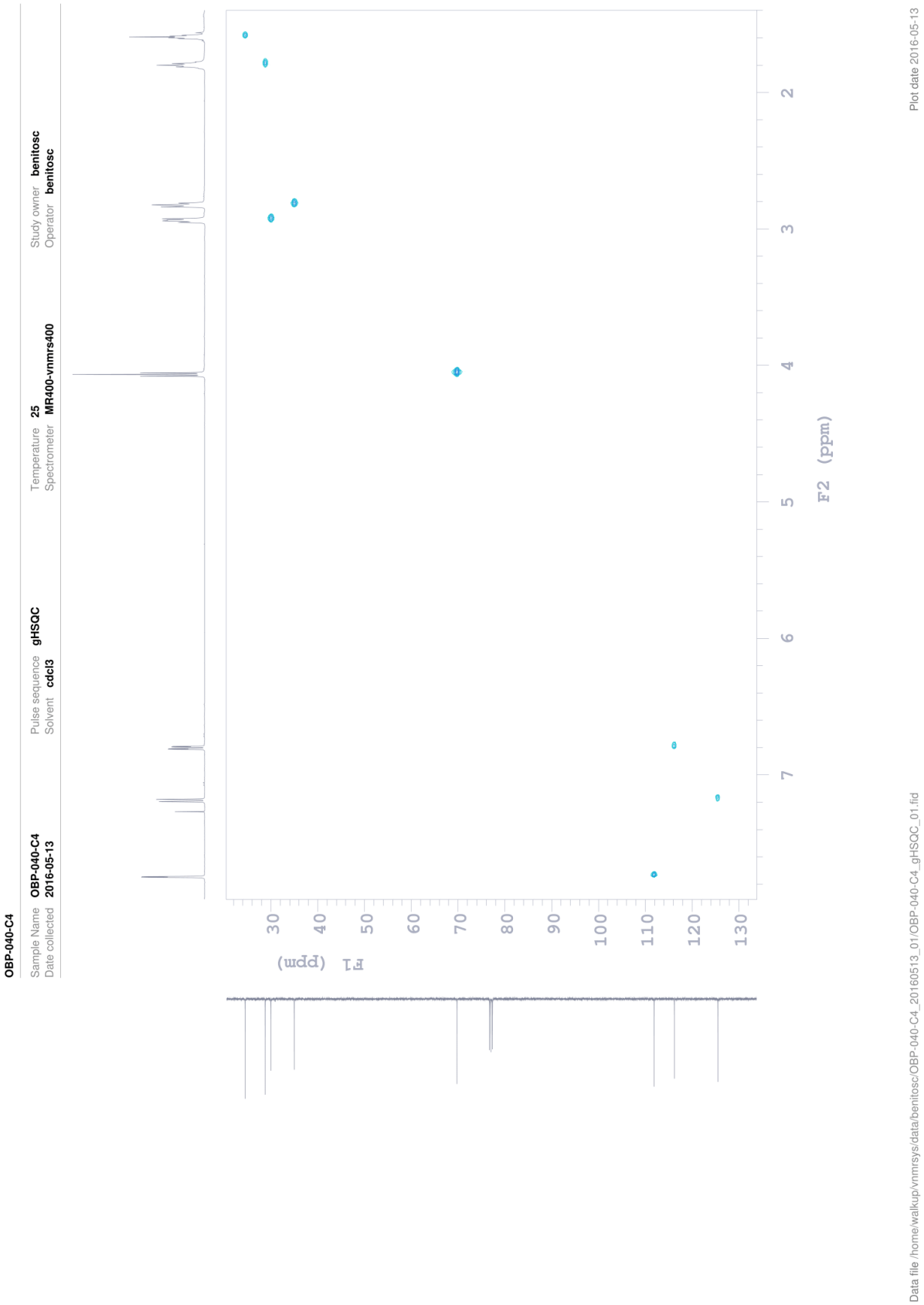

Figure 70. HSQC NMR spectrum of compound *Z*-1a.

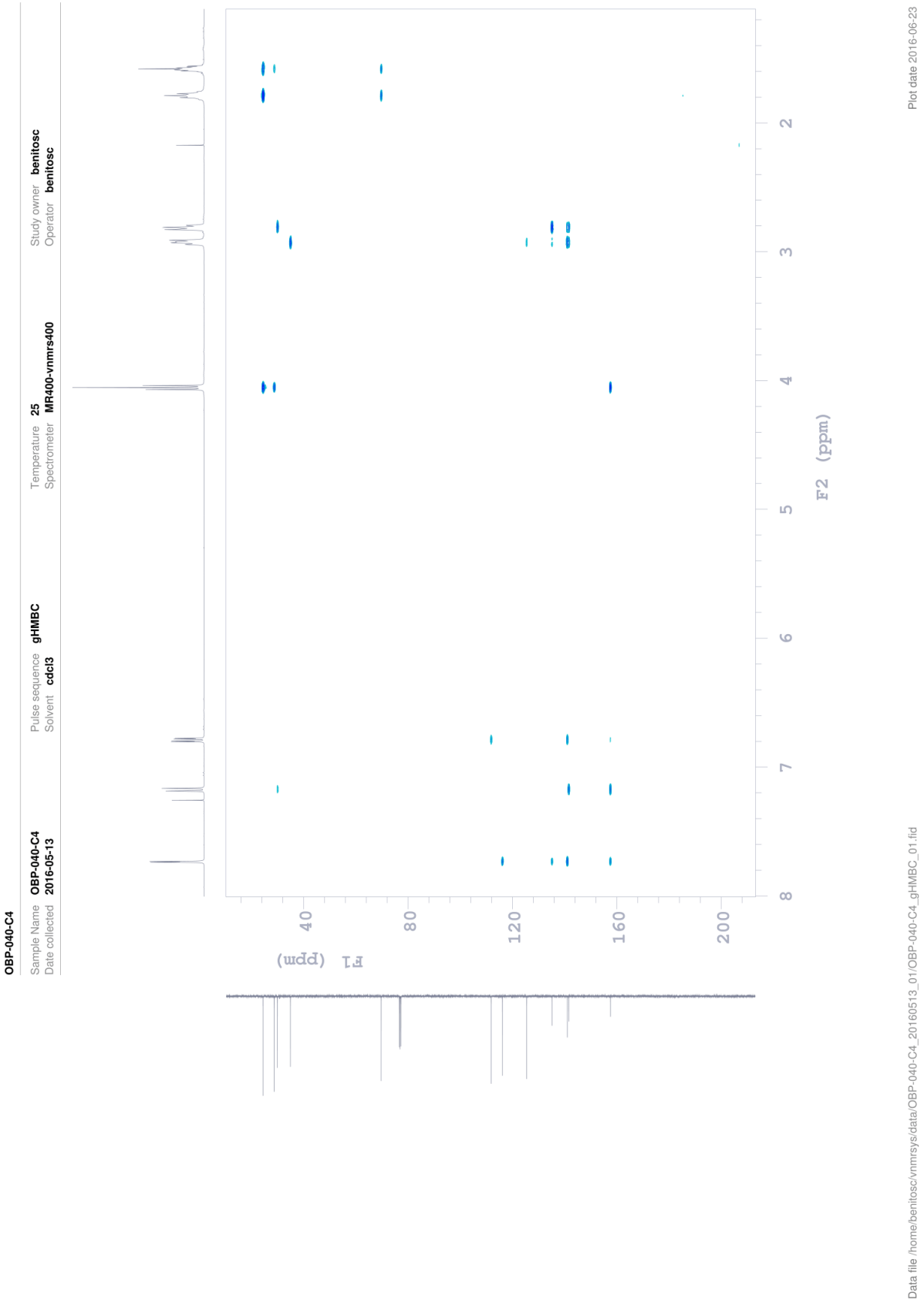

Figure 71. HMBC NMR spectrum of compound *Z*-1a.

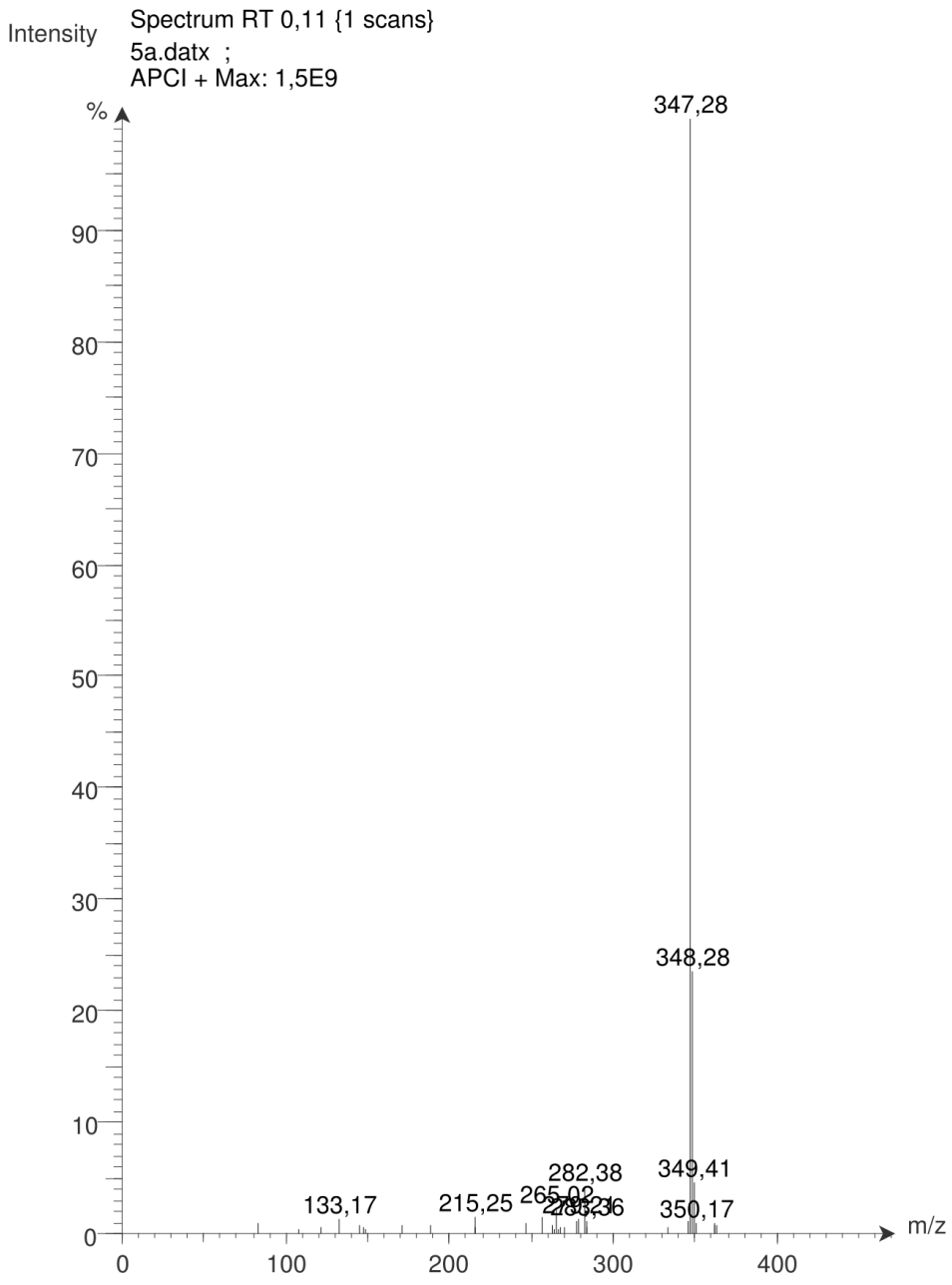

Figure 72. MS spectrum of compound *Z*-1a.

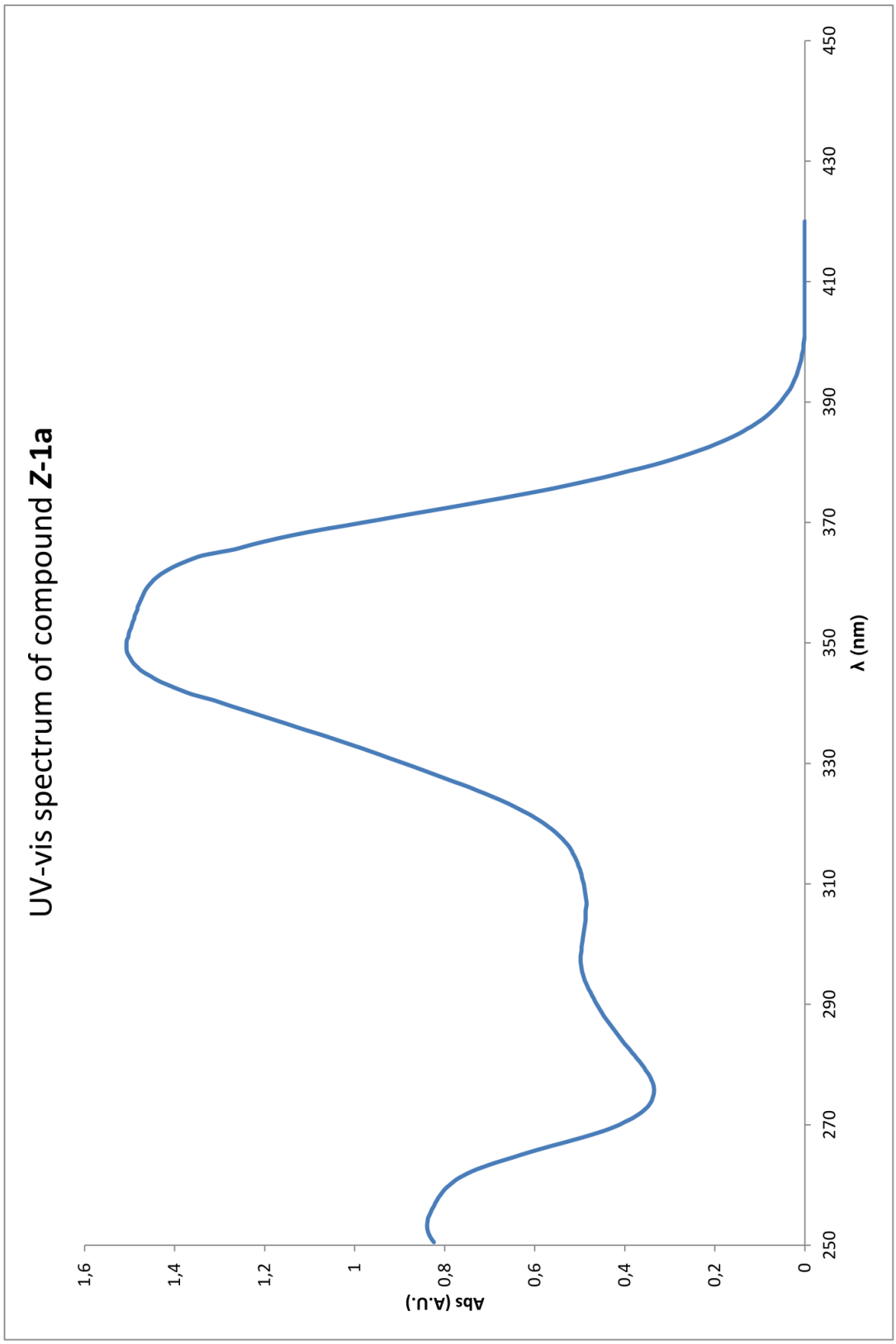

Figure 73. UV-vis spectrum of compound *Z*-1a.

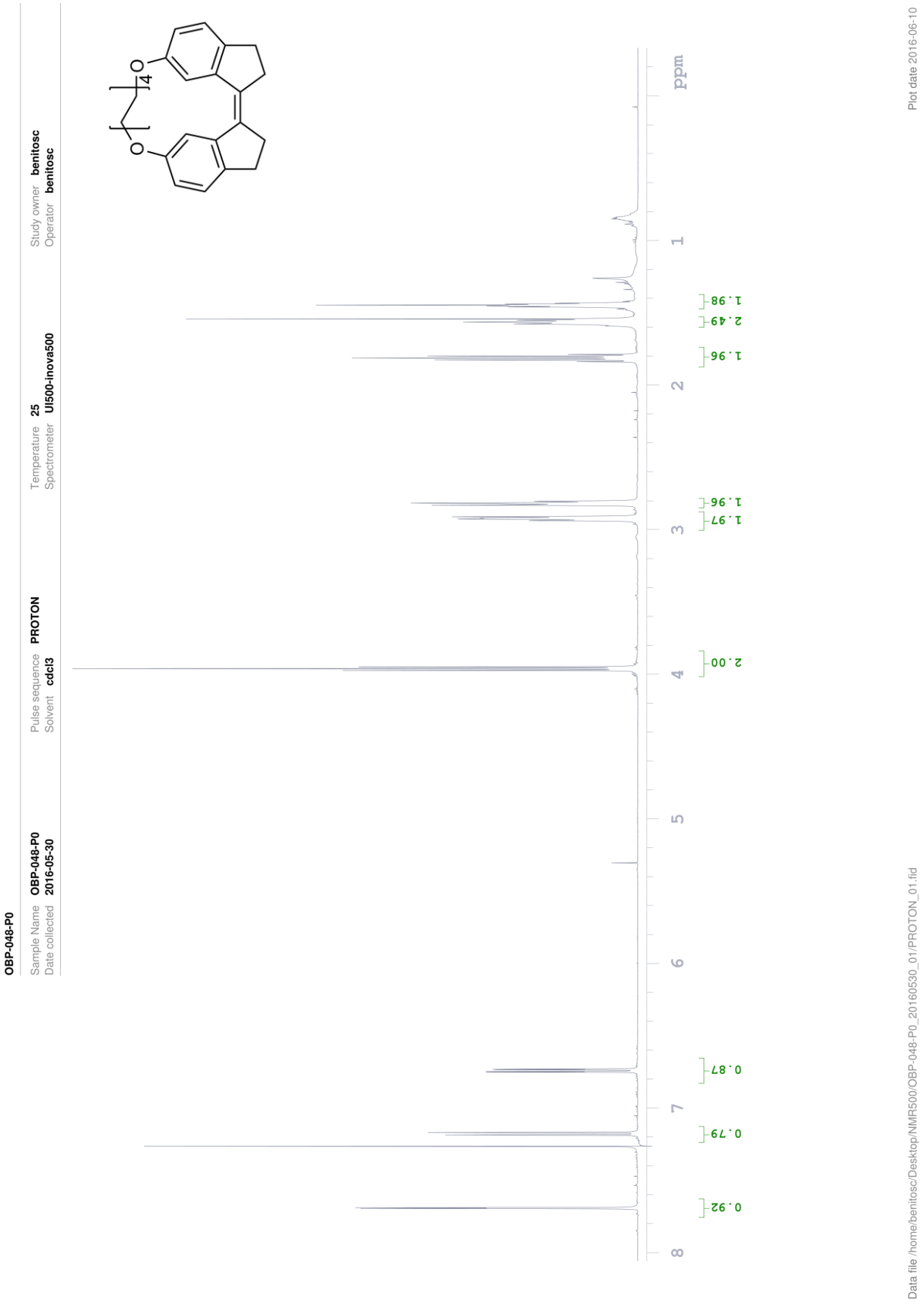

Figure 74. ^{1}H-NMR spectrum of compound *Z*-1b.

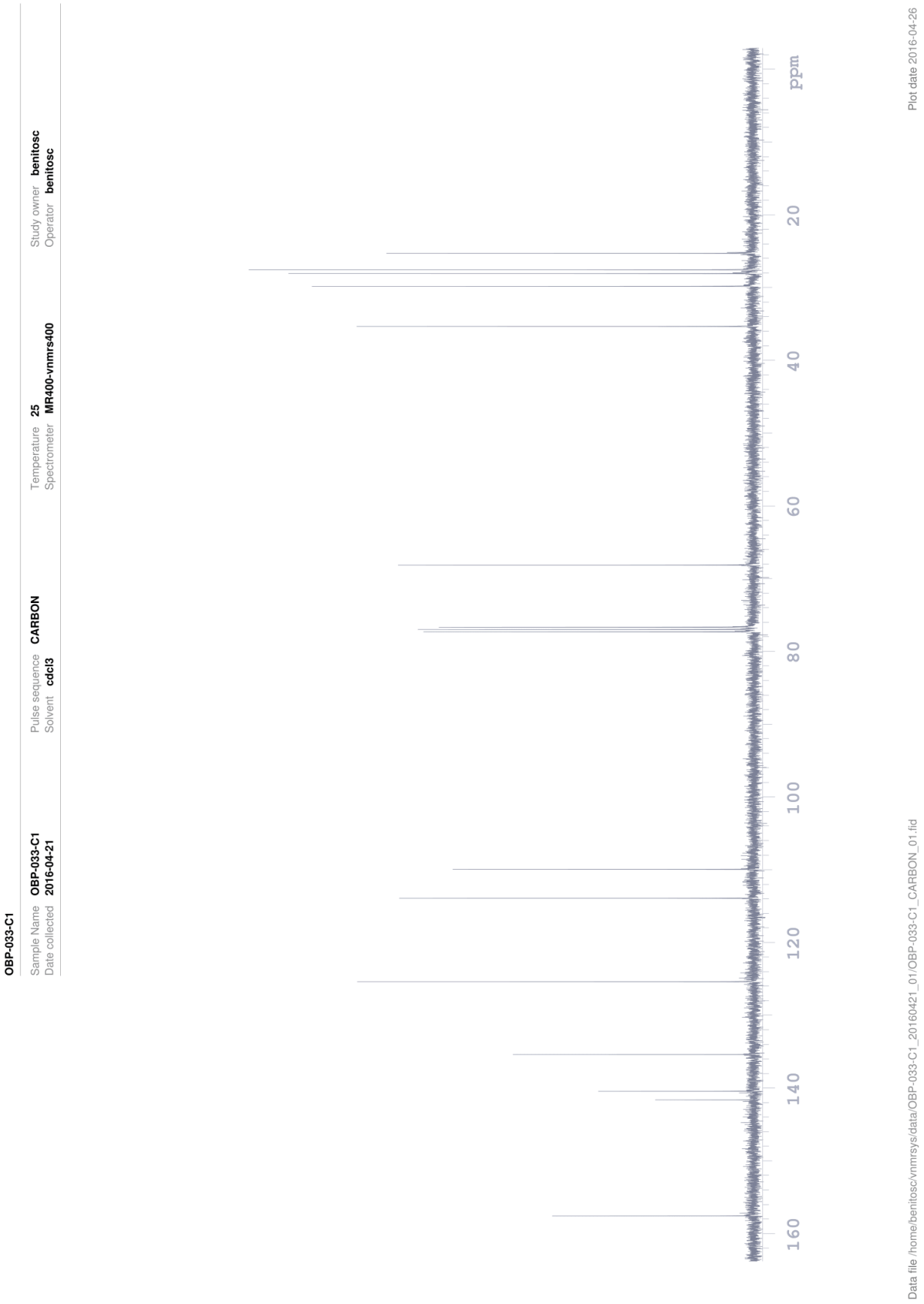

Figure 75. ^{13}C-NMR spectrum of compound *Z*-1b.

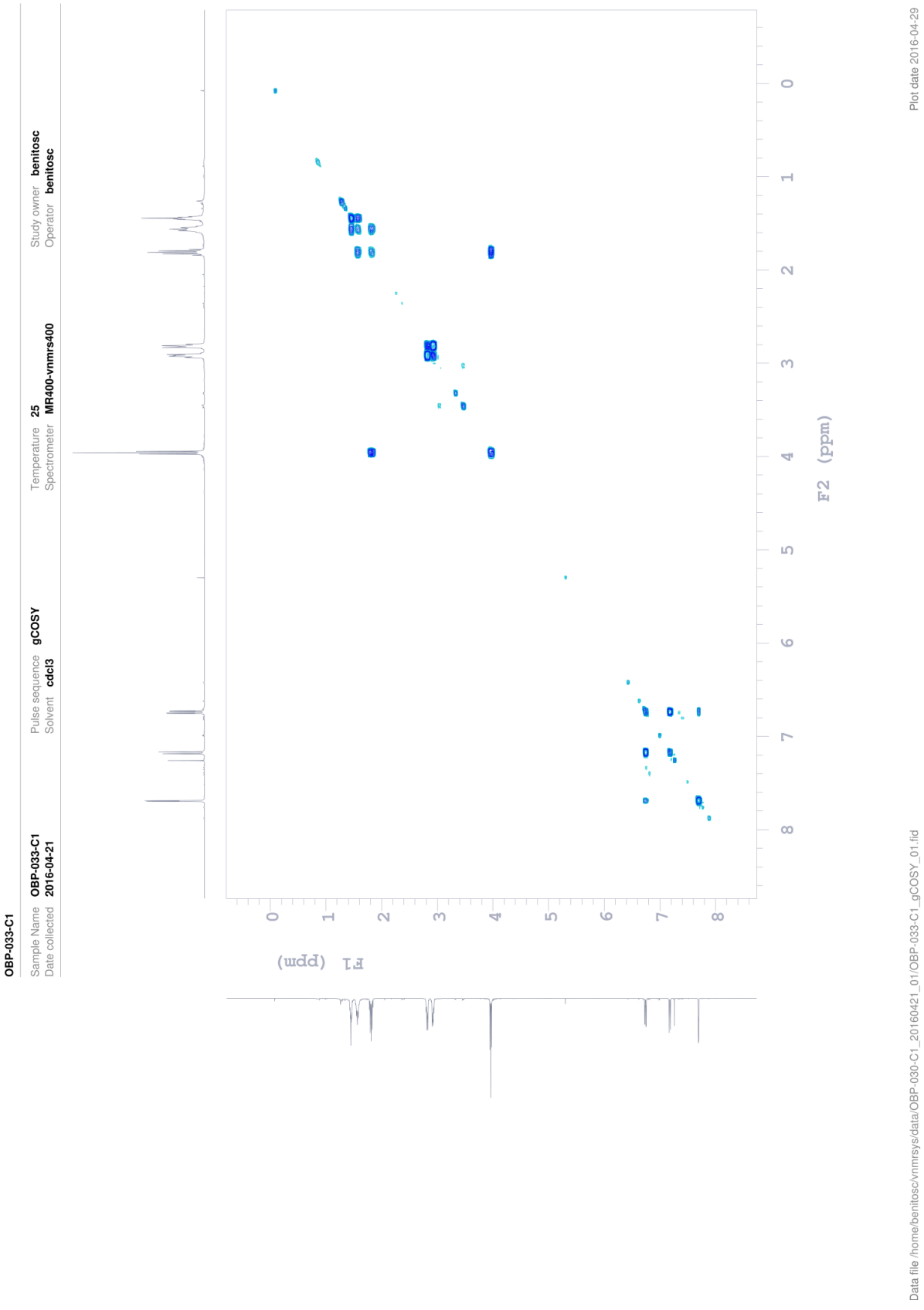

Figure 76. COSY NMR spectrum of compound *Z*-1b.

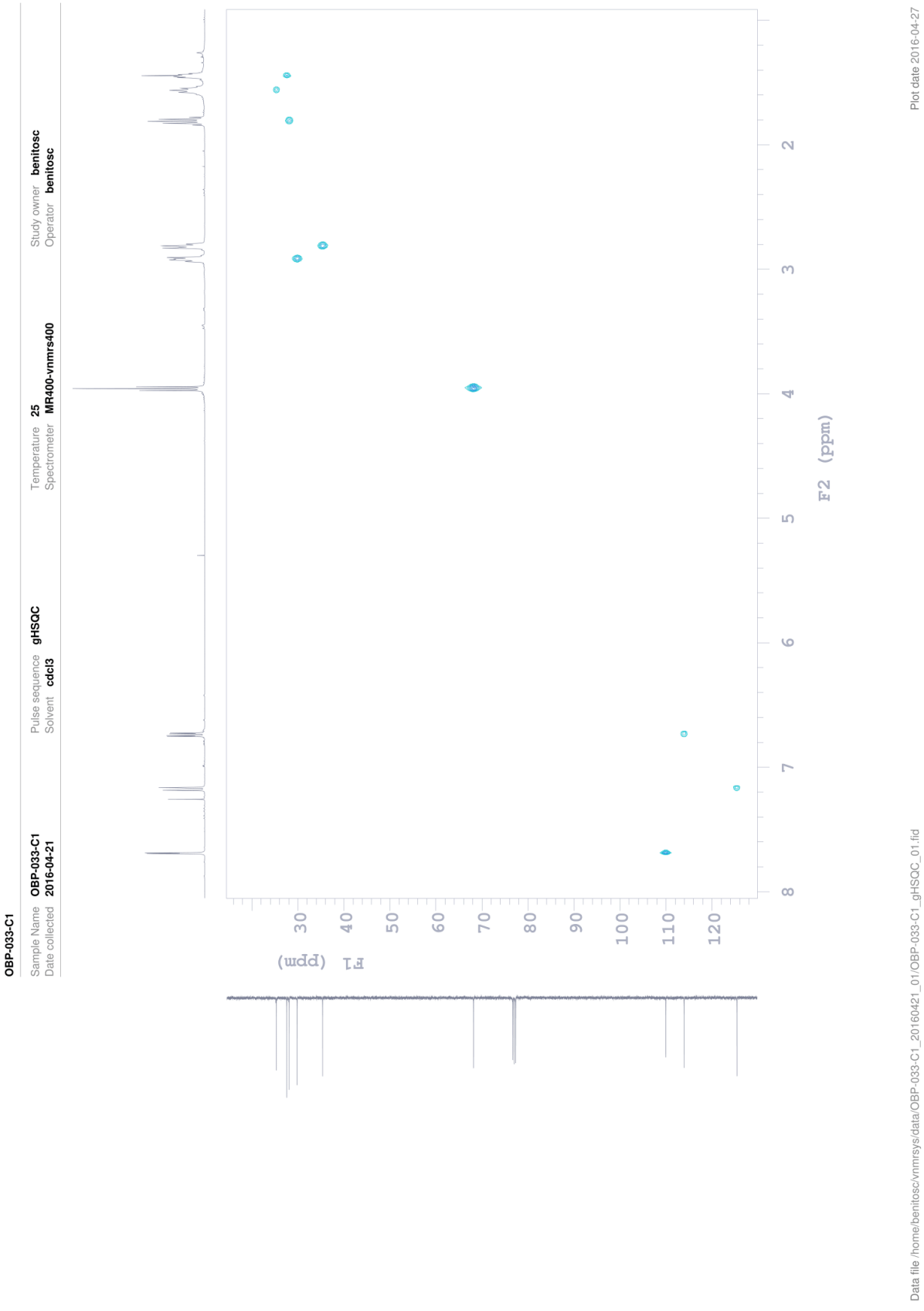

Figure 77. HSQC NMR spectrum of compound *Z*-1b.

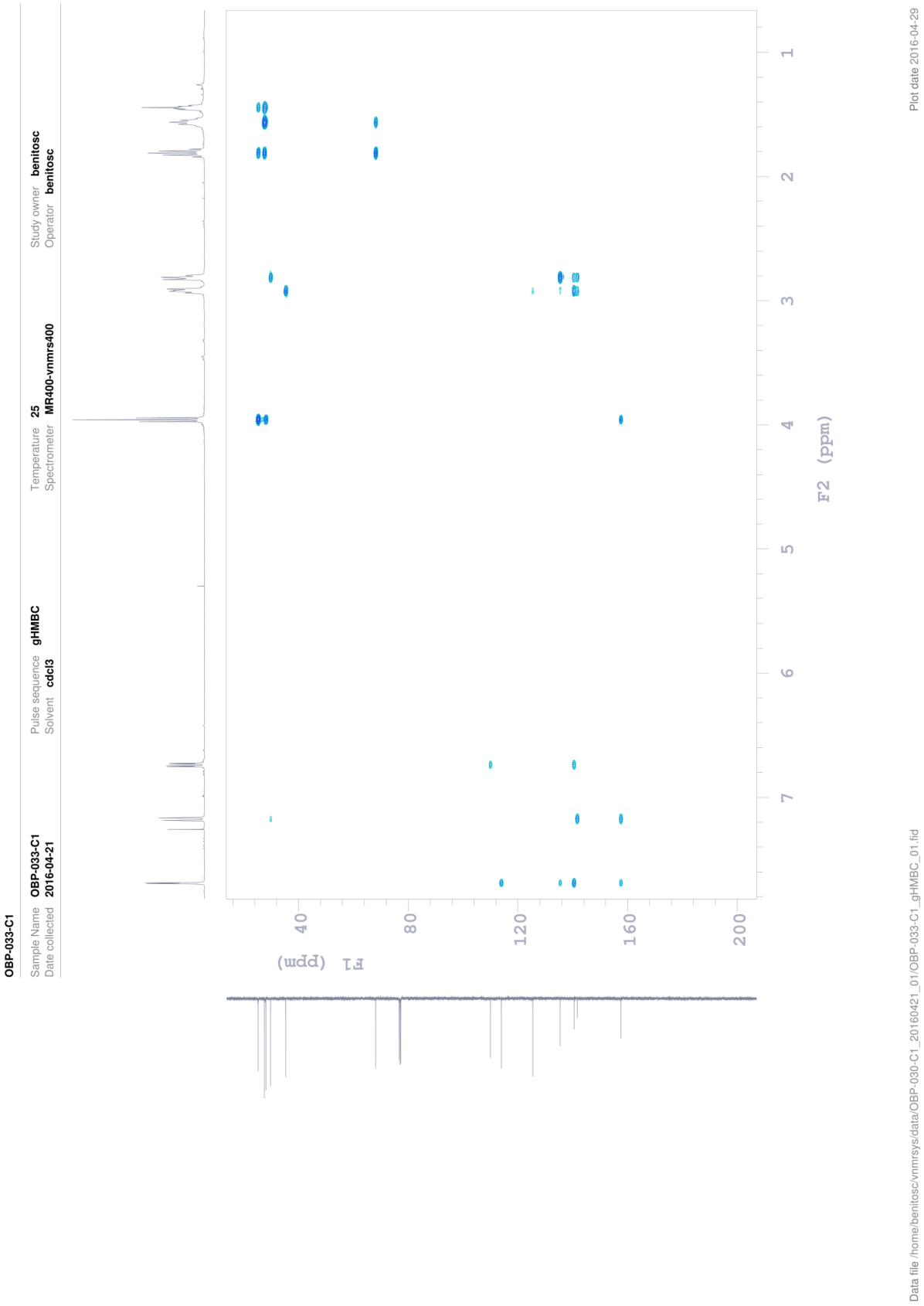

Figure 78. HMBC NMR spectrum of compound *Z*-1b.

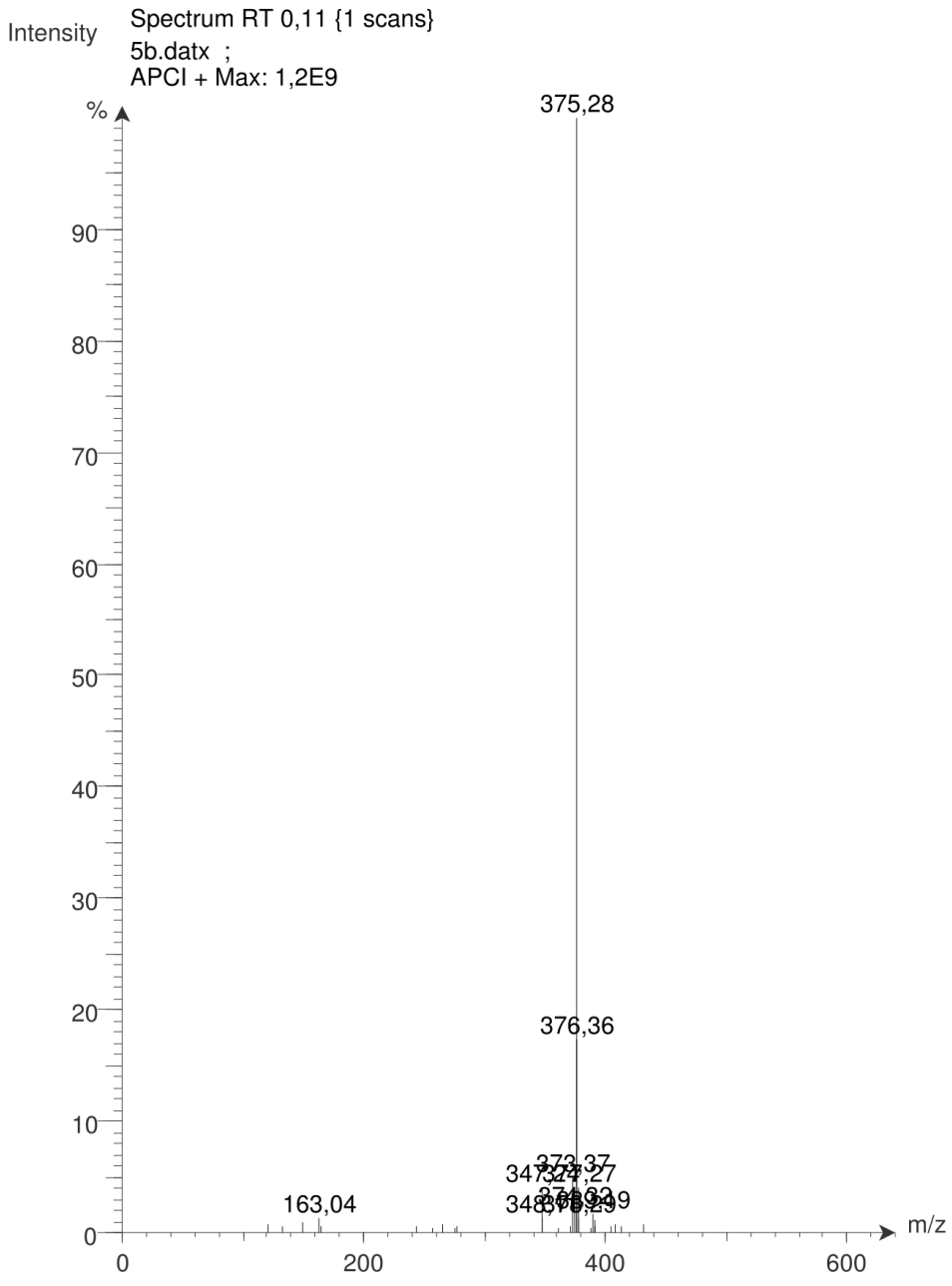

Figure 79. MS spectrum of compound *Z*-1b.

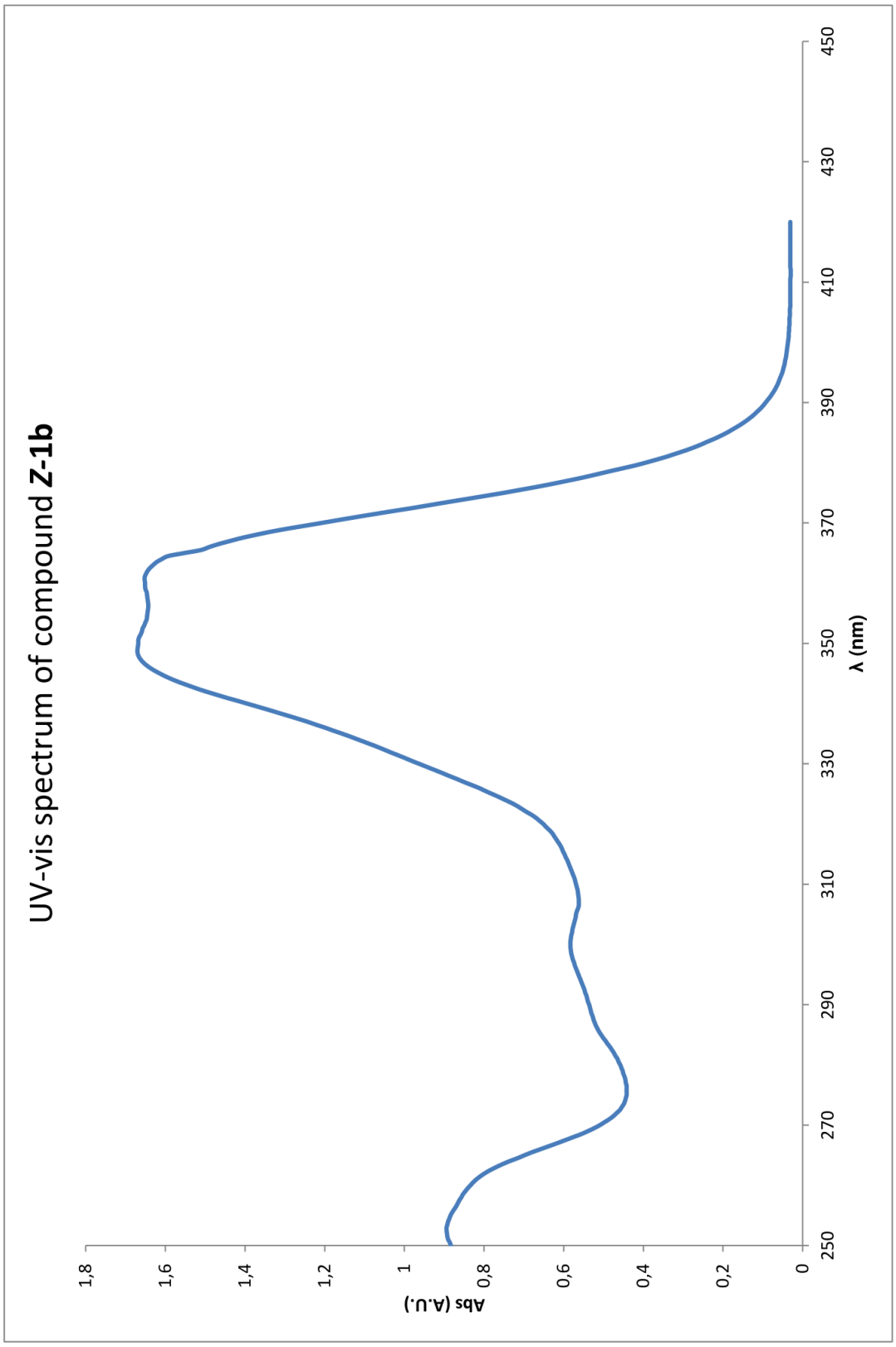

Figure 80. UV-vis spectrum of compound Z-1b.

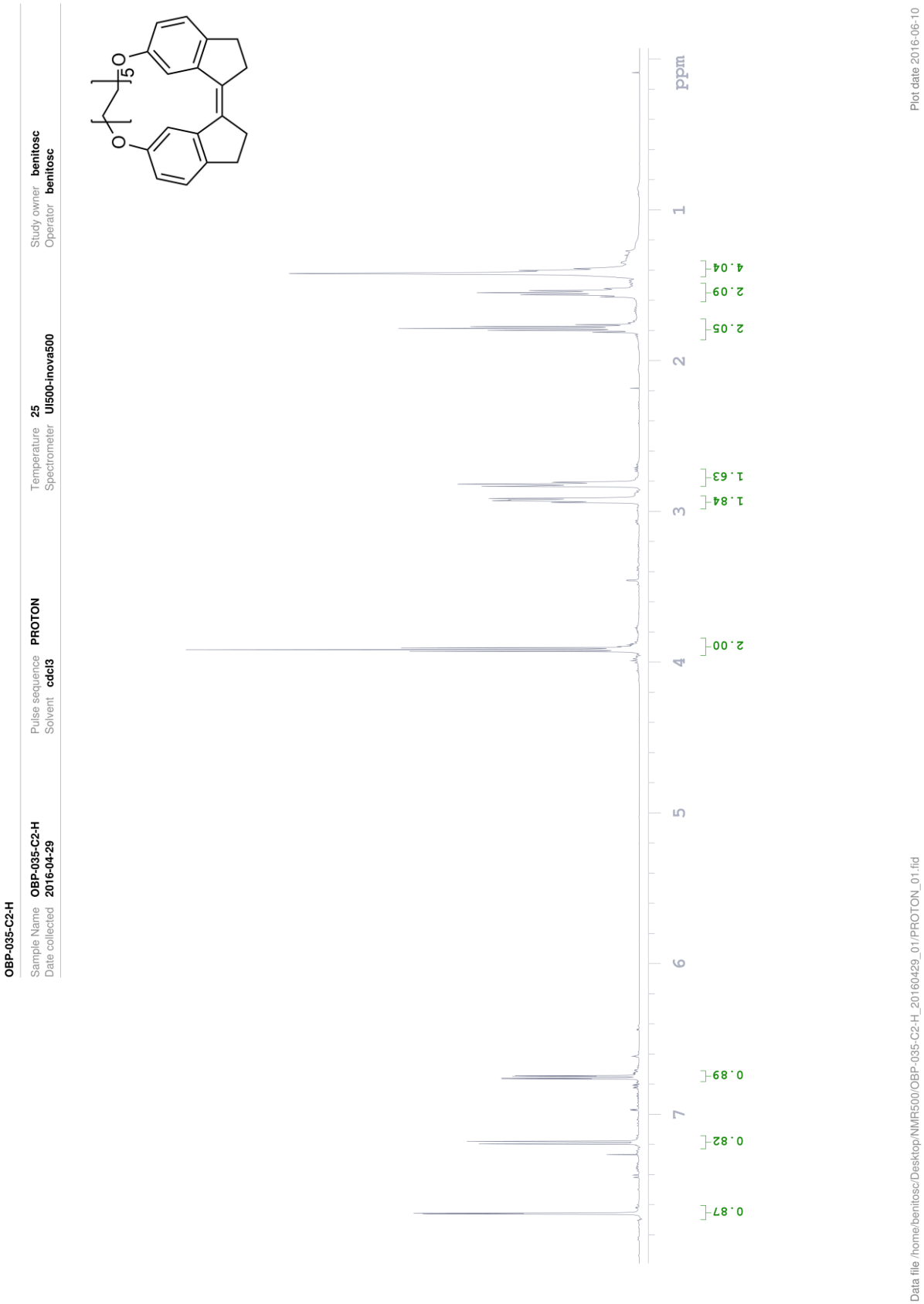

Figure 81. ^{1}H-NMR spectrum of compound *Z*-1c.

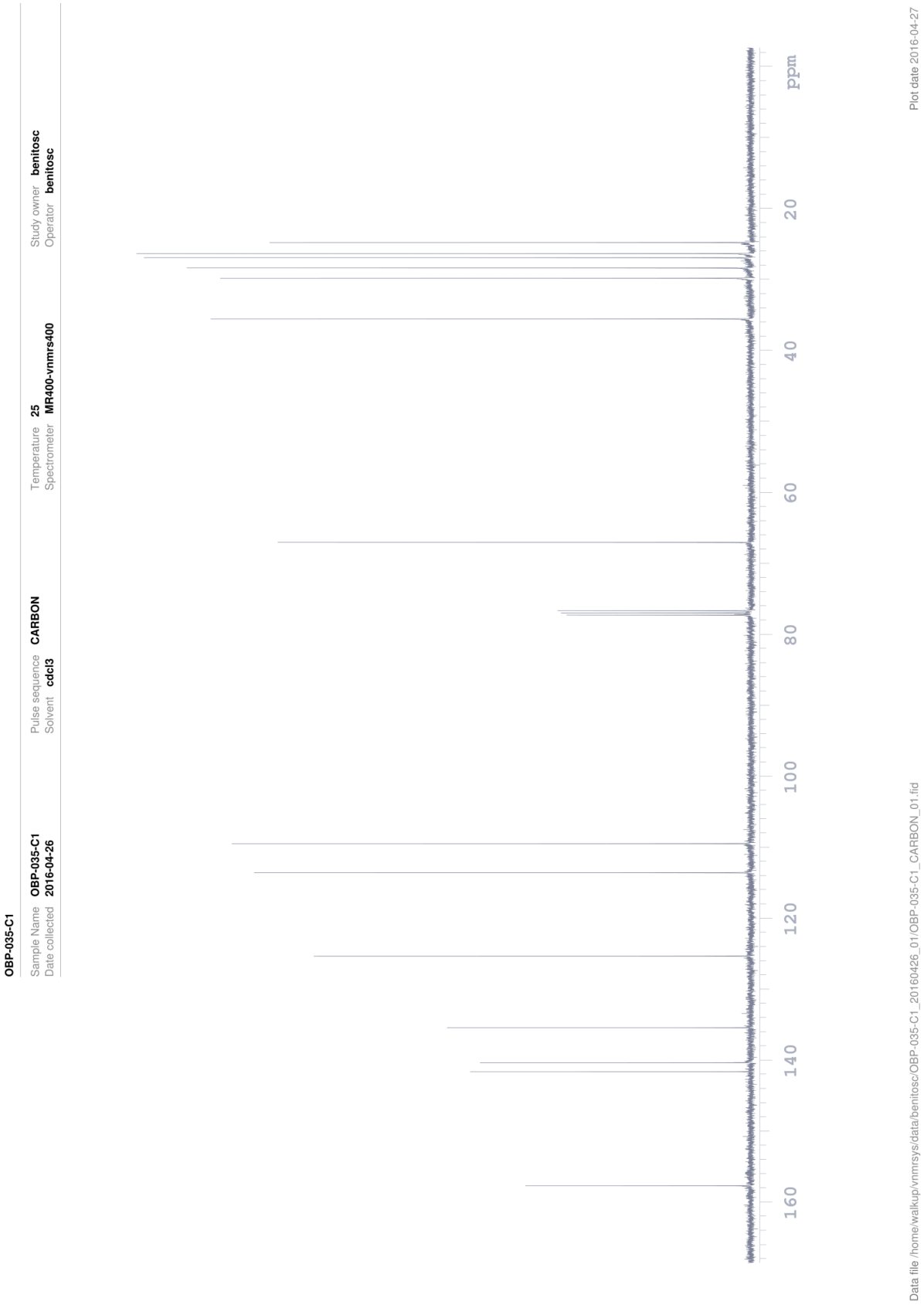

Figure 82. ^{13}C-NMR spectrum of compound *Z*-1c.

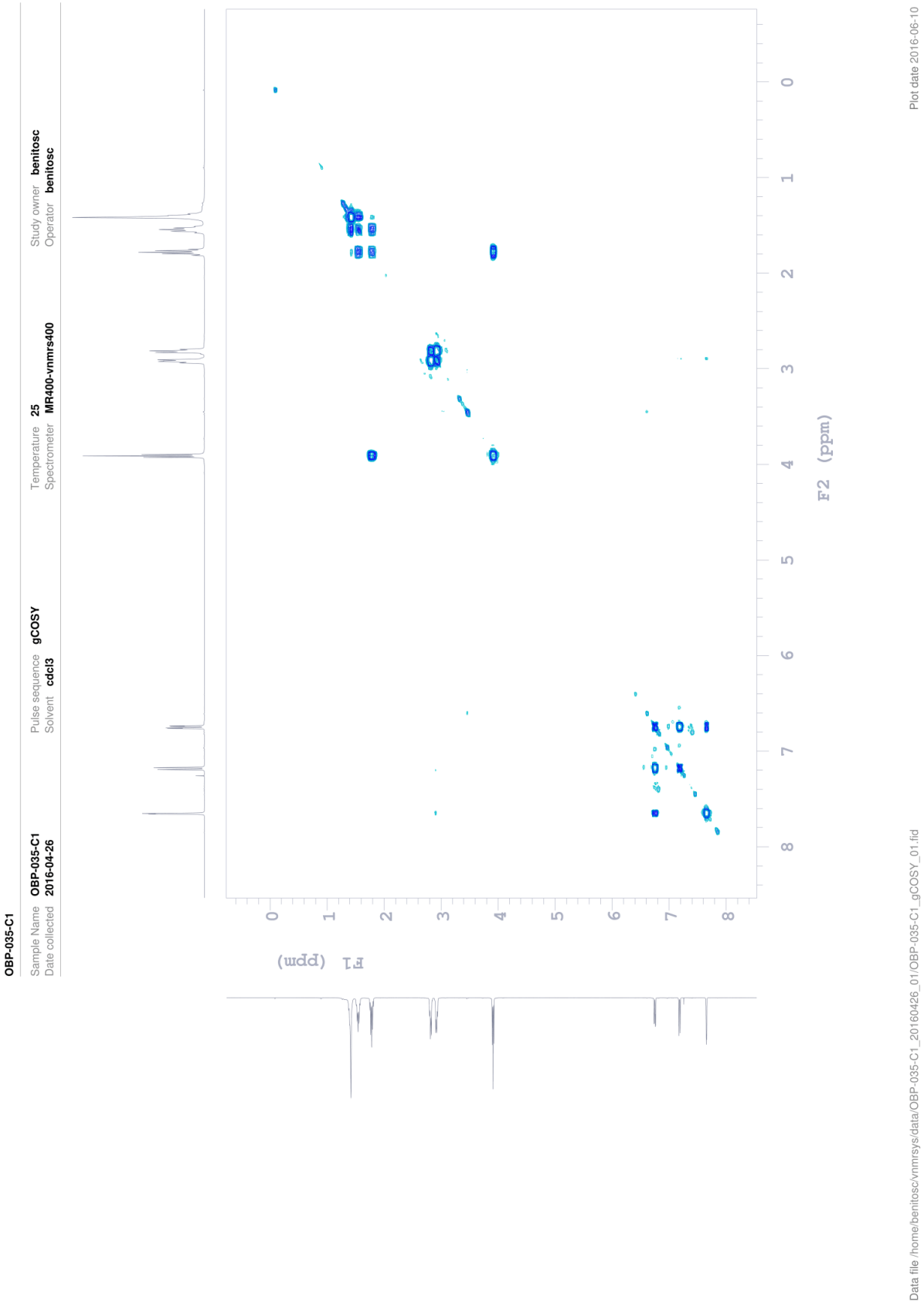

Figure 83. COSY NMR spectrum of compound Z-1c.

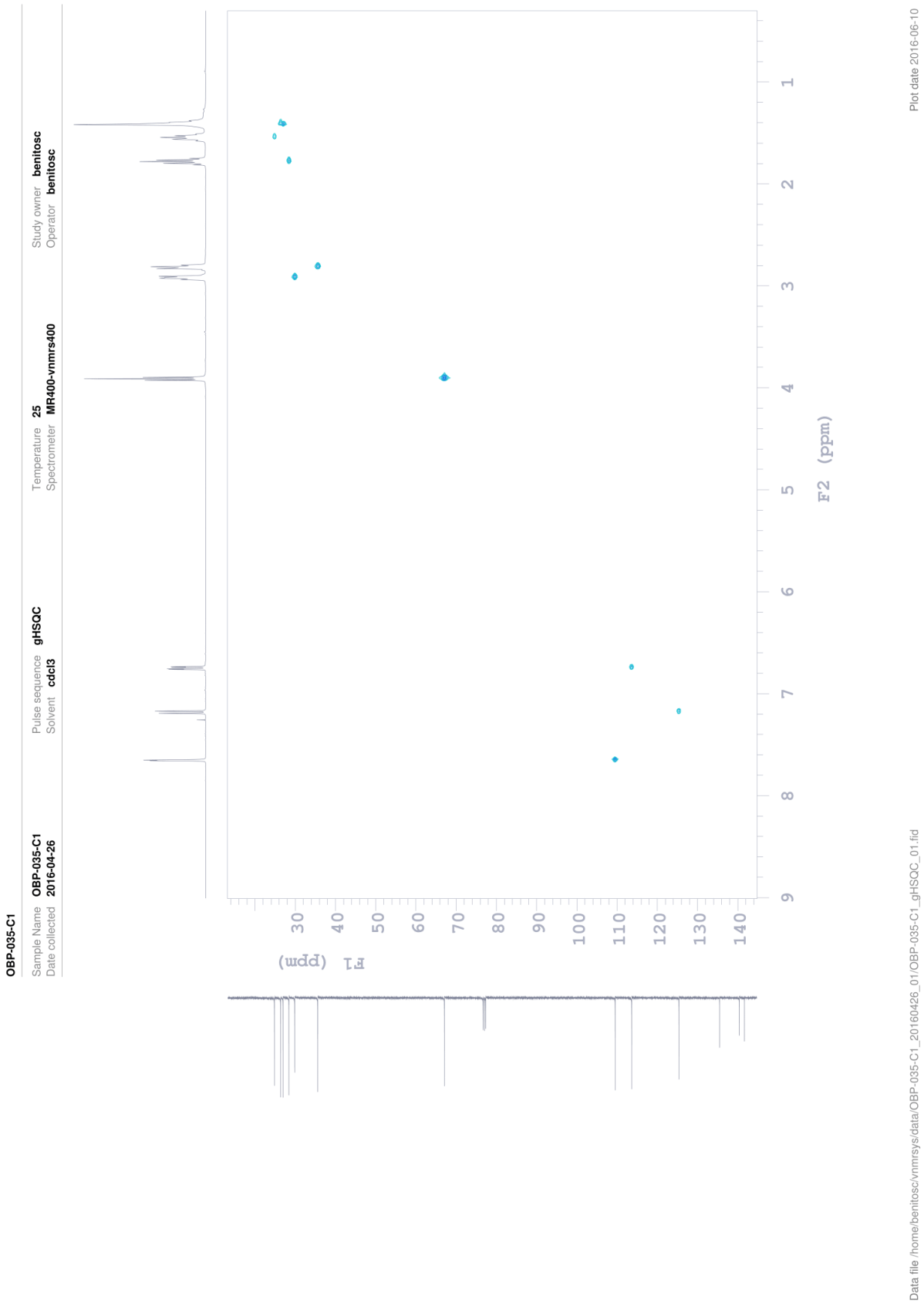

Figure 84. HSQC NMR spectrum of compound *Z*-1c.

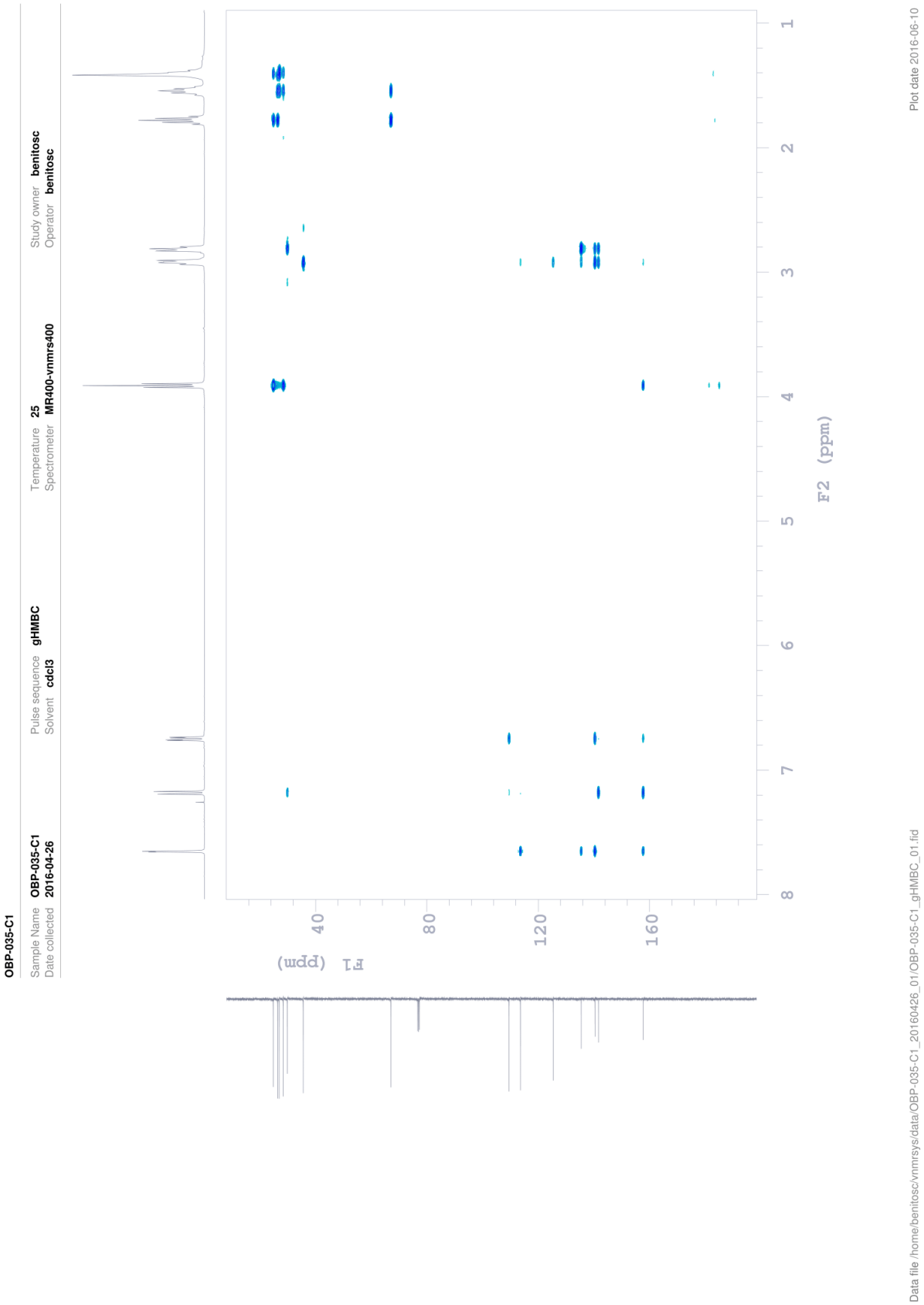

Figure 85. HMBC NMR spectrum of compound *Z*-1c.

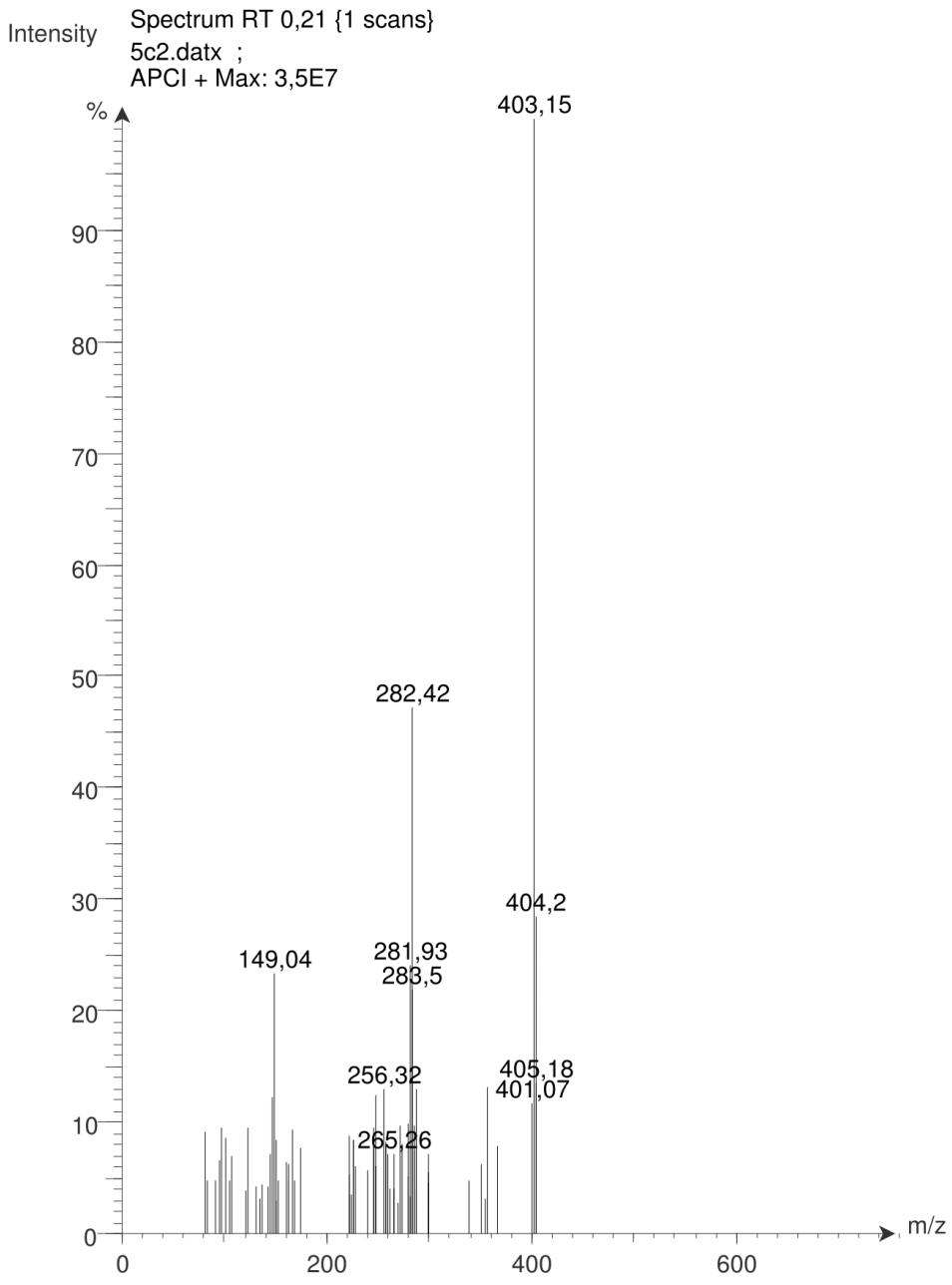

Figure 86. MS spectrum of compound *Z*-1c.

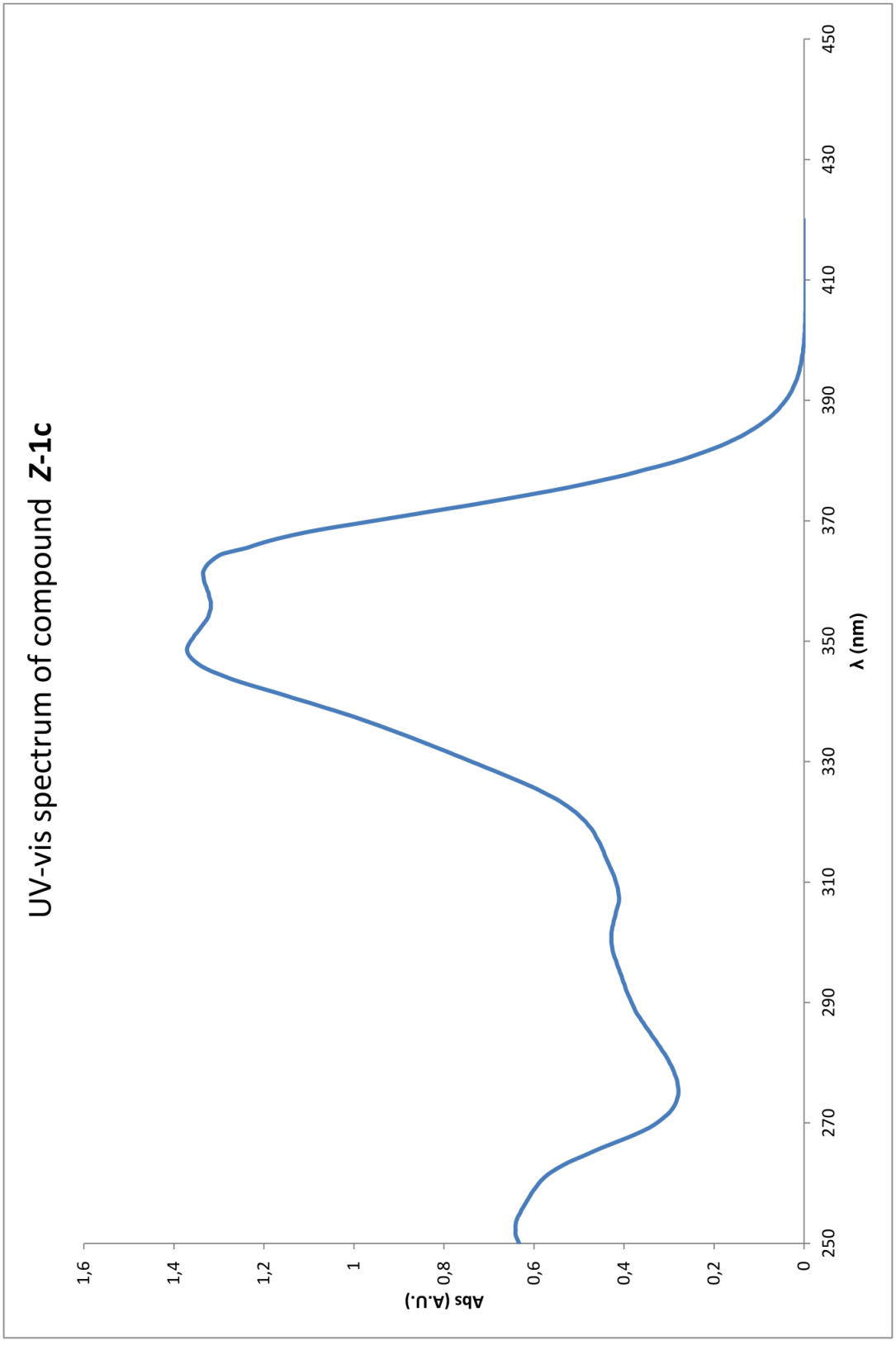

Figure 87. UV-vis spectrum of compound *Z*-1c.

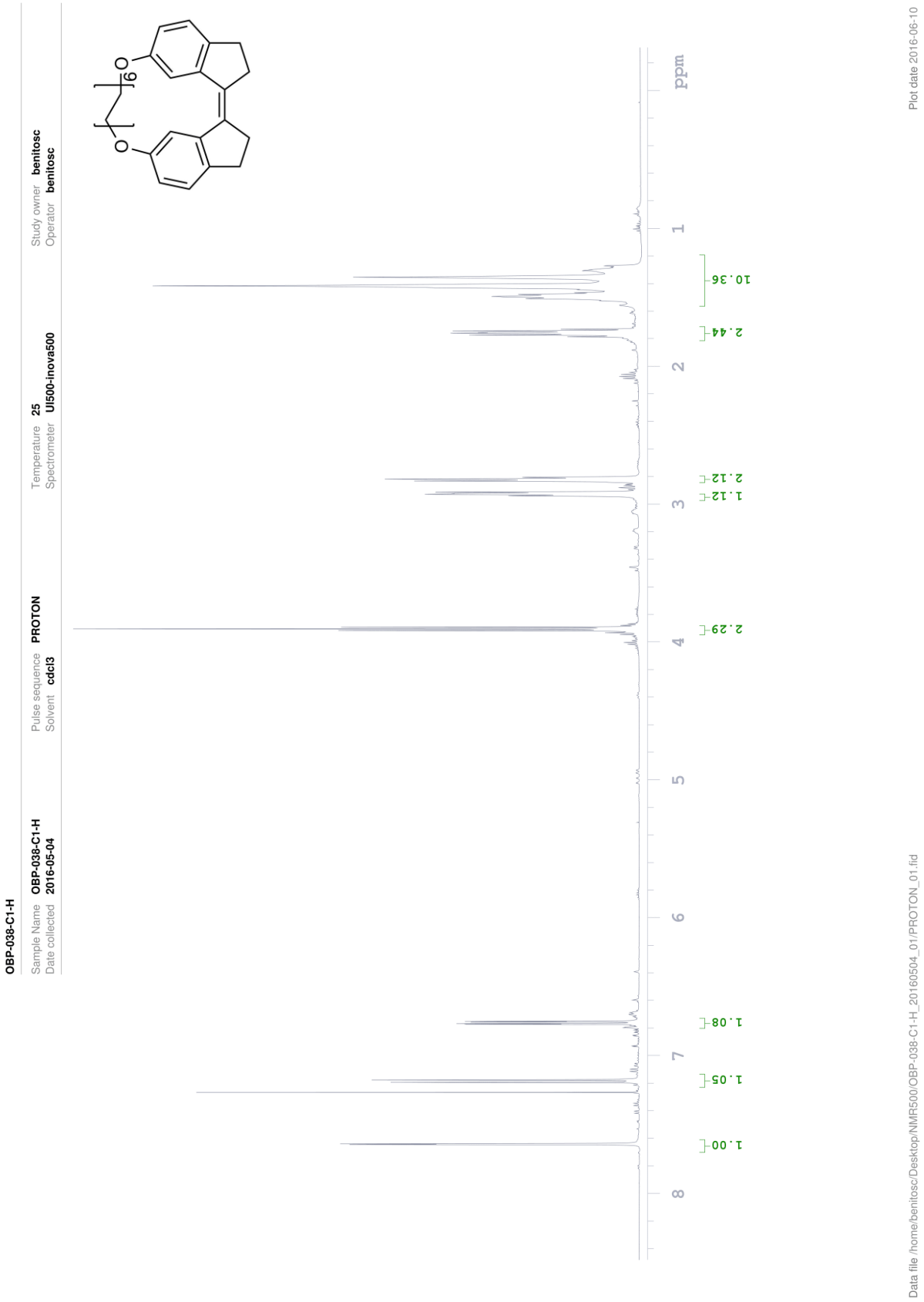

Figure 88. ^{1}H-NMR spectrum of compound *Z*-1d.

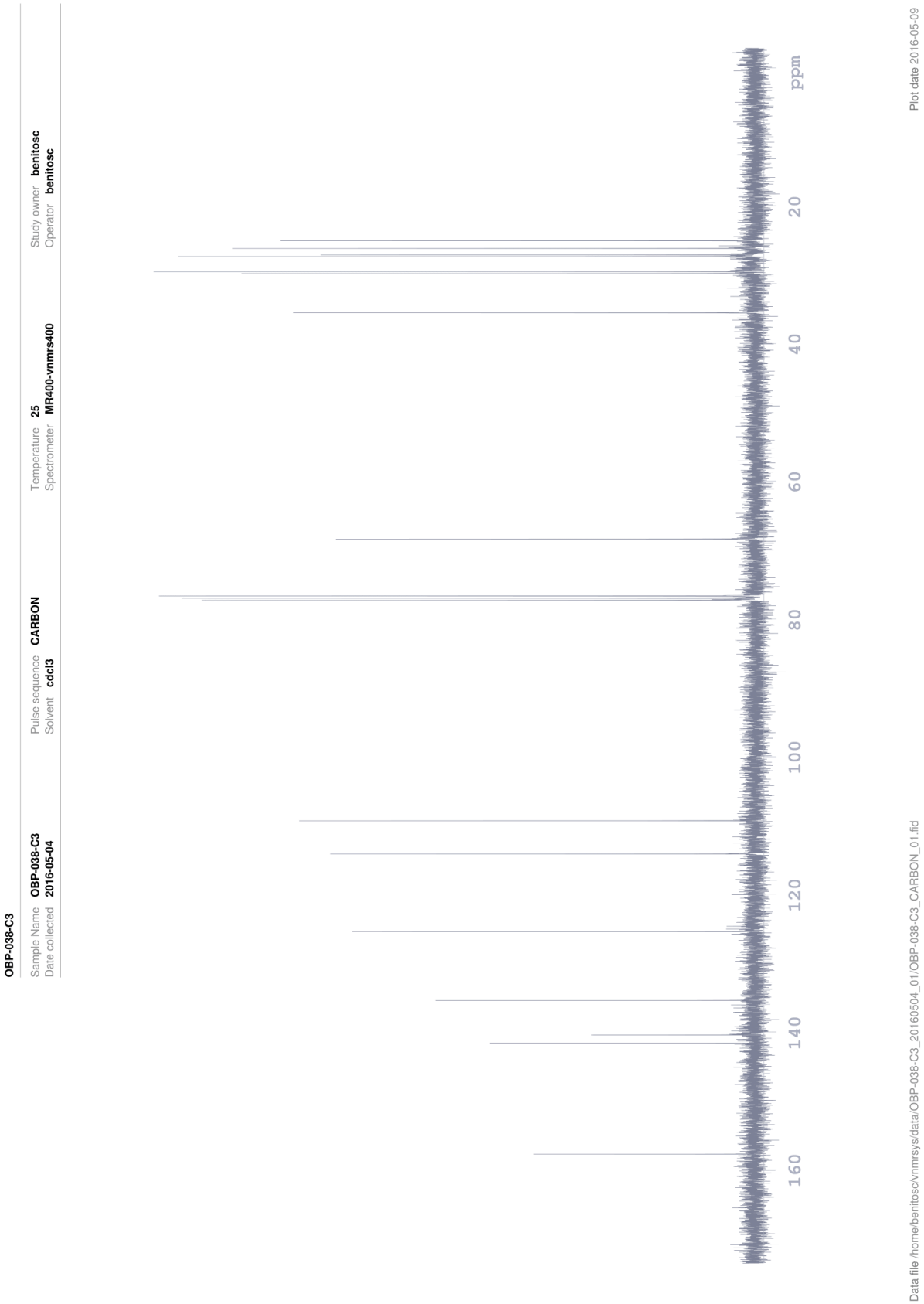

Figure 89. ^{13}C-NMR spectrum of compound *Z*-1d.

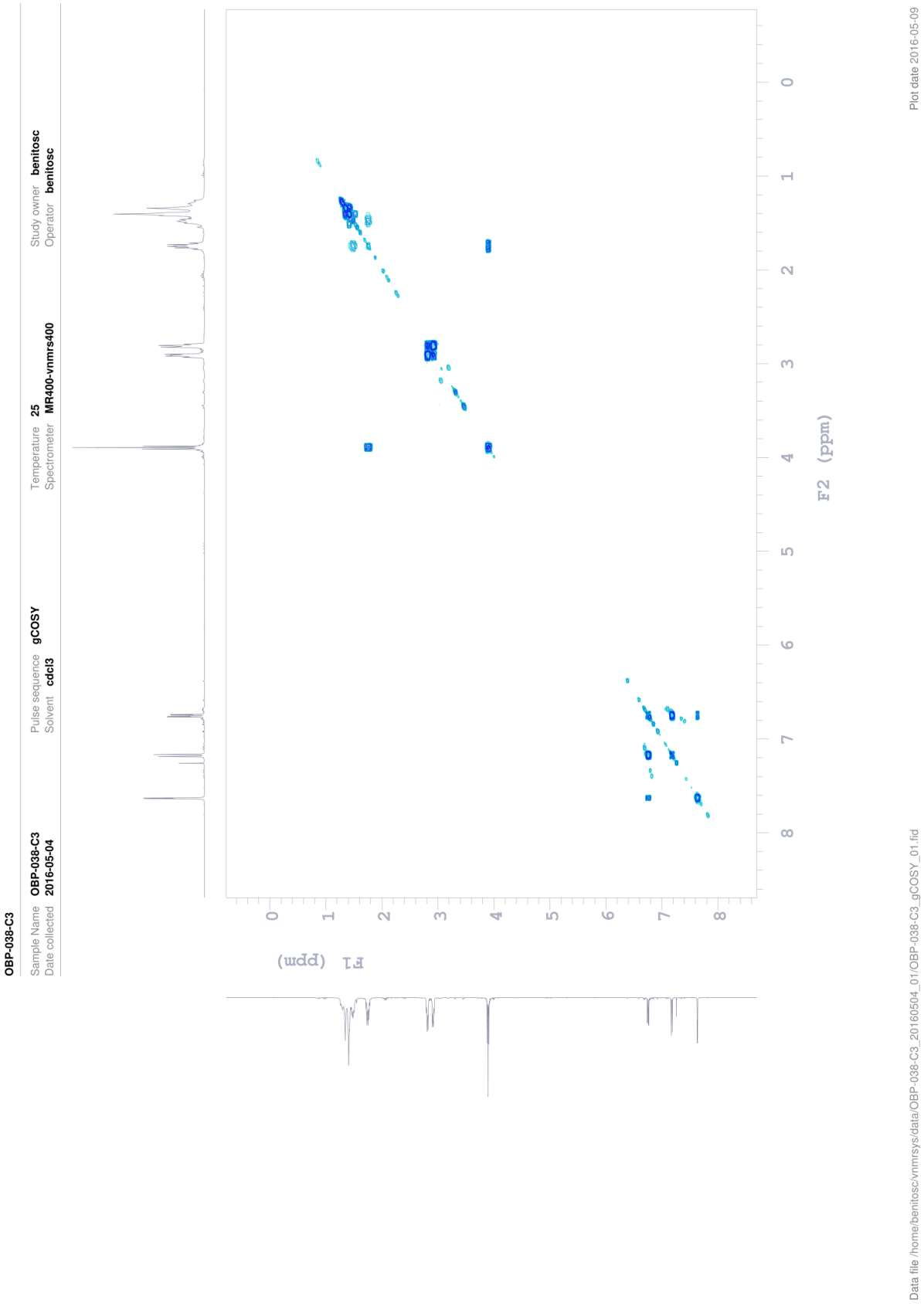

Figure 90. COSY NMR spectrum of compound Z-1d.

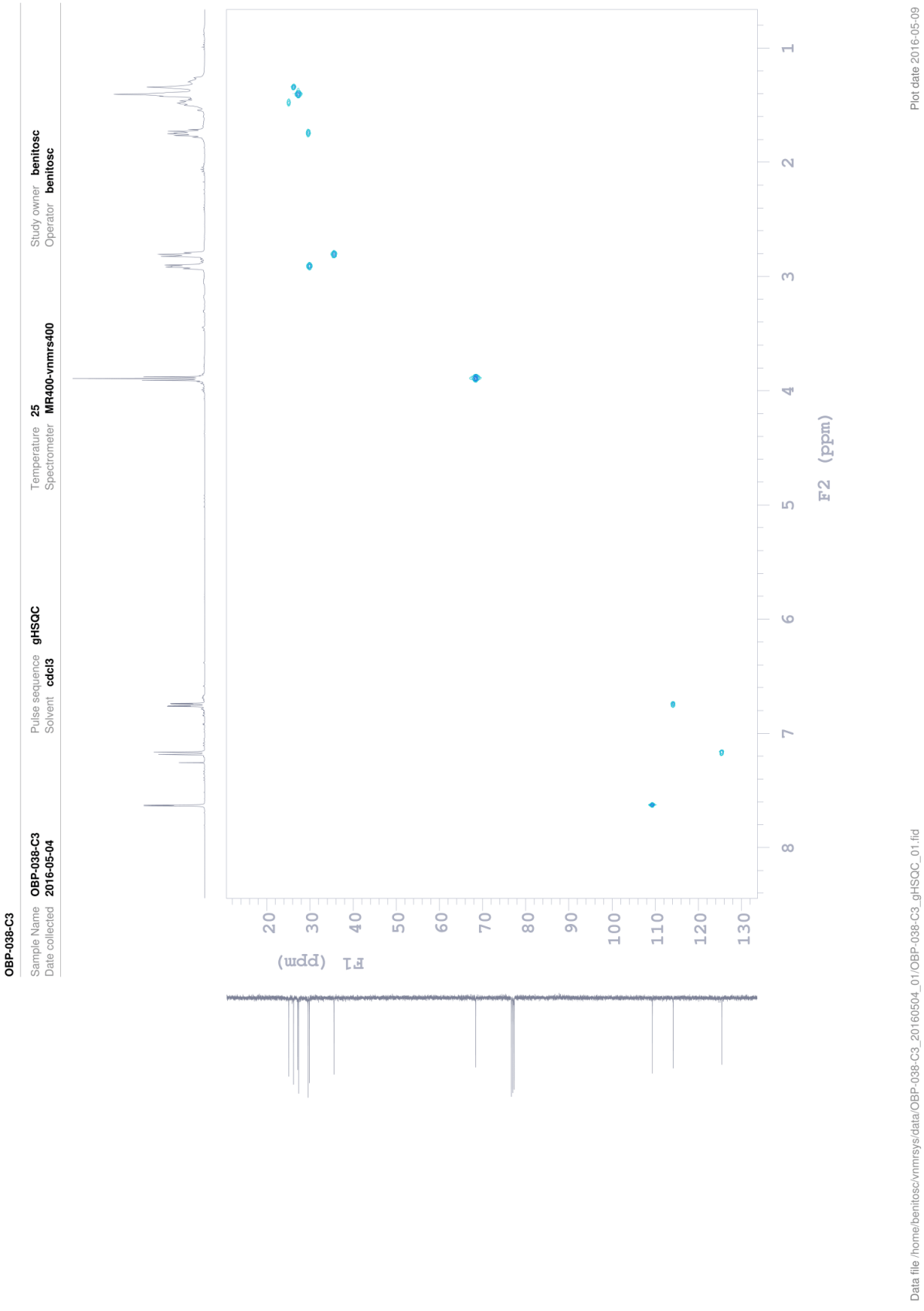

Figure 91. HSQC NMR spectrum of compound *Z*-1d.

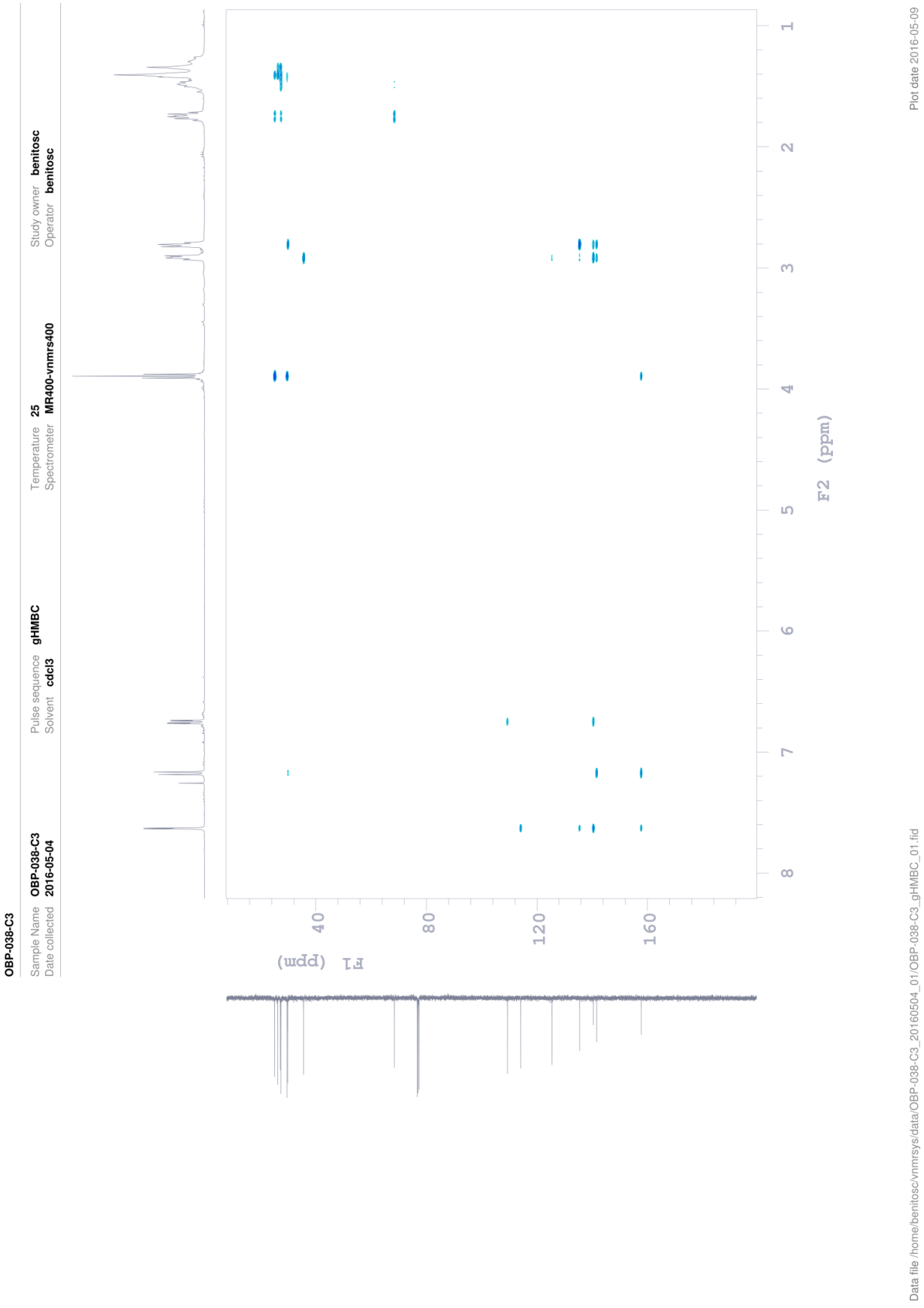

Figure 92. HMBC NMR spectrum of compound *Z*-1d.

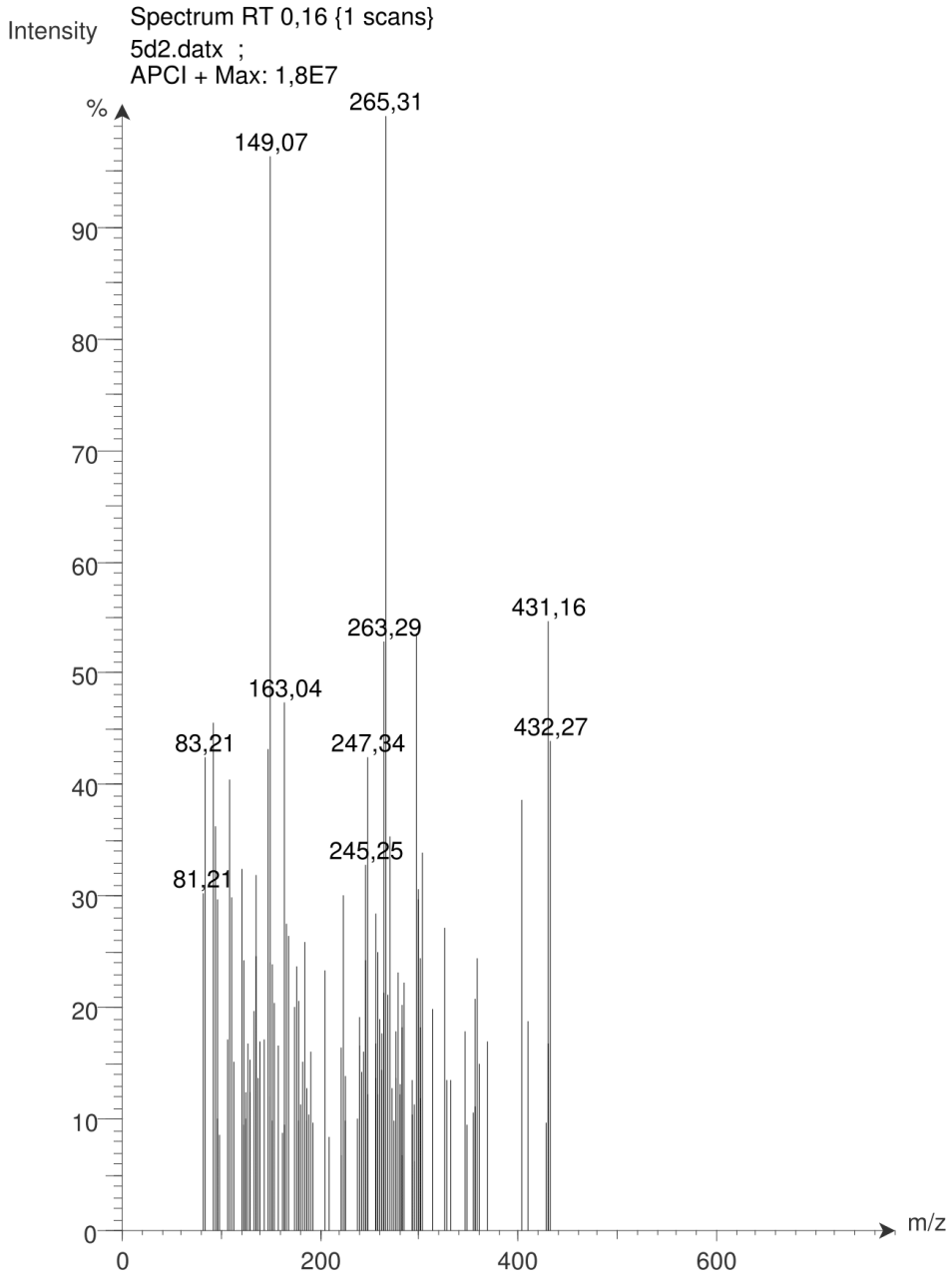

Figure 93. MS spectrum of compound 2d.

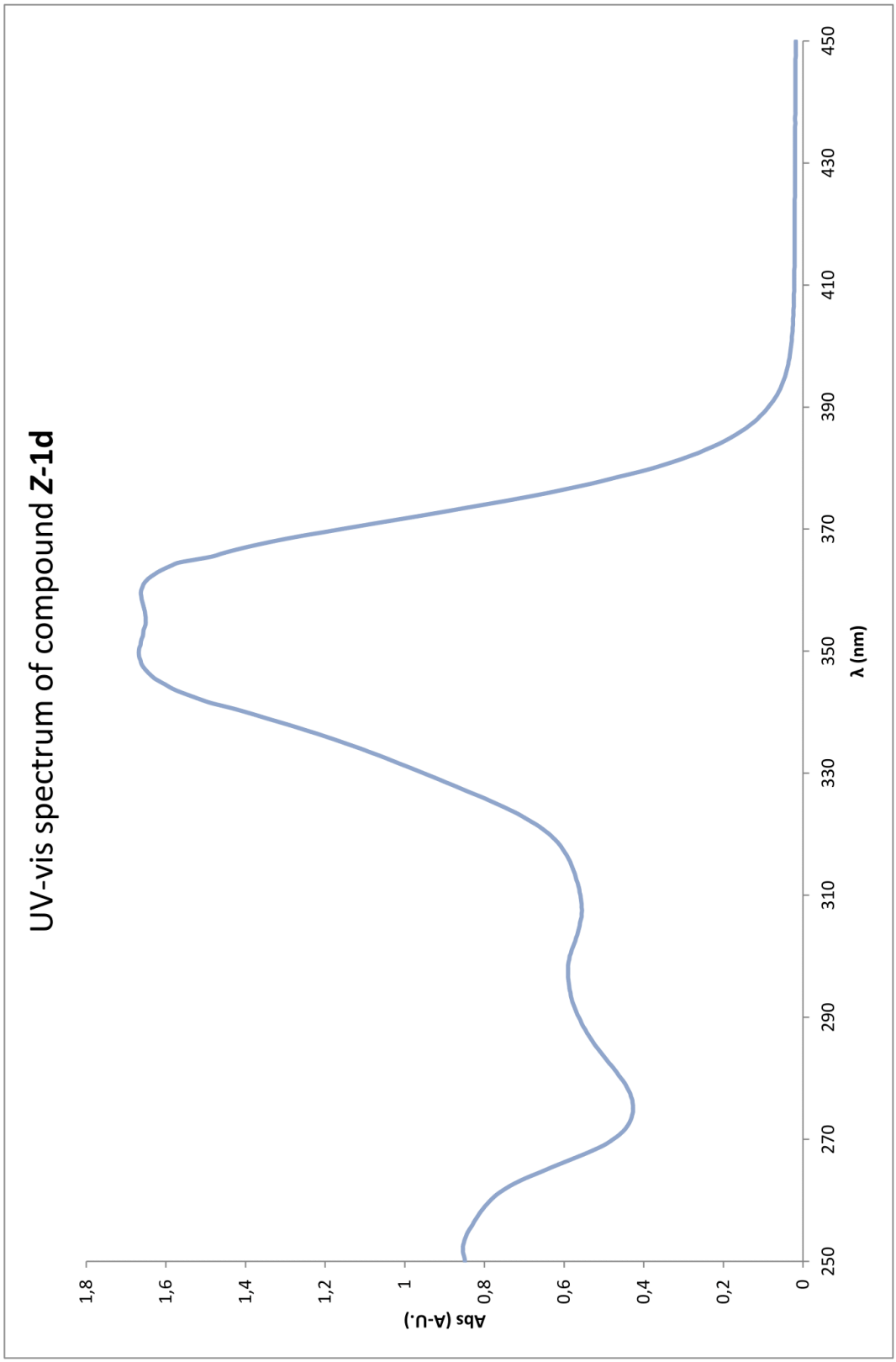

Figure 94. UV-vis spectrum of compound *Z*-1d.

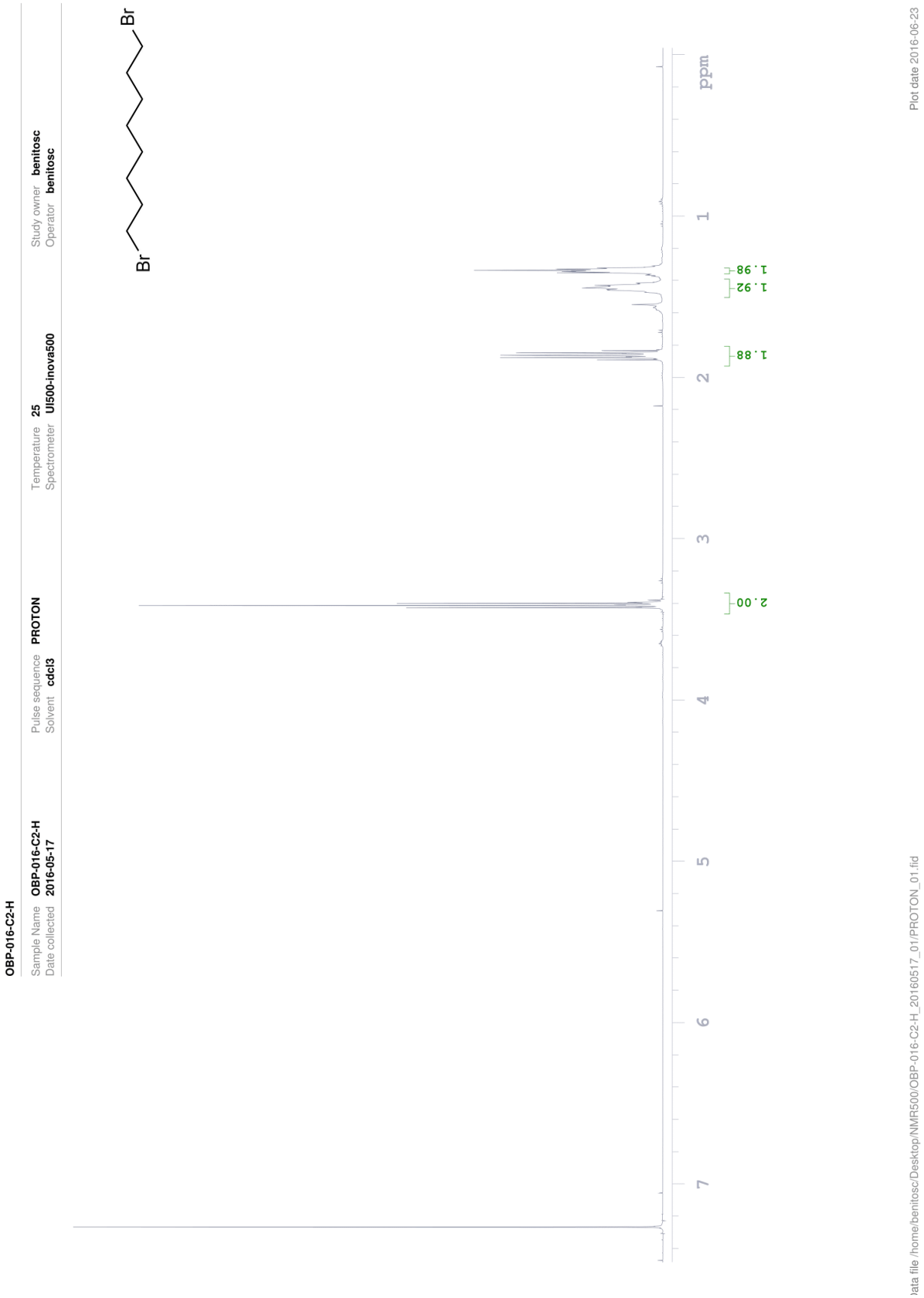

Figure 95. ^{1}H-NMR spectrum of 1,8-dibromooctane.

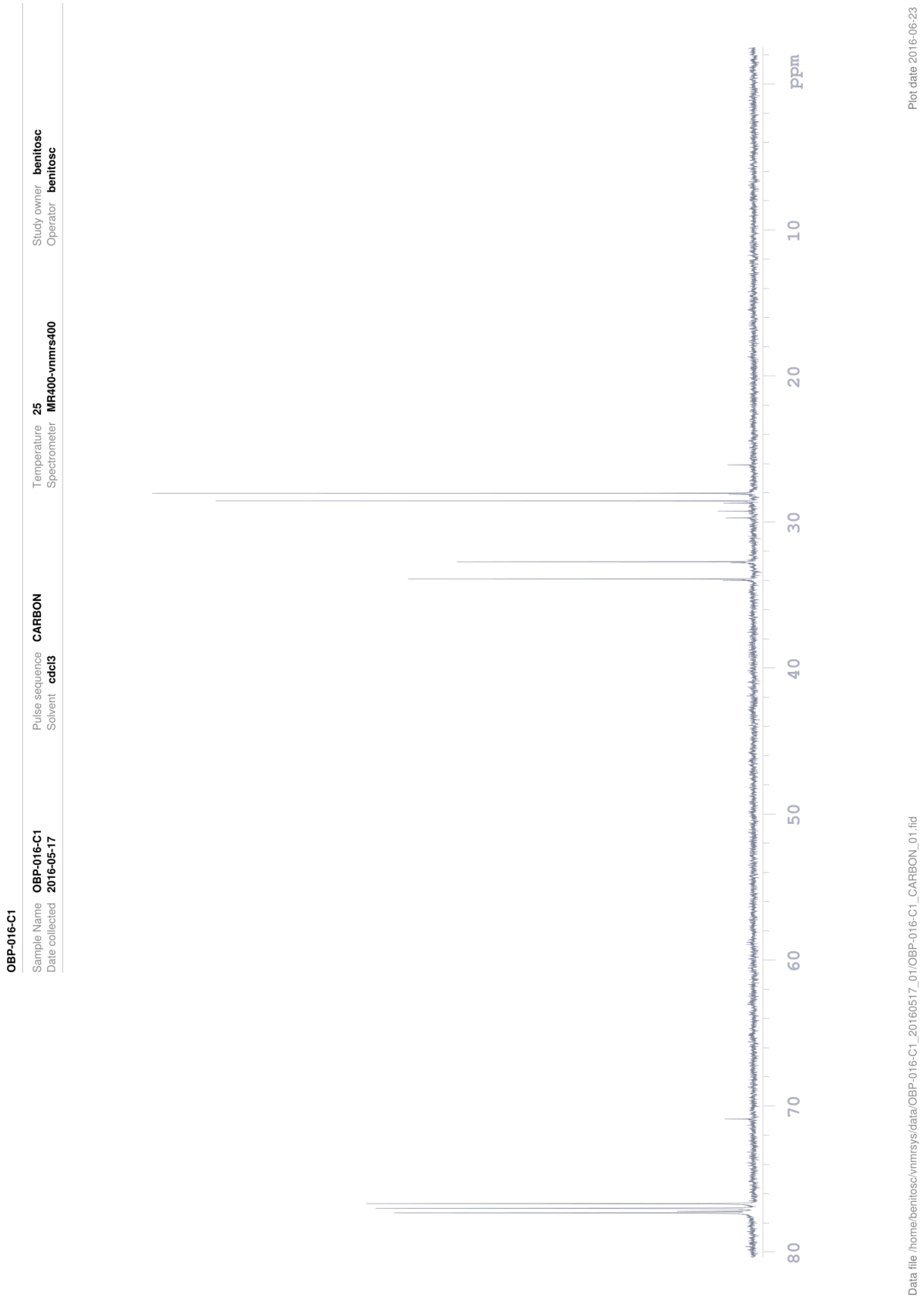

Figure 96. ^{13}C-NMR spectrum of 1,8-dibromooctane.

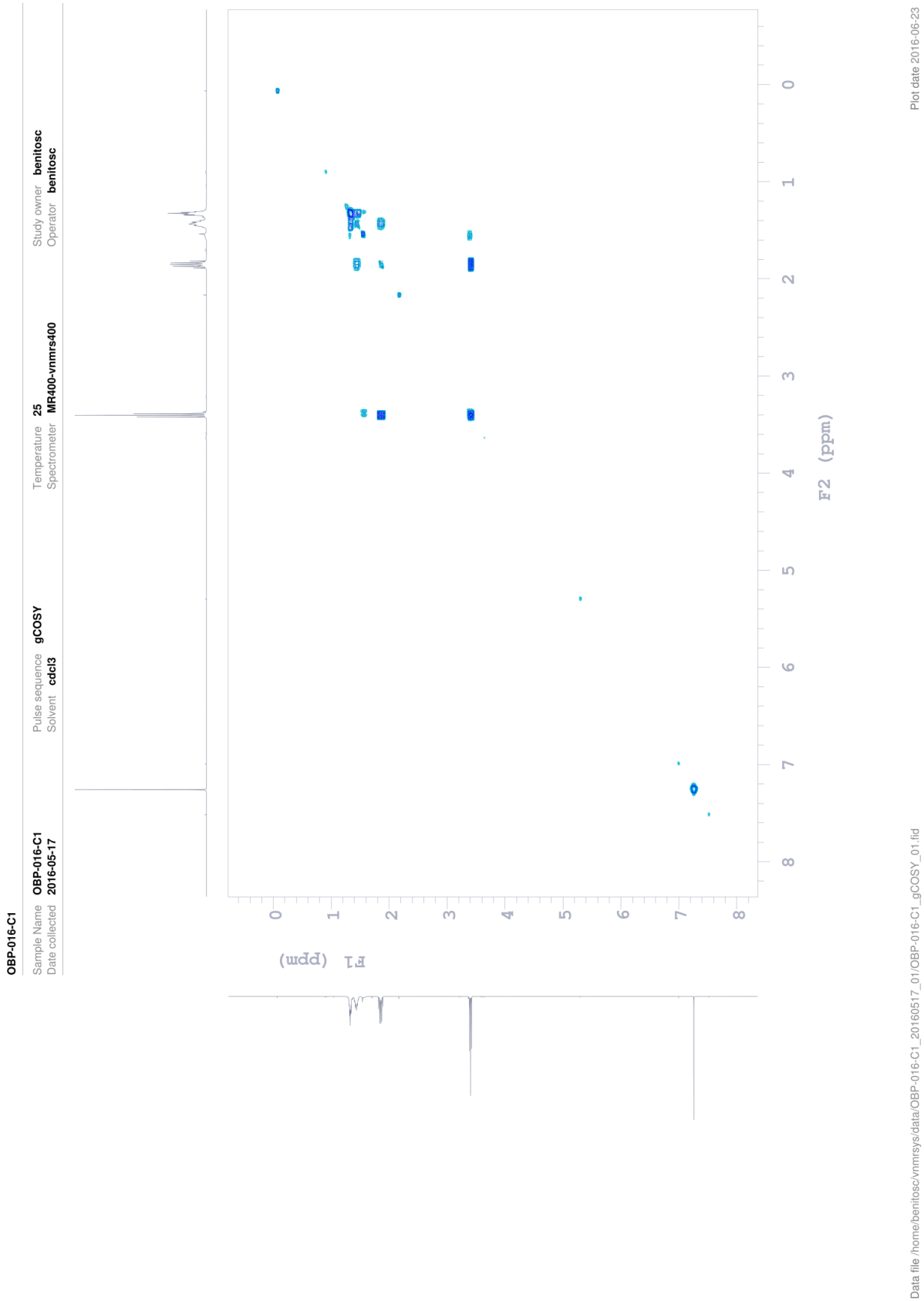

Figure 97. COSY NMR spectrum of 1,8-dibromooctane.

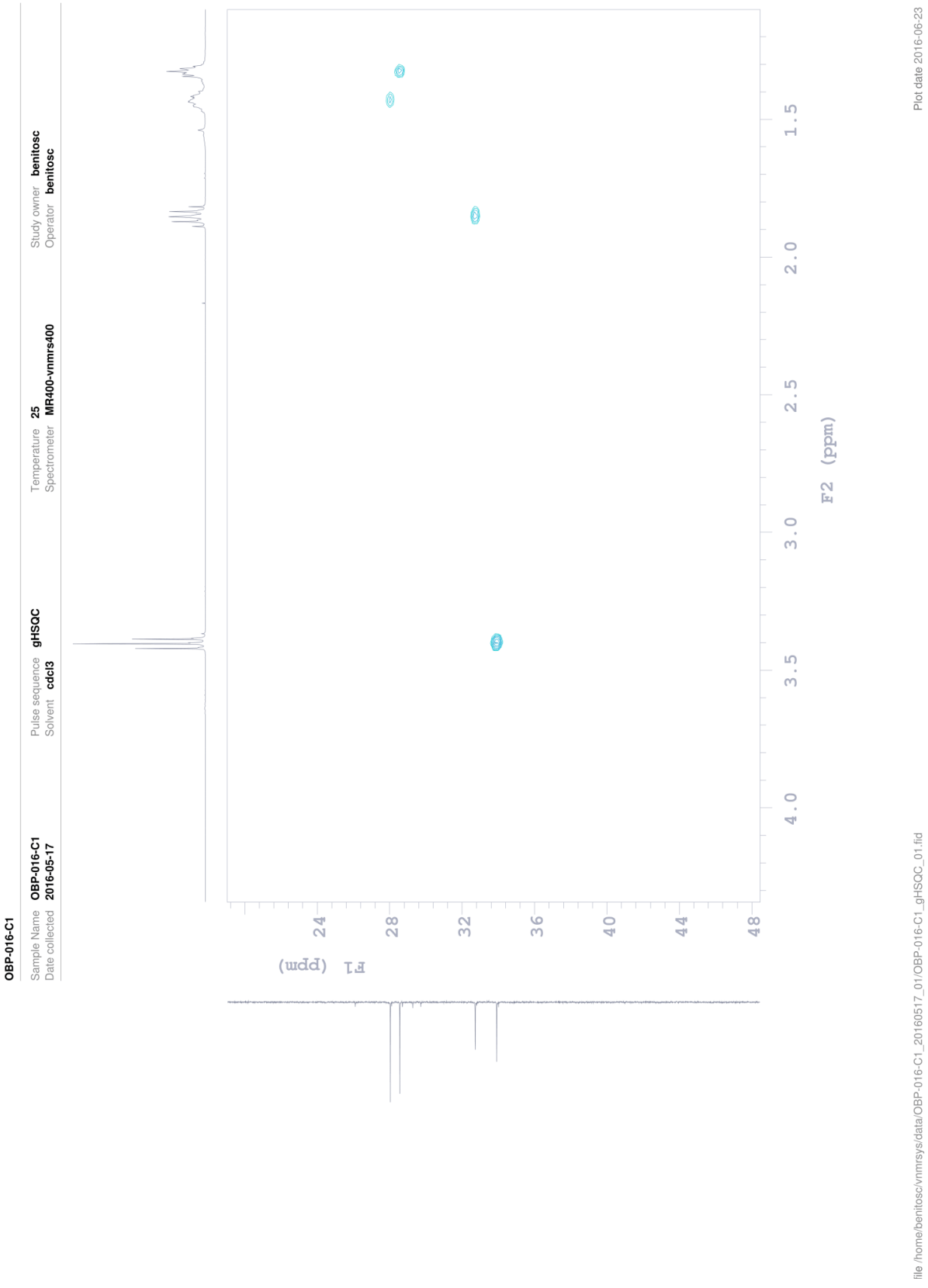

Figure 98. HSQC NMR spectrum of 1,8-dibromooctane.

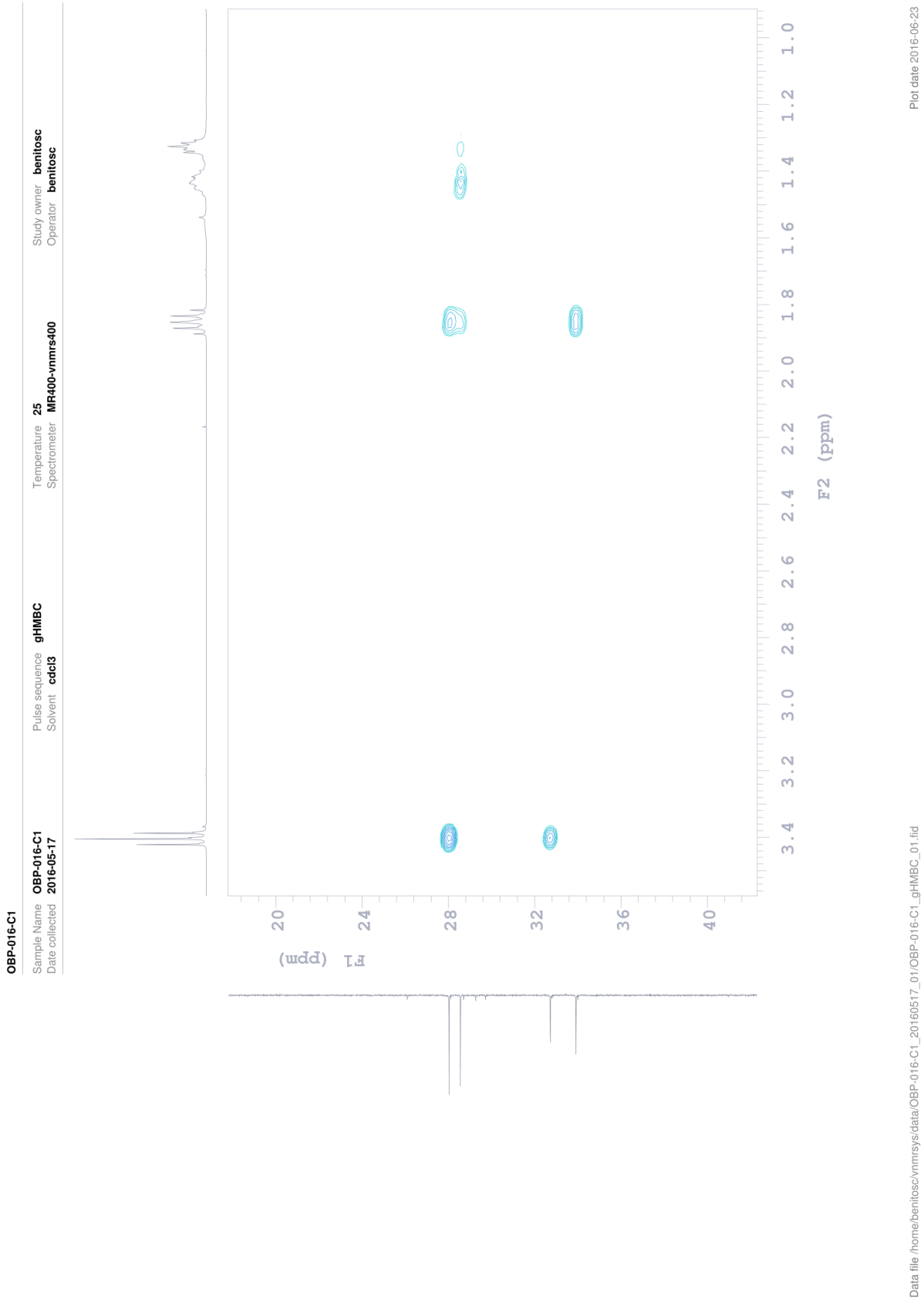

Figure 99. HMBC NMR spectrum of 1,8-dibromooctane.